RADIOLOGY AND ONCOLOGY

December 2008
Vol. 42 No. 4
Ljubljana

ISSN 1318-2099

PRAVI TRENUTEK ZA NOV ZAČETEK

Odobrena indikacija za prehod med adjuvantnim zdravljenjem

AROMASIN®
eksemestan

BISTVENE INFORMACIJE IZ POVZETKA GLAVNIH ZNAČILNOSTI ZDRAVILA
AROMASIN® 25 mg obložene tablete
Sestava in oblika zdravila: obložena tableta vsebuje 25 mg eksemestana. **Indikacije:** adjuvantno zdravljenje žensk po menopavzi, ki imajo invazivnega zgodnjega raka dojke s pozitivnimi estrogenskimi receptorji in so se uvodoma vsaj 2 leti zdravile s tamoksifenom. Zdravljenje napredovalega raka dojke pri ženskah z naravno ali umetno povzročeno menopavzo, pri katerih je bolezen napredovala po antiestrogenski terapiji. Učinkovitost še ni bila dokazana pri bolnicah, pri katerih tumorske celice nimajo estrogenskih receptorjev. **Odmerjanje in način uporabe:** 25 mg enkrat na dan, najbolje po jedi. Pri bolnicah z zgodnjim rakom dojke je treba zdravljenje nadaljevati do dopolnjenega petega leta adjuvantnega hormonskega zdravljenja oz. do recidiva tumorja. Pri bolnicah z napredovalim rakom dojke je treba zdravljenje nadaljevati, dokler ni razvidno napredovanje tumorja. **Kontraindikacije:** znana preobčutljivost na učinkovino zdravila ali na katero od pomožnih snovi, ženske pred menopavzo, nosečnice in doječe matere. **Posebna opozorila in previdnostni ukrepi:** predmenopavzni endokrini status, jetrna ali ledvična okvara, bolniki z redkimi prirojenimi motnjami, kot so fruktozna intoleranca, malabsorpcija glukoze-galaktoze ali insuficienca saharoze-izomaltase. Lahko povzroči alergijske reakcije ali zmanjšanje mineralne gostote kosti. Ženskam z osteoporozo ali tveganjem zanjo je treba izrecno izmeriti gostoto kosti s kostno denzitometrijo, in sicer na začetku zdravljenja in nato redno med zdravljenjem. **Medsebojno delovanje z drugimi zdravili:** sočasna uporaba zdravil - npr. rifampicina, antiepileptikov (npr. fenitoina ali karbamazepina) ali zeliščnih pripravkov s šentjaževko - ki inducirajo CYP 3A4, lahko zmanjša učinkovitost Aromasina. Uporabljati ga je treba previdno z zdravili, ki se presnavljajo s pomočjo CYP 3A4 in ki imajo ozek terapevtski interval. Kliničnih izkušenj s sočasno uporabo zdravila Aromasin in drugih zdravil proti raku ni. Ne sme se jemati sočasno z zdravili, ki vsebujejo estrogen, saj bi ta izničila njegovo farmakološko delovanje. **Vpliv na sposobnost vožnje in upravljanja s stroji:** po uporabi zdravila je lahko psihofizična sposobnost za upravljanje s stroji ali vožnjo avtomobila zmanjšana. **Neželeni učinki:** neželeni učinki so bili v študijah ponavadi blagi do zmerni. *Zelo pogosti (> 10 %):* vročinski oblivi, bolečine v sklepih, utrujenost, slabost, nespečnost, glavobol, močnejše znojenje, blago zvišanje alkalne fosfataze. **Način in režim izdajanja**: zdravilo se izdaja le na recept, uporablja pa se po navodilu in pod posebnim nadzorom zdravnika specialista ali od njega pooblaščenega zdravnika. **Imetnik dovoljenja za promet:** Pfizer Luksembourg SARL, 283, route d'Arlon, L-8011 Strassen, Luksemburg. **Datum zadnje revizije besedila:** 9.12.2005
Pred predpisovanjem se seznanite s celotnim povzetkom glavnih značilnosti zdravila.

Pfizer

Podrobnejše informacije o zdravilu so na voljo pri:
Pfizer, podružnica za svetovanje s področja farmacevtske dejavnosti, Ljubljana, Letališka cesta 3c, 1000 Ljubljana

RADIOLOGY AND ONCOLOGY

Editorial office
Radiology and Oncology
Institute of Oncology
Zaloška 2
SI-1000 Ljubljana
Slovenia
Phone: +386 1 5879 369
Phone/Fax: +386 1 5879 434
E-mail: gsersa@onko-i.si

December 2008
Vol. 42 No. 4
Pages 173-239
ISSN 1318-2099
UDC 616-006
CODEN: RONCEM

Aims and scope
Radiology and Oncology is a journal devoted to publication of original contributions in diagnostic and interventional radiology, computerized tomography, ultrasound, magnetic resonance, nuclear medicine, radiotherapy, clinical and experimental oncology, radiobiology, radiophysics and radiation protection.

Editor-in-Chief
Gregor Serša
Ljubljana, Slovenia

Executive Editor
Viljem Kovač
Ljubljana, Slovenia

Deputy Editors
Andrej Cör
Ljubljana, Slovenia

Igor Kocijančič
Ljubljana, Slovenia

Editorial Board
Karl H. Bohuslavizki
Hamburg, Germany
Maja Čemažar
Ljubljana, Slovenia
Christian Dittrich
Vienna, Austria
Metka Filipič
Ljubljana, Slovenia
Tullio Giraldi
Trieste, Italy
Maria Gődény
Budapest, Hungary
Vassil Hadjidekov
Sofia, Bulgaria
Marko Hočevar
Ljubljana, Slovenia
Maksimilijan Kadivec
Ljubljana, Slovenia
Miklós Kásler
Budapest, Hungary
Michael Kirschfink
Heidelberg, Germany
Janko Kos
Ljubljana, Slovenia
Tamara Lah Turnšek
Ljubljana, Slovenia
Damijan Miklavčič
Ljubljana, Slovenia
Luka Milas
Houston, USA
Damir Miletić
Rijeka, Croatia
Maja Osmak
Zagreb, Croatia
Branko Palčič
Vancouver, Canada
Dušan Pavčnik
Portland, USA
Geoffrey J Pilkington
Portsmouth, UK
Ervin B. Podgoršak
Montreal, Canada
Uroš Smrdel
Ljubljana, Slovenia
Primož Strojan
Ljubljana, Slovenia
Borut Štabuc
Ljubljana, Slovenia
Ranka Štern-Padovan
Zagreb, Croatia
Justin Teissié
Tolouse, France
Sándor Tóth
Orosháza, Hungary
Gillian M. Tozer
Sheffield, UK
Andrea Veronesi
Aviano, Italy
Branko Zakotnik
Ljubljana, Slovenia

Advisory Committee
Marija Auersperg Ljubljana, Slovenia; ***Tomaž Benulič*** Ljubljana, Slovenia; ***Jure Fettich*** Ljubljana; ***Valentin Fidler*** Ljubljana, Slovenia; ***Berta Jereb*** Ljubljana, Slovenia; ***Vladimir Jevtič*** Ljubljana, Slovenia; ***Stojan Plesničar*** Ljubljana, Slovenia; ***Živa Zupančič*** Ljubljana, Slovenia

Publisher
Association of Radiology and Oncology

Affiliated with
Slovenian Medical Association – Slovenian Association of Radiology, Nuclear Medicine Society,
Slovenian Society for Radiotherapy and Oncology, and Slovenian Cancer Society
Croatian Medical Association – Croatian Society of Radiology
Societas Radiologorum Hungarorum
Friuli-Venezia Giulia regional groups of S.I.R.M.
(Italian Society of Medical Radiology)

Copyright © Radiology and Oncology. All rights reserved.

Reader for English
Vida Kološa

Key words
Eva Klemenčič

Secretary
Mira Klemenčič

Design
Monika Fink-Serša

Printed by
Imprint d.o.o., Ljubljana, Slovenia

Published quarterly in 600 copies

Beneficiary name: DRUŠTVO RADIOLOGIJE IN ONKOLOGIJE
Zaloška cesta 2,
1000 Ljubljana
Slovenia
Beneficiary bank account number: SI56 02010-0090006751
IBAN: SI56020100090006751
Our bank name: Nova Ljubljanska banka, d.d.,
Ljubljana, Trg republike 2,
1520 Ljubljana; Slovenia
SWIFT: LJBASI2X

Subscription fee for institutions EUR 100, individuals EUR 50

The publication of this journal is subsidized by the Slovenian Research Agency.

Indexed and abstracted by:
Science Citation Index Expanded (SciSearch®)
Journal Citation Reports/Science Edition
Scopus
EMBASE/Excerpta Medica
Open J-gate
Chemical Abstracts
Biomedicina Slovenica

This journal is printed on acid- free paper

Radiology and Oncology is available on the internet at: http://www.onko-i.si/radioloncol and http://www.versita.com

ISSN 1581-3207

RADIOLOGY AND ONCOLOGY

Ljubljana, Slovenia
December 2008
Vol. 42 No. 4

ISSN 1318-2099
UDC 616-006
CODEN: RONCEM

CONTENTS

Radiology and Oncology is covered in *Science Citation Index Expanded (SciSearch®), Journal Citation Reports/Science Edition, Scopus, EMBASE/Excerpta Medica, Open J-gate, Chemical Abstracts, Biomedicina Slovenica*

Radiol Oncol 2008; 42(4): 173-80. *doi:10.2478/v10019-008-0018-0*

research article

What is the most common mammographic appearance of T1a and T1b invasive breast cancer?

Maja Podkrajšek[1], Janez Žgajnar[2], Marko Hočevar[2]

[1]Department of Radiology and [2]Department of Surgical Oncology, Institute of Oncology Ljubljana, Slovenia

Background. *Data about the mammographic appearance of breast cancer smaller than 10 mm are very limited and different authors use different mammographic criteria. The aim of this study was to determine the most common mammographic appearance of small invasive breast cancers (T1a and T1b).*

Patients and methods. *The study group consisted of 100 women with 102 small (1-10 mm) invasive breast cancers detected on mammography at a single institution in 16 months period. The mammographic appearance of tumours was classified as: mass, mass with associated calcifications, only calcifications or others (asymmetric density and architectural distortion).*

Results. *The most common mammographic appearance was a mass without calcifications (60/102; 59%). Additional 12/102 (11%) tumours had a mammographic appearance of a mass with associated calcifications. Only microcalcifications were detected in 12 (11 %) and asymmetric density and architectural distortion in 18 breast cancers (18 %). Most (44/60) cancers which presented mammographically as a mass had stellate margins. The proportion of castig type calcifications was higher in women under 50 years.*

Conclusions: *The most common mammographic finding of small breast cancer is a mass with stellate margins independent of the age of patients. Calcifications with/without mass are more common in woman under 50 years.*

Key words: breast cancer; mammographic appearance; microcalcifications, stellate; casting; asymmetric density

Introduction

Breast cancer is the most common non-cutaneous cancer in European women. In Slovenia 1020 new cases and 425 deaths from breast cancer are estimated in 2005. An average Slovenian woman has a lifetime risk of 1 in 16 for developing breast cancer.[1]

Received 13 October 2008
Accepted 5 November 2008

Correspondence to: Prof. Marko Hočevar, MD, PhD, Institute of Oncology Ljubljana, Zaloška 2, SI-1000 Ljubljana, Slovenia. Phone: +386 1 5879 534; Fax: +386 1 5879 407; E-mail: mhocevar@onko-i.si

Mammography can identify breast cancers too small to palpate on physical examination. Clinical trials have established that screening with mammography may decrease breast cancer mortality, because breast cancers detected on screening mammography are smaller and more likely not to have spread to regional lymph nodes as compared with breast cancers detected at physical examination.[2-4] Additionally, since breast cancers detected on screening mammography are smaller, they can be more often treated with breast conservation and with less-toxic systemic therapy.[5]

Table 1. Classification of mammographic findings

1	Mass without calcifications:
	with stellate margins
	round/oval mass
2	Mass with calcifications
3	Only calcifications:
	casting
	powdery
	crushed-stone like
4	Others:
	asymmetric density
	architectural distorsion

Table 2. Distribution of mammographic findings in 102 small breast cancers

		No	%
1	Mass without calcifications	**60**	59
	stellate	44	
	round or oval	16	
2	Mass with calcifications	**12**	11
	powdery	1	
	crushed-stone like	2	
	casting	9	
3	Only calcifications	**12**	12
	powdery	3	
	crushed-stone like	1	
	casting	8	
4	Other	**18**	18
	asymmetric density	14	
	architectural distortion	4	
	Total:	**102**	100%

If we want to detect with mammography small breast cancers, we have to use the accurate mammographic criteria for early (T1a and T1b) invasive breast cancers. However, there are only a few publications in the literature about the mammographic appearance of breast cancer smaller than 10 mm.[6] Additionally, there is unfortunately no standardized approach - different authors use different mammographic criteria for breast cancers smaller than 10 mm.

The aim of this study was to determine the most common mammographic findings of small invasive breast cancers (T1a and T1b).

Patients and methods

In the 16 months period (from September 2003 to December 2004) 100 consecutive women (aged 36-77 years; mean 59 years) with 102 pathologically proven small (pT1a and pT1b) breast cancers were treated at the Institute of Oncology in Ljubljana, Slovenia. Most of the cancers were non-palpable (80/102) and detected on screening mammography. Palpable cancers were tumours which were palpable in the same quadrant as histologically proven tumours and which were cytologically proven for cancer (C5) without imaging modality.

Mammographic lesions were classified according to BIRADS:[7] 4 lesions as R2, 28 lesions as R3, 66 as R4 and 4 as R5. Free hand fine needle aspiration biopsy (FNAB) was performed in all 20 patients with palpable tumours. Cytology was positive (C5) in 14/20 patients and non diagnostic (C1) in 6/20. In these six patients, as well as in all other cases (80/102) of non palpable tumour, image guided FNAB (58 cases) or core biopsy (28 cases) was performed. In 51 cases biopsy guidance was done by the ultrasound (US) and in 35 by the stereotaxy.

Preoperative diagnosis of breast cancer was established in 67 patients (C5 in 48 cases and B5 in 19 cases) with nonpalpable tumours. Occult lesion localization (40/67 by stereotaxy and 27/67 by US) with 30-60 MBq of ^{99m}Tc labeled nanocolloid (Nanocol®) in 0.2 ml saline was performed on the morning of surgery. Tumourectomy

Table 3. Distribution of mammographic findings in 28 small breast cancers in women under the age of 50 years

		No	%
1	Mass without calcifications	**11**	39
	stellate	10	
	round or oval	1	
2	Mass with calcifications	**6**	21,5
	powdery	0	
	crushed-stone like	2	
	casting	4	
3	Only calcifications	**6**	21,5
	powdery	2	
	crushed-stone like	1	
	casting	3	
4	Other	**5**	18
	asymmetric density	4	
	architectural distortion	1	
	Total:	**28**	100%

(58/67), quadrantectomy (3/67) or mastectomy (6/67) were combined with a sentinel lymph node biopsy (SLNB).

In 31 patients with preoperative C3/C4 (22 patients) or B2-4 (9 patients) radioguided occult lesion localization (ROLL) and excisional biopsy were performed. ROLL was performed in 26 cases under stereotaxic and in 5 cases under sonographic control. After the histological diagnosis of breast cancer (B5), in the second surgical procedure re-excision of the primary site (22 patients), quadrantectomy (2 patients) or mastectomy (3 patients) and SLNB was performed. In four patients only SLNB was performed because of adequate margins (more than 10 mm) after the excisional biopsy.

Two patients with palpable cytologically proven breast cancers (C5) underwent tumourectomy and axillary dissection because preoperative US examination and US guided FNAB of the axillary lymph nodes revealed metastases in lymph nodes.[8]

All mammographic images were reviewed by a single radiologist (PM), who has a special interest and dedication in breast radiology. Mammographic findings were classified according to Table 2, as seen in Table 1. A mass is defined as a lesion seen in two different projections, while a density is observed only in a single projection according to Samardar.[9]

Pathologic characteristics of primary tumours included size, histologic type, grade (according to Bloom, Richardson and Elston), status of axillary lymph nodes, estrogen and progesteron receptors and HER2 status. The histological type of breast cancers was as follows: invasive ductal, invasive lobular, tubular, mucinous, medullary and papillary.

For the statistical analysis descriptive statistical methods were used.

Results

The mean size of breast cancers was 8.1 mm (range 4-10 mm; pT1a in 18 and pT1b in84 cases). Histologically 86/102 (84%) were invasive ductal, 14/102 (14%) invasive lobular and 2/102 (2%) invasive tubular cancers. There were 48/102 (47%) grade I, 41/102 (40%) grade II and 13/102 (13%) grade III cancers. The great majority of patients (98/100) had no metastasis in lymph nodes. Estrogen and progesteron receptors were positive in 91 patients, while there were only 8 patients with positive HER2 tumours.

The most frequent mammographic finding was a stellate mass without calcifications, which was seen in 44/102 (43%) cancers (Table 2). Casting type calcifications were found in 17/102 (17%) cancers.

There were 28 patients younger than 50 years and Table 3 shows mammographic findings in this group of patients. The most frequent mammographic finding was a stel-

Table 4. The association between mammographic appearance and histologic type and grade of the tumor

		IDC	ILC	ITC	Gradus III	Gradus I	Gradus II
1	Mass without calcifications	**51**	**8**	**1**	**6**	**32**	**22**
	stellate	40	4		4	24	16
	round or oval	11	4	1	2	8	6
2	Mass with calcifications	**9**	**2**	**1**	**5**	**5**	**2**
	powdery	1				1	
	crushed-stone like	1		1	1	1	
	casting	7	2		4	3	2
3	Only calcifications	**12**			3	**3**	**6**
	powdery	3					3
	crushed-stone like	1				1	
	casting	8			3	2	3
4	Other	**14**	**4**			**8**	**10**
	asymmetric density	10	4			7	7
	architectural distortion	4				1	3
	Total:	**86**	**14**	**2**	**13**	**48**	**41**

IDC invasive ductal carcinoma, ILC invasive lobular carcinoma, ITC invasive tubular carcinoma

late mass without calcifications, which was seen in 10/28 (36%) cancers. Casting type calcifications were seen in 7/28 (25%) of these cancers.

Table 4 shows the distribution of mammographic findings as compared to the histological type and histological grade of 102 small breast cancers.

Invasive lobular cancers were found in 14% (14/102) of invasive small breast cancers and were mammographically seen as a mass or asymmetric density in 12/14 (86%) cases. No invasive lobular cancer was mammographically seen as only calcifications.

Table 5 shows the distribution of mammographic findings as compared to histological type and histological grade of 28 small breast cancers in women under the age of 50. There were 22/28 (79%) grade II and III tumours in this group of young patients.

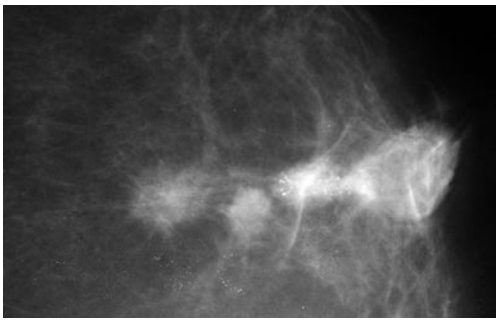

Figure 1. 48 years old women with three breast carcinomas. First stellate mass without calcifications on mammography. Histologically proven as 1cm large invasive breast carcinoma, grade 2. Second stellate mass with casting calcifications on mammography. Histologically proven as 0.9 cm large invasive breast carcinoma, grade 3. Third round mass without calcifications on mammography. Histologically proven as 0.7 cm large invasive breast carcinoma, grade 1.

Figure 1 shows mammographic appearance of three different synchronous cancers in a single woman.

Table 5. The association between mammographic appearance and histological type and grade of the tumor in women under 50 years

		IDC	ILC	ITC	Gradus II	Gradus I	Gradus III
1	Mass without calcifications	**10**	1		**1**	**1**	**9**
	stellate	9	1		1	1	8
	round or oval	1					1
2	Mass with calcifications	**5**		**1**	**1**	**3**	**2**
	powdery						
	crushed-stone like			1			2
	casting	4			1	3	
3	Only calcifications	**4**	**2**		3	**1**	**2**
	powdery	2			1		1
	crushed-stone like		1				1
	casting	2	1		2	1	
4	Other	**5**			3	**1**	**1**
	asymmetric density	4			2	1	1
	architectural distortion	1			1		
	Total:	**24**	**3**	**1**	**8**	**6**	**14**

IDC invasive ductal carcinoma, ILC invasive lobular carcinoma, ITC invasive tubular carcinoma

Discussion

The most common mammographic finding in small breast cancers (T1a and T1b) in our study was a stellate mass without calcifications. It was found in 44/102 (43%) of small breast cancers. This is consistent with results of other published series.[6-14] Additional 16/102 (16%) of small breast cancers have mammographic appearance of a round/oval mass without calcifications. Calcifications with/without mass were present in 24/102 (24%) of small breast cancers.

The important finding of our study was that the distribution of mammographic findings in small breast cancers varied with age. In the group of younger women (< 50 years) with higher breast density, a stellate mass without calcifications was still the most common mammographic finding. It was found in 10/28 (36%) of small breast cancers. However, the proportion of circular/oval shaped tumours was much smaller in this group of women. There was only a single woman (1/28) with a mammographic finding of a circular/oval shaped tumour. On the other hand, calcifications with/without mass are much more common mammographic findings in younger women. In our series, 12/28 (43%) of small breast cancers appeared mammographically as calcifications. Half (6/12) of them with a mass and half of them without it.

More importantly, the majority of calcifications were of the casting type. Tabar[6] proved by the multivariate analysis that the mammographic appearance of small breast cancers was an independent prognostic factor. In his study the mammographic appearance of casting type calcifications was more predictive of a long-term survival than clas-

Figure 2. Mediolateral oblique view of the right breast with BIRADS category 4. Mammographic finding of 0.8 cm large asymmetric density. Patologically proven as invasive ductal carcinoma grade 2.

sic prognostic factors (tumour size, histological grade and lymph node status). The 20-year survival rate was 72% for women with small breast cancers accompanied by casting – type calcifications. All other women with small breast cancers had an excellent survival regardless of lymph node status, histological grade or treatment.[6]

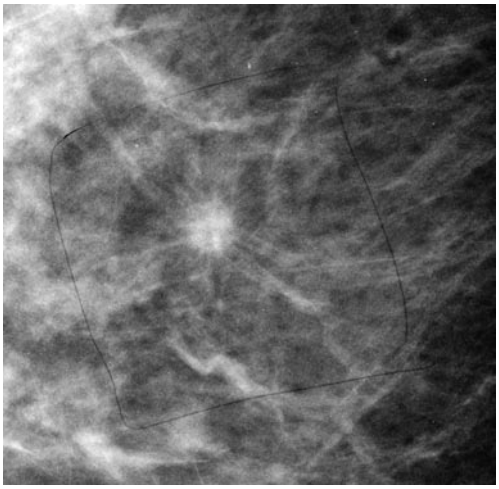

Figure 3. Stellate mass without calcifications on mammography. Histologically proven as 0.5 cm large invasive breast carcinoma, grade 2.

Casting type calcifications are associated significantly with a positive lymph node status and poorer histological grade.[6] In our series there were only two patients with lymph node metastases. Both of them had tumours accompanied by casting type calcifications. The majority of our patients with small breast cancers accompanied by casting type calcifications also had a higher histological grade (grade III in 7/15 and grade II in 5/15).

Asymmetric breast findings define as four different types: asymmetric breast tissue, densities seen in one projections, ar-

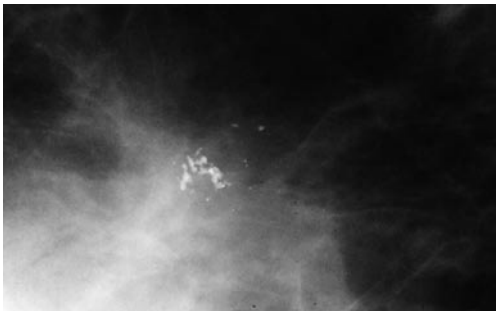

Figure 4. Crushed- stone like calcifications on mammography. Histologically 0.6 cm large invasive breast carcinoma, grade 1.

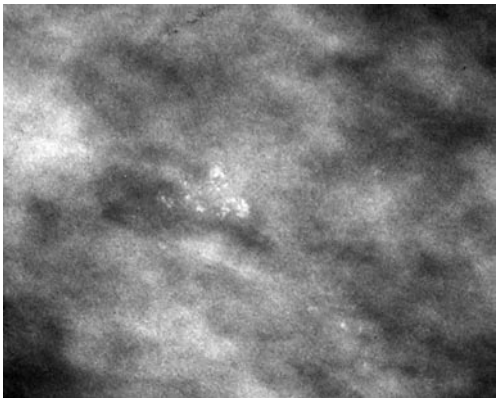

Figure 5. Powdery type of calcifications on mammography. Histologically proven as 0.4 cm large invasive breast cancer, gradus 1.

chitectural distortion, and focal asymmetric densities.[8,9] We have observed an architectural distortion (a focal area of breast tissue appears distorted with no definable central mass) and a focal asymmetric density also in our study. From 102 small breast cancers, 14 (14%) were seen as a focal asymmetric density and 4 as an architectural distortion. Interestingly, 4/14 (26%) of focal asymmetric density proved histologically to be invasive lobular cancers. Invasive lobular cancers accounts for 5-10% of all breast cancers and can often manifest as an area of distortion or asymmetry.[10] In our series we found 14% of invasive lobular cancer, that in 86% appeared as spiculated mass or focal asymmetric density. There was no case of an invasive lobular cancer which would appear mammographically as calcifications only. This is in agreement with results of Tjurfjell.[13]

Samardar[15] defined that palpable mass associated with a focal area of breast asymmetry or architectural distortion is very often malignant. We found in our series only 20 palpable small breast cancers and they all appeared mammographically as a mass with/without calcifications.

Conclusions

Most of the T1a and T1b breast cancers are nonpalpable. The most common mammographic finding in these cancers is stellate mass without calcifications. Calcifications are more frequent mammographic findings in younger patients. Fourteen % of small breast cancers appear mammographically as a focal asymmetric density. Invasive lobular cancer never appears mammographically as calcifications only.

References

1. Primic Zakelj M. Cancer incidence in Slovenia 2005. Ljubljana: Institute of Oncology Ljubljana. Cancer Registry of Slovenia; 2008.

2. Fletcher SW, Elmore JG. Clinical practice. Mammographic screening for breast cancer. *N Engl J Med* 2003; **348:** 1672-80.

3. Leitch AM, Dodd GD, Costanza M, Linver M, Pressman P, McGinnis L, et al. American Cancer Society guidelines for the early detection of breast cancer: update 1997. *CA Cancer J Clin* 1997; **47:** 150-3.

4. Tabar L, Vitak B, Chen HH, Prevost TC, Duffy SW. Update of the Swedish Two-County Trial of breast cancer screening: histologic grade-specific and age-specific results. *Swiss Surg* 1999; **5:** 199-204.

5. Barth RJ, Jr., Gibson GR, Carney PA, Mott LA, Becher RD, Poplack SP. Detection of breast cancer on screening mammography allows patients to be treated with less-toxic therapy. *Am J Roentgenol* 2005; **184:** 324-9.

6. Tabar L, Tony Chen HH, Amy Yen MF, Tot T, Tung TH, Chen LS, et al. Mammographic tumor features can predict long-term outcomes reliably in women with 1-14-mm invasive breast carcinoma. *Cancer* 2004; **101:** 1745-59.

7. Rissanen TJ, Makarainen HP, Mattila SI, Karttunen AI, Kiviniemi HO, Kallioinen MJ, et al. Wire localized biopsy of breast lesions: a review of 425 cases found in screening or clinical mammography. *Clin Radiol* 1993; **47:** 14-22.

8. Obenauer S, Hermann KP, Grabbe E. Applications and literature review of the BI-RADS classification. *Eur Radiol* 2005; **15:** 1027-36.

9. Kocijancic I, Rener M, Vidmar K. Simultaneous occurence of fat necrosis and carcinoma after breast injury in a traffic accident. *Eur J Ultrasound* 2000; **11:** 213-6.

10. Burrell HC, Pinder SE, Wilson AR, Evans AJ, Yeoman LJ, Elston CW, et al. The positive predictive value of mammographic signs: a review of 425 non-palpable breast lesions. *Clin Radiol* 1996; **51:** 277-81.

11. Franceschi D, Crowe JP, Lie S, Duchesneau R, Zollinger R, Shenk R, et al. Not all nonpalpable breast cancers are alike. *Arch Surg* 1991; **126:** 967-70.

12. Sickles EA. Mammographic features of 300 consecutive nonpalpable breast cancers. *Am J Roentgenol* 1986; **146:** 661-3.

13. Thurfjell MG, Lindgren A, Thurfjell E. Nonpalpable breast cancer: mammographic appearance as predictor of histologic type. *Radiology* 2002; **222:** 165-70.

14. Tinnemans JG, Wobbes T, Holland R, Hendriks JH, Van der Sluis RF, Lubbers EJ, et al. Mammographic and histopathologic correlation of nonpalpable lesions of the breast and the reliability of frozen section diagnosis. *Surg Gynecol Obstet* 1987; **165:** 523-9.

15. Samardar P, de Paredes ES, Grimes MM, Wilson JD. Focal asymmetric densities seen at mammography: US and pathologic correlation. *Radiographic*s 2002; **22:** 19-33.

case report

Obliterative hepatocavopathy – ultrasound and cavography findings

Ramazan Kutlu

Department of Radiology, Inonu University School of Medicine, Malatya, Turkey

Backgound. *Obliterative hepatocavopathy is a relatively new term for the definition of primary inferior vena cava thrombosis and membranous obstruction of inferior vena cava that were included in Budd-Chiari syndrome.*

Case report. *In this report, cavography and ultrasound findings of a case with a complete occlusion of inferior vena cava in a 36 year-old female patient who has been followed up with the diagnosis of hepatitis B related cirrhosis for 5 years were presented.*

Conclusions. *Although this disease classically treated by surgery (e.g. portal or mesenteric–systemic shunting, liver transplantation), also interventional radiology procedures e.g. transjugular intrahepatic portosystemic shunting, percutaneous hepatic vein angioplasty and/or stent placement), now play an important role in the management[4].*

Key words: obliterative hepatocavopathy; cavography; ultrasound; inferior vena cava

Introduction

The complete inferior vena cava (IVC) obstruction develops as a result of primary IVC thrombosis.[1] Although in the earlier literature this entity was included in Budd-Chiari syndrome, obliterative hepatocavopathy (OH) is currently being used to define this condition.[1] In this report, we present cavography and ultrasound features of this rare entity in a 36 year-old female patient.

Received 20 September 2008
Accepted 28 October 2008

Correspondence to: Assoc. Prof. Ramazan Kutlu, M.D., PhD, Department of Radiology, Inonu University School of Medicine, Turgut Ozal Medical Center, 44069 Malatia, Turkey. Phone: +90 422 341 0660 (Extn: 5703); Fax: +90 422 341 0834 (Attn: Dr. Ramazan Kutlu); E-mail: rkutlu@inonu.edu.tr

Case report

A 36 year-old female patient who has been followed with the diagnosis of chronic liver disease (Child B, score 7) due to hepatitis B for 5 years was referred to our radiology department for portal Doppler evaluation. She had splenomegaly and moderate ascites. Upper gastrointestinal endoscopy revealed esophageal varices. She had been receiving beta blockers and diuretics. Her CA-125 level was found to be increased (234 U/mL).

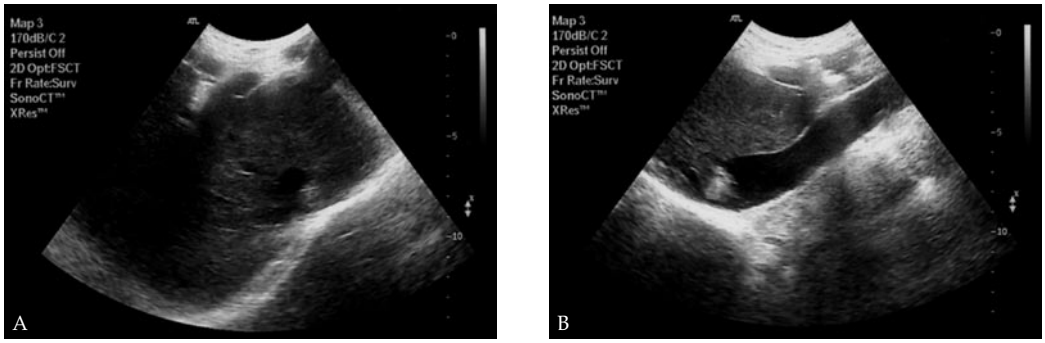

Figure 1. Gray scale axial (A) and sagittal (B) US images show hyperechoic, solid material at the posterolateral part of distal IVC.

Gray scale (Figure 1 A,B) and Doppler (Figure 2 A-C) US examinations showed compressed hepatic veins, hepatopedal portal flow, and no blood flow into the right atrium through distal IVC which was thrombosed. The abdominal CT examination revealed the absence of intrahepatic portion of IVC. The patient didn't undergo MR examination due to claustrophobia. Cavography was performed using right femoral vein access. Firstly, a large vein was erroneously accessed and a test injection before introducer placement demonstrated that this vein was a large collateral vein extending to the right side of the body and ultimately draining to the intercostal, pericardiophrenic and right subclavian vein (Figures 3 A-E). Secondly, the right femoral vein was catheterized and inferior cavography revealed a complete occlusion of distal 4 cm of IVC connecting to the right atrium and retrograde flow into the prominent collaterals in the late series (Figures 4 A,B). The selective catheterization of the hepatic veins showed hepatic vein confluence and weak filling (Figure 5A) and a small vein below hepatic confluence draining to IVC (Figure 5B). Superior vena cavography

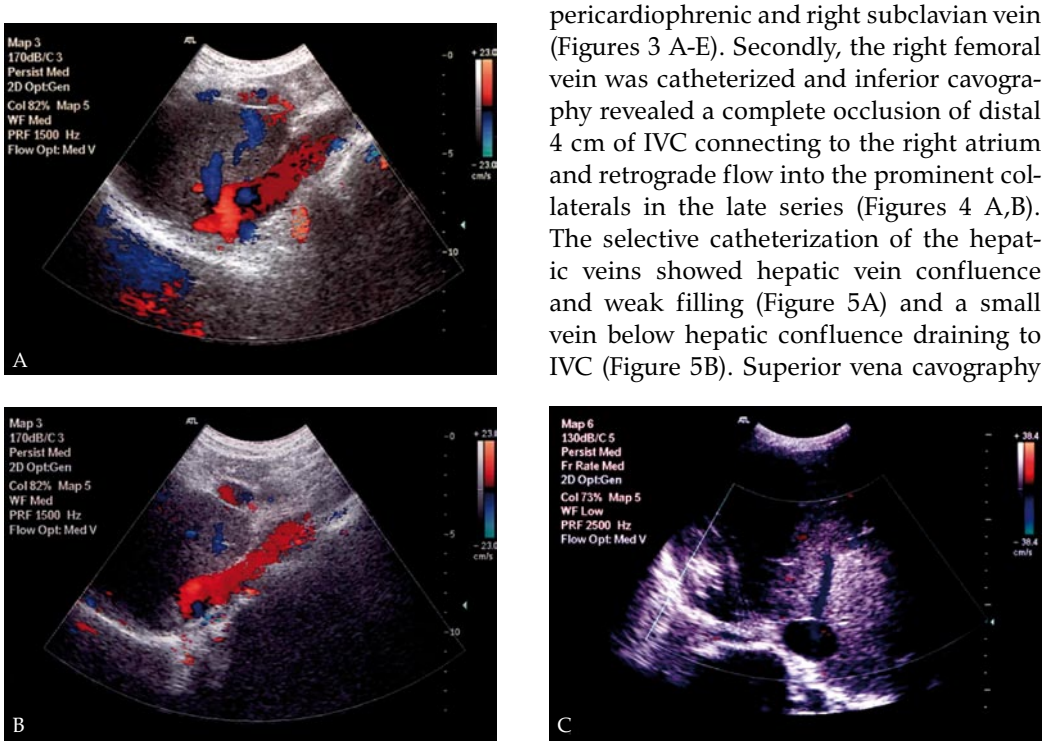

Figure 2. Sagittal (A, B) Doppler US images slight filling of hepatic vein and complete occlusion of distal IVC. Subcostal oblique image (C) reveals a relatively small hepatic vein below the hepatic confluence.

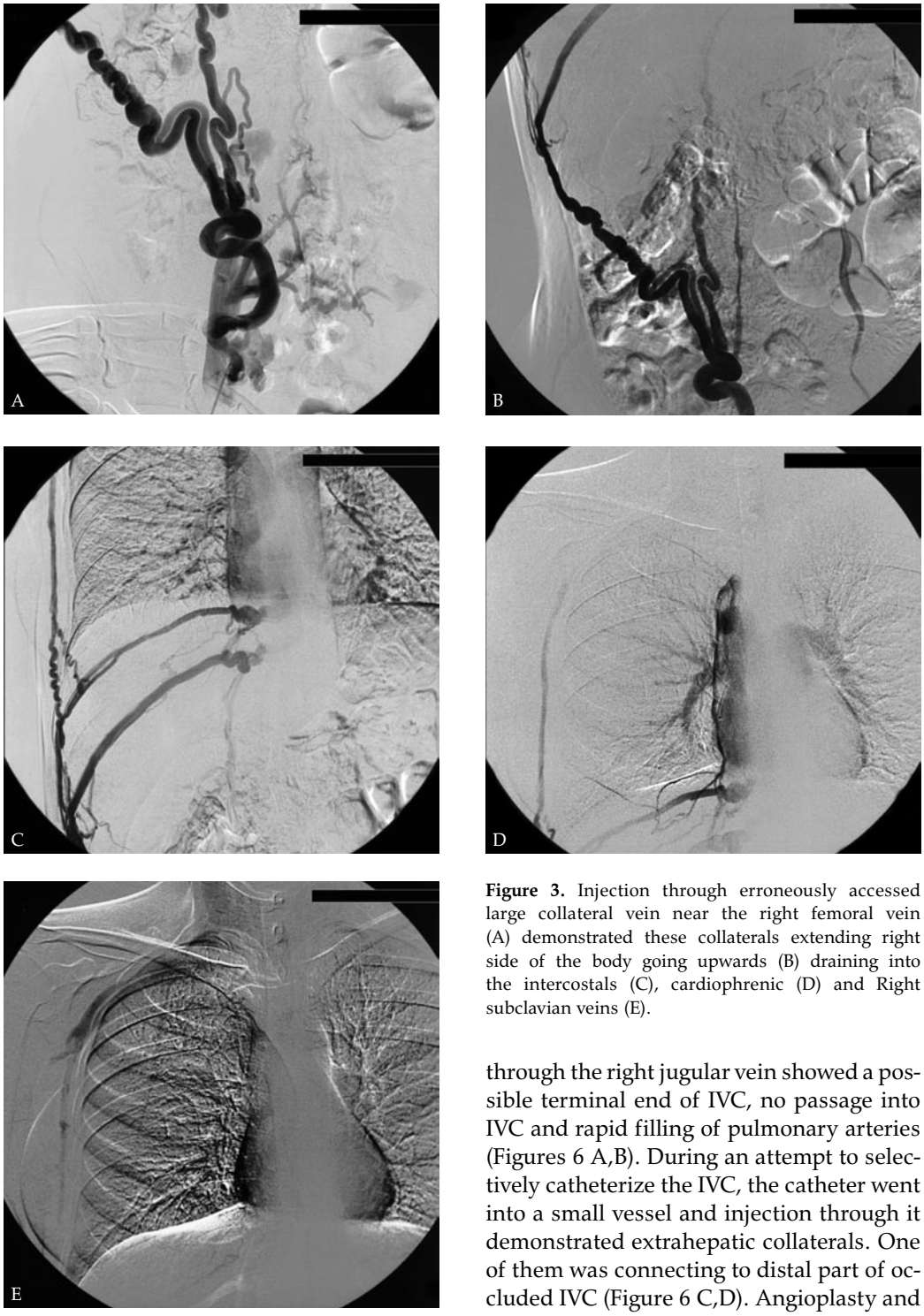

Figure 3. Injection through erroneously accessed large collateral vein near the right femoral vein (A) demonstrated these collaterals extending right side of the body going upwards (B) draining into the intercostals (C), cardiophrenic (D) and Right subclavian veins (E).

through the right jugular vein showed a possible terminal end of IVC, no passage into IVC and rapid filling of pulmonary arteries (Figures 6 A,B). During an attempt to selectively catheterize the IVC, the catheter went into a small vessel and injection through it demonstrated extrahepatic collaterals. One of them was connecting to distal part of occluded IVC (Figure 6 C,D). Angioplasty and

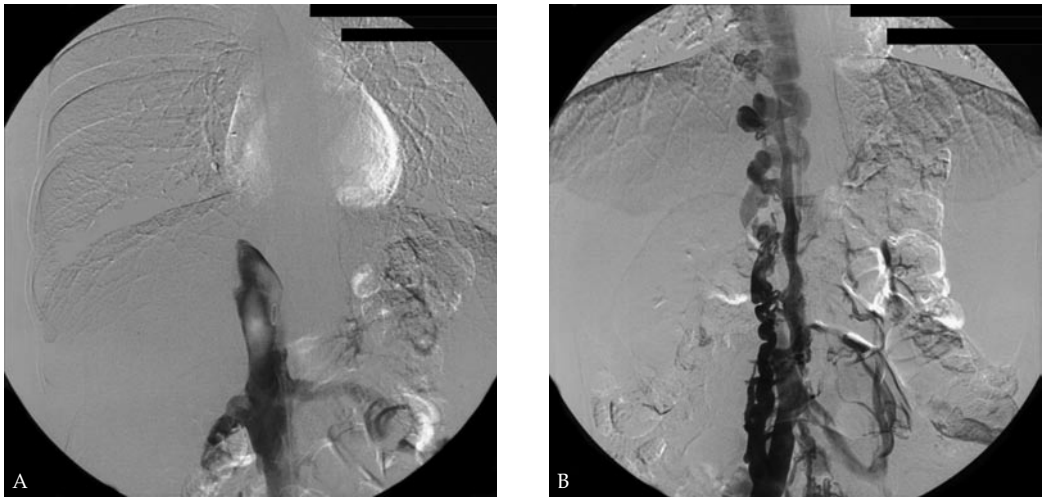

Figure 4. Cavography performed with 6F pigtail catheter which could not passed into right atrium showed complete occlusion of distal IVC (A). Due to downward flow in the late series, markedly dilated and tortuous paraspinal collaterals were seen (B).

stent placement were considered but the patient did not accept the intervention.

Discussion

OH is a relatively new term proposed to define primary IVC thrombosis and membranous obstruction of the IVC.[1] These two conditions were included in Budd-Chiari syndrome which was defined as hepatic venous outflow obstruction at any level from the small hepatic veins to the junction of the IVC and the right atrium, regardless of the cause of obstruction.[2] Occlusion and stenosis of the IVC are squeals of primary IVC thrombosis.[1] Although the majority of these cases are idiopathic, as in our case,

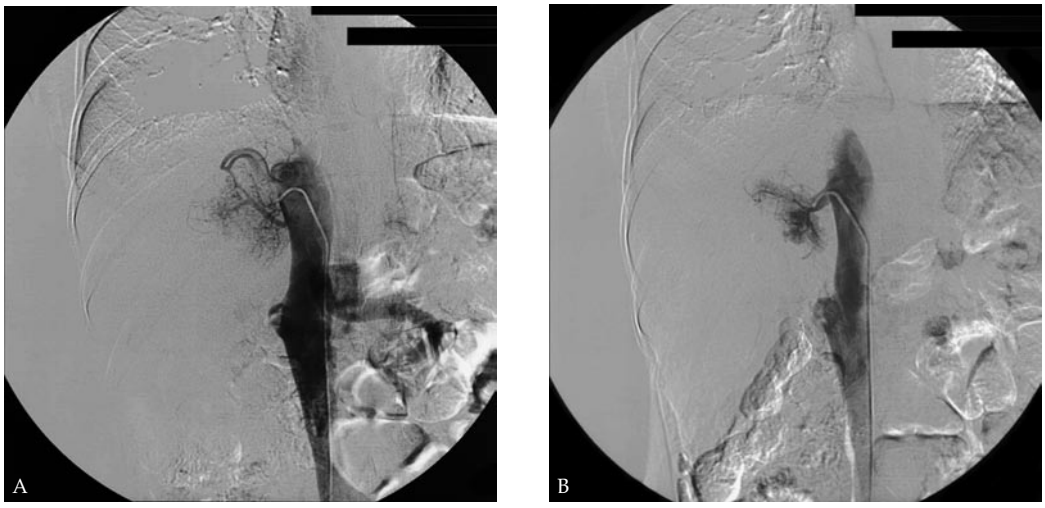

Figure 5. Selective hepatic vein injection showed a part consistent with hepatic vein confluence and tangle of vessels in the area of hepatic veins (A) and a small vein that had been seen during Doppler examination (B).

Figure 6. Superior venacavogram through introducer in right jugular vein shows no passage into IVC (A) and rapid filling of pulmonary arteries (B). Selective catheterization with a multipurpose catheter shows extrahepatic collaterals and filling of pulmonary arteries due to backflow (C), and in the later phases collateral connecting to occluded distal IVC appears and than IVC fills.

thrombotic or hypercoagulable conditions (like coagulation factor deficiency or mutation, myeloproliferative disorders, oral contraceptive use, pregnancy etc) could be observed in OH.[1] If all hepatic veins become occluded, blood is coming from hepatic artery drain into either portal veins or collateral vessels. Retrograde flow in the portal vein occurs and portocaval shunts develop. As the occlusion progresses, blood circulation changes appear in and around liver. Intrahepatic or subcapsular hepatic venous collaterals are a distinctive feature of Budd–Chiari syndrome.[2,3] In complete IVC obstruction, large shunts form between the IVC and the ascending lumbar vein continuous with the azygos and hemiazygos veins or paravertebral veins. The increased pressure in the ascending lumbar/hemiazygos and azygos veins may result in retrograde flow in the intercostal and subcutaneous veins.

Due to mainly difficulties in the differential diagnosis of primary hepatic vein thrombosis and primary IVC thrombosis, the epidemiology of primary IVC thrombosis is not well established and adults are affected more frequently, but OH could be seen at any age.[1] The clinical presentation is acute and very serious like in the case of vena cava superior sindrom.[1,4] Hepatomegaly, ascites, abdominal pain, fever and leg oedema appear quite fast, but the clinical course could be chronic with repeated acute episodes characterized by ascites, hepatomegaly, and pain.[1] Due to the circulatory disturbances caused by IVC obstruction, patients commonly show marked venous dilatation over the body trunk.[1] Our case had no visible venous dilatation over the body trunk possibly due to the collateral between occluded distal IVC and right atrium.

The radiological imaging provides a definitive diagnosis of OH. In addition to demonstrating thrombus within the IVC and hepatic vein problems, ultrasonography also demonstrates caudate lobe enlargement, splenomegaly, ascites, stenotic veins, membrane, intrahepatic collateral veins connecting with enlarged hepatic veins, vein to-vein anastomoses, a patent and enlarged inferior right hepatic vein opening into the IVC, and absence of normal respiratory changes in the IVC. Doppler US could delineate flow disturbances and direction. CT and MRI assess hepatomegaly, ascites, enlarged caudate lobe, splenomegaly, collateral vessels, and the thrombus occluding the IVC. MRI depict the level of an obstructing membrane or web within the IVC.[1] Hepatic venography delineates occluded veins, slow flow in attenuated venous branches, and rapid shunting into the portal vein. Additionally, wedged hepatic venography will demonstrate the "spider's web" network.[1] Cavography is one of the most important imaging modality in the evaluation of IVC obstruction. It confirms the level of obstruction, occluding thrombus, mural thrombosis, membrane, and extrahepatic collateral vessels.[1] Based on cavography findings three types of IVC obstruction were defined; type I, a thin membrane is present in the vena cava, type II, there is an absent segment of the IVC of variable length, type III, the vena cava is not visualized, and only dilated collateral channels are demonstrated.[2] According to this classification, our case appears to be type II.

Although this disease classically treated by surgery (e.g. portal or mesenteric-systemic shunting, liver transplantation), interventional radiology procedures e.g. transjugular intrahepatic portosystemic shunting, percutaneous hepatic vein angioplasty and/or stent placement also plays an important role in the management – like in the others severe vascular complicated cases.[3,5,6]

References

1. Okuda K. Inferior vena cava thrombosis at its hepatic portion (obliterative hepatocavopathy). *Semin Liver Dis* 2002; **22:** 15-26.

2. Sakamoto N, Koizumi K, Asahina Y, Tazawa J, Maeda M, Marumo F, et al. Primary Budd-Chiari syndrome due to complex venous anomalies. *Abdom Imaging* 1997; **22:** 499-501.

3. Janssen HL, Garcia-Pagan JC, Elias E, Mentha G, Hadengue A, Valla DC; European Group for the Study of Vascular Disorders of the Liver. Budd-Chiari syndrome: a review by an expert panel. *J Hepatol* 2003; **38:** 364-71.

4. Vodvářka P, Števerák P. Algorithm for percutaneous stenting in patients suffering from superior vena cava syndrome. *Radiol Oncol* 2000; **34:** 349-55.

5. Wu T, Wang L, Xiao Q, Wang B, Li S, Li X, et al. Percutaneous balloon angioplasty of inferior vena cava in Budd-Chiari syndrome-R1. Int J Cardiol 2002; **83:** 175-8.

6. Gjikolli B, Hadžihasanović B, Jaganjac S, Herceglija E, Nikšić M, Hadzimehmedagić A, et al. Treatment of complicated case with subclavia steal syndrome and stenosis of common iliac artery. *Radiol Oncol* 2008; **42:** 1-12.

case report

Gastric gastrointestinal stromal tumour

Ivan Žokalj[1], Renata Čulinović-Čaić[2], Zvonimir Magaš[2], Zlatko Pavčec[1], Hussein Saghir[1], Jasminka Igrec[1], Miljenko Marotti[3]

[1]Department of Radiology and Ultrasound, County Hospital Čakovec, Croatia;
[2]Department of Surgery, County Hospital Čakovec, Croatia
[3]Department of diagnostic and interventional radiology, University Hospital "Sisters of Mercy", Zagreb, Croatia

Background. *Gastrointestinal stromal tumours (GISTs) are the most common mesenchymal tumours of the digestive tract. These tumours can not be simply divided into benign and malignant forms. There is a continuum from benign to malignant forms. The tumour size and mitotic activity have strong influence on GISTs behaviour. Tumour behaviour also varies according to the site of the origin. The site of the tumour origin can be anywhere along the digestive tract, in the mesentery or omentum. GISTs are mainly benign tumours, about 70-80%, usually found in the gastric wall. We report a case of 70-year old female with gastric form of GIST.*

Case report. *The patient has undergone abdominal ultrasound (US) because of a palpable lump in the epigastrium, which mainly revealed hyperechogenic round mass with small hypoechogenic areas in the central part. On the abdominal computed tomography (CT) a large expansive mass with heterogeneous structure was depicted in the gastric wall. The mass had higher attenuation coefficients on the periphery and lower in the central part. During the surgery the large exophytic tumour of the gastric wall has been found. The diagnosis of gastric GIST has been obtained after the patohistologic and imunohistochemical analysis.*

Conclusions. *Gastrointestinal stromal tumours may be the statistically rare tumours (0.1%-0.3% of all gastrointestinal tumours) but when we have the patient with a round, mainly exophytic mass on the wall of the gastrointestinal tract or peritoneum, GIST must be taken into consideration. Cross-sectional imaging methods like US and CT allow the preoperative diagnosis of the tumour and staging.*

Key words: gastrointestinal stromal tumours; computed tomography

Received 3 November 2008
Accepted 18 November 2008

Correspondence to: Ivan Žokalj, MD, Department of Radiology and Ultrasound, County Hospital Čakovec, Ivana Gorana Kovačića 1e, 40000 Čakovec, Croatia. Phone: +385 40 375 297; E-mail: ivan.zokalj@ck.t-com.hr

Introduction

Gastrointestinal stromal tumours (GISTs) are currently defined as mesenchymal tumours of the gastrointestinal tract, mainly KIT (CD117)-positive.[1] These tumours usually affect the population over 50 years, rarely patients younger than 40 years of age, and are extremely rare in the child-

hood.[1-3] The frequency of GISTs is about 10 to 20 cases per million persons, according to the Miettinen and Lasota.[4] GISTs can arise anywhere through the gastrointestinal tract but they can also occur in the *omentum*, mesentery and *retroperitoneum* as a primary tumour. In 70% of cases GISTs arise in stomach, the second most frequent site is small intestine (20-30%). Other less frequent sites are anus, rectum, colon and oesophagus.[4] GISTs of gastrointestinal tract commonly arise in the *muscularis propria* of the stomach or intestinal wall, usually in the outer muscular layer. That is the reason why GISTs have an exophytic growth pattern in majority of the cases and usually manifest themselves as large extraluminal abdominal masses. Clinical features of GISTs depend on the size and anatomic location of the tumour. They can be presented with mild signs and symptoms of anaemia caused by occult bleeding in the gastrointestinal tract or they can have a dramatic picture with *hematemesis*, *melena*, abdominal pain and signs of intestinal obstruction.[5,6]

Histogenetically gastrointestinal stromal tumours probably originate from interstitial cells of Cajall (or the native KIT-positive gut pacemaker cell) which intermediates between the GI autonomic nervous system and smooth muscle cells regulating GI motility and autonomic nerve function. This postulate is made on the expression of KIT on GISTs tumour cells.[1,7]

Larger forms of GISTs are usually centrally cystic, positioned extraluminally, while smaller GISTs are subserosal and intramural solid tumours, rarely polypod intraluminal ones.[1] GISTs can generally be divided into three groups: spindle cell type (70%), epithelioid type (20%) and mixed spindle and epithelioid cel type.[7] Gastric GISTs can be histologically divided into two groups, four spindle cell subtypes (sclerosing spindle cell, palisaded-vacuolate spindle cell, hypercellular spindle cell, sarcomatous spindle cell) and four epitheloid subtypes (sclerosing epithelioid GIST with syncytitial pattern, epitheloid GIST with dyscohesive pattern, hypercellular epitheloid GIST, sarcomatous epitheloid GIST). Sarcomatous subtype is highly cellular form of GIST with a marked mitotic activity (more than 20 per 50 HPFs).[9] The most important feature for immunohistochemical differentiation between GISTs and other similar soft-tissue tumours are the antigens on the surface of the tumour cells, especially KIT tyrosine kinase receptor (CD117) which has been found in more than 95% of GISTs. There are other antigens which are less specific for GISTs but are commonly expressed, like CD34 and nestin. GISTs sometimes express smooth muscle cell markers (like smooth muscle cell actin-SMA), but are usually negative for desmin, the muscle type intermediate filament protein.[1] KIT imunoreactivity has shown to be very useful in the treatment of GISTs with immunotherapy as well as in diagnostics. The immunotherapy of GISTs is based on targeting of tyrosine kinase receptors with a selective KIT-tyrosine kinase inhibitor (STI-571, imatinib mesylate). The drug acts as a selective c-kit blocker.[6]

The contrast-enhanced computed tomography (CT) is currently widely available diagnostic imaging method and the imaging modality of choice for patients with abdominal mass suspected for GISTs.[7]

The standard initial treatment for GISTs, even in non-resectable cases, is the surgical treatment. Some authors propose the immediate treatment with imatinib for unresectable and/or metastatic disease.[8]

Case report

A 70-year old female patient underwent abdominal ultrasound (US) because of pal-

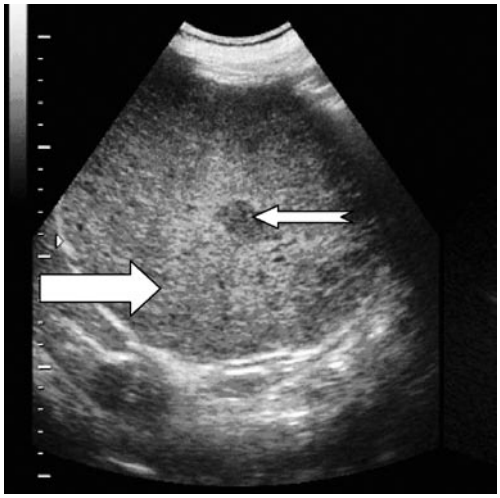

Figure 1. Abdominal ultrasound – axial plain. Large round hyperechogenic expansive mass (white arrow) with small hypoechogenic areas in the central part (white notched arrow).

pable mass in the upper abdomen. The patient suffered from inapetency without vomiting and weight loss, hematemesis or melena. US revealed a large round hyperechogenic expansive mass with small hypoechogenic areas in the central part. There were no signs of focal lesions in parenchymal abdominal organs or lymphadenopathy (Figure 1).

The next step in diagnostics was computed tomography (CT) of the abdomen, performed with three postcontrast phases and distension of gastrointestinal (G-I) tract with 1000ml of water. CT depicted a large intraperitoneal mass in the upper abdomen, ventrally placed and sharply demarcated from surrounding structures except from stomach. The lesion had a heterogeneous structure on native and postcontrast scans with higher attenuation coefficients on periphery and lower in the central part (about 30HU on precontrast and 60HU on postcontrast scans). There were no significant changes in attenuation values centrally between precontrast and all series of postcontrast scanns. No lymphadenopathy or focal lesions in the parenchymal organs have been found. The working (imaging) diagnosis of mesenchymal tumour of the stomach wall (probably GIST) has been established (Figure 2).

The upper G-I tract follow through with barium showed elongated stomach with sharply demarcated contours and concavely impressed lesser curvature (Figure 3).

The patient has been treated surgically with a complete gross resection. During the explorative laparatomy a large tumour in the upper abdomen with origins on the lesser curvature of the stomach without lymphadenopathy has been found (Figure 4).

The material obtained during surgery has been sent to the pathohystologic analysis and immunochemical evaluation. The gross pathologic feature of the specimen was an encapsulated mass of medium firm consistency, measuring 18 cm in largest diameter. On cut section the tumour was whitish and greyish with dispersed areas of swirling structure. Predominant histological features were spindle shaped cells with scant cytoplasm and big nucleus without nucleolus. The tumour cells formed swirling structures and tracks. Focal areas of degeneration and small areas of tumour tissue necrosis were found.

Three mitoses per 50 consecutive high power fields (HPF) have been detected.

The immunohistochemical analysis showed that the tumour cells were CD117(C-kit), CD 34 and BCL2 positive, SMA -/+ and S-100 negative. The diagnosis of gastrointestinal stromal tumour was established.

Discussion

GIST is usually placed in the stomach and small intestine. The gastric form is especially common between other possible locations, 50 to 70% of GISTs are located in the stomach, 33% of cases in the small

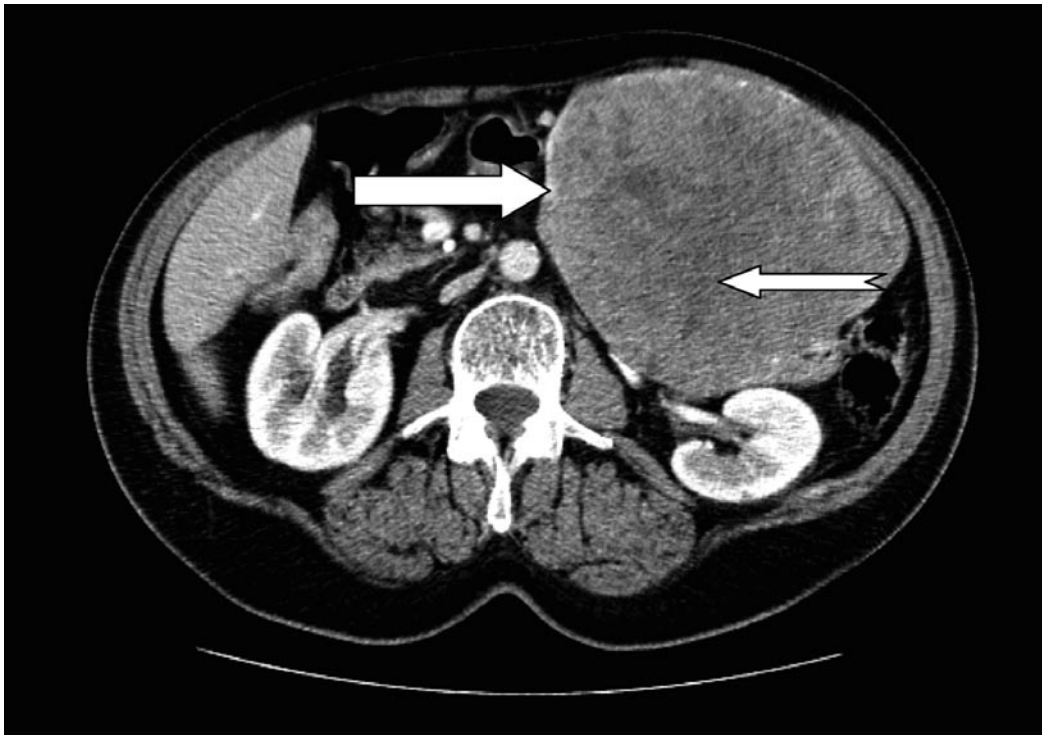

Figure 2. Abdominal CT post-contrast axial scan. Large round expansive mass in the upper abdomen with heterogeneous structure sharply demarcated from surrounding structures depicted on this scan. Higher attenuation coefficients on periphery (white arrow) and lower in the central part were detected on native and postcontrast scans (white notched arrow).

intestine, 5 to 15% in rectum and colon and only 1 to 5% in oesophagus.[2,10] GISTs can originate outside of the gastrointestinal wall, in mesentery or peritoneum in 10% of cases, but they are extremely rare retroperitoneally. Both sexes are equally affected by GISTs, commonly between 40 and 70 years. The small intestine GISTs are usually more aggressive and have a more grave prognosis than GISTs which originate in other segments of G-I tract.[3,11]

The factors that worsen the prognosis of GISTs are location (all extragastric locations), size of the tumour (bigger than 5cm), advanced age of the patient, metastasis at the time of tumour manifestation, tumour tissue necrosis and high mitotic index (more than five mitosis per 50 high-power fields).[4,10,11] In 10 to 30% of GISTs malignant forms have been diagnosed.[4] The two most important factors that influence GISTs prognosis are the tumour size and mitotic index. Currently it is believed that only tumours with diameter smaller than 1 cm can be considered as definitely benign on clinicopathologic features.[12] The patient presented in this report has few bad prognostic factors, age of 70 years and the tumour largest diameter of 18 cm.

Clinical features of GISTs depend on the tumour size and anatomic location of the tumour, they can be mild signs and symptoms of anaemia caused by occult bleeding in the gastrointestinal tract or dramatic picture with hematemesis, melena, abdominal pain and signs of intestinal obstruction.[5] GIST of the stomach, small and large intestine and anorectum usually manifest with gas-

trointestinal bleeding from mucosal ulcerations. The other common clinical features are abdominal pain, nausea, dysphagia, vomiting, weight loss and palpable abdominal mass.[13,14] The leading clinical feature of the case presented in this article was palpable abdominal mass in the epigastrium. G-I tract obstruction can be manifested in 10 to 30% of cases, usually in the cases of the small intestine GIST. The biliary tract and the renal obstruction may be the clinical feature of the duodenal GIST.[13,15]

The tumour is usually covered with an affected organ serosa. In the cases of the surrounding structures infiltration by the GIST the primary tumour has more often smooth and broad pushing than insinuating fascicles. The typical location of the first recurrence of GIST is in the abdomen. Liver is the most common metastatic site, in 65% of cases. The lung and bone metastases usually develop later than liver metastases. Lymph node metastases are very rare for the difference to lymphoma and leiomyosarcoma.[1,12,16]

Computed tomography (CT) and magnetic resonance imaging (MRI) are used for the radiologic diagnostic evaluation of patients with abdominal mass suspected for GIST. Contrast-enhanced CT is currently an imaging method of choice for diagnosing of GISTs, staging and surgical planning because of its wide availability. Endoscopic ultrasound can be used for the evaluation of the local extent in patients with small tumours which have been found incidentally during endoscopy. MRI is a better imaging method for the evaluation of patients with rectal GISTs. MRI is indicated for the evaluation of liver lesions which can not be characterized definitely on CT scans and in cases of contrast-enhance CT is contraindicated.[8,17,18] The factors that influence CT features of GISTs are size of the tumour, aggressiveness of the tumour and time of presentation during the course of the disease.[18] The typical CT finding of primary GIST is a large mass with heterogeneous structure because of usually centrally placed necrosis, haemorrhage, or cystic degeneration. In fact, the tumour can be so large that it is difficult to define its origin. On postcontrast scans the tumour is usually presented as a hypervascular and well-enhancing heterogeneous mass. Ulceration and fistulisation to the lumen of GI tract are often seen in GIST patients. Small GISTs are commonly presented as homogenous masses.[18] MRI can be used to follow-up the operated patients and to evaluate response in the patients on an adjuvant therapy with imatinib. Fluorine-18-fluorodeoxyglucose (FDG) positron emission tomography (PET) is recommended in patients on imatinib therapy which need an early detection of tumour response to imatinib because of the possibility for the surgical resection after the cytoreduction with imatinib.[17] There is no need to perform PET scan in every GIST patient after the complete surgical resection of the tumour. PET can be performed

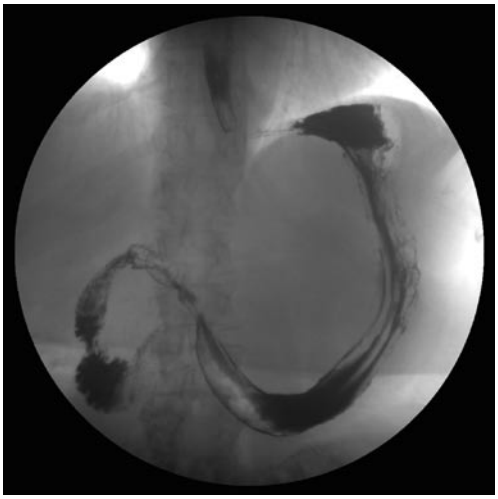

Figure 3. Upper gastrointestinal tract follow through with barium – anteroposterior projection – elongated stomach with sharply demarcated contours and concavely impressed lesser curvature.

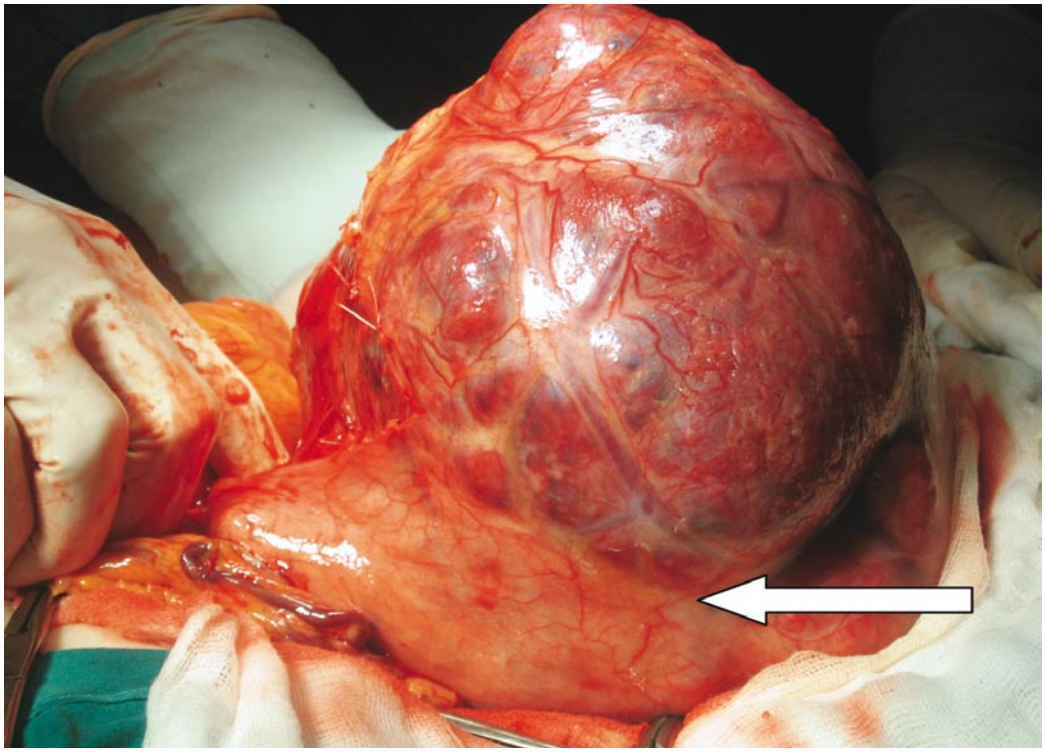

Figure 4. Explorative laparatomy – a large tumour in the upper abdomen with origins on the lesser curvature of the stomach (white arrow).

on patients with CT or /and MRI images suspected for metastases.[8,17,18]

The imaging diagnosis of GIST can be suggested when CT depicts a large, mainly extraluminal tumour arising from the stomach or small bowel wall with heterogeneous contrast material enhancement (with higher attenuation coefficients peripherally and lower coefficients in the central part). Metastases are usually presented in the liver and on the peritoneum, but a lymph node enlargement is very rarely depicted.[18,19,20] A triphasic CT scanning technique with scanning of the native scans and post-contrast scans after the intravenous injection of contrast material in an arterial and a porto-venous phase with delays of 20-30 s and 70-80 s, respectively, is preferred for baseline scans and follow-ups during and after the treatment.[17,18]

Unlike GISTs, lymphomas usually cause lymph node enlargement and circumferential bowel wall thickening which homogenously enhances on post-contrast scans. Carcinoid tumours commonly arise in the terminal ileum often stimulating a desmoplastic reaction with calcifications. A local infiltration and a visceral obstruction are common radiologic features of the carcinoma, very often in large tumours. Metastases of the bowel wall are usually multifocal masses in patients with a history of primary known malignancy.[18,20,21]

It is still difficult to make a differentiation between GIST and other soft-tissue tumours like leiomyosarcoma, intraabdominal fibromatosis of the bowel wall, malignant tumours of nerve sheath and the tumours of vascular origin with radiological and pathological methods.[21]

Pathohystology accomplished with immunohystochemistry still remain the gold standard for diagnosing of GIST. The transabdominal biopsy is not recommended because of the possibility of seeding the tumour cells.[16]

GISTs are commonly positive for KIT (CD117), a tyrosine kinase growth factor receptor. KIT positivity is usually strong and pancytoplasmic, but some epithelioid forms of GISTs of the stomach may be weakly CD117 positive or even negative.[1] We must be aware and analyse the KIT positivity together with other clinical signs, imaging method findings and immunohistochemical test results because there are few other tumours which are generally CD117 positive like small cell carcinoma of the lung, mastocytoma, seminoma and extramedullary myeloid tumour. Tumours like metastatic melanoma, clear cell sarcoma, Ewing sarcoma family of tumours, childhood neuroblastoma and angiosarcoma also sometimes express CD 117.[22]

Among other GIST markers CD34, the hematopoetic progenitor cell antigen plays an important role because it can be found in 80 to 85% of gastric GISTs and 50% of small intestinal GISTs. CD34 is usually expressed on endothelial cells, subsets of fibroblasts and neoplasms related to these cell types.[9] Small intestinal GISTs more often than gastric GISTs express muscle cell markers like SMA. Smooth muscle fibers can be interspersed with SMA and desmin positive GIST intratumoral spindle cells during the infiltration of tumour; in this situation we can have a false muscle marker positivity. The SMA positivity is a favourable prognostic factor for the gastric and small intestinal forms of GIST. The detection of S100 protein is relatively rare in GISTs, it seems to be an adverse prognostic factor in gastric GISTs.[1,9] Nestin is a type VI intermediate filament protein typical of many stem cells which can be found in most of the cases of GISTs but also in GI schwanomas.[23]

The surgical resection is the standard initial treatment for GISTs. Until the beginning of an application of imatinib (the specific tyrosine kinase inhibitor) in GIST therapy, surgery was the only way of the treatment because the conventional chemotherapy and the radiation therapy proved inefficient. Generally speaking about 85% of patients with primary localized form of GIST, they can be treated with a complete gross resection, but approximately 50% of those patients develop the tumour recurrence.[12] The patient presented in this article was treated with a complete resection of the tumour. The application of imatinib mesylate for the GIST treatment was a successful introduction of molecularly targeted therapy for the treatment of solid tumours. The imatinib therapy is used for the treatment of unresectable cases, recurrent or metastatic cases. Surgery or ablative modalities can be used when the disease becomes amenable to gross resection due to changes initiated by imatinib, or when the tumour develops resistance to imatinibe treatment.[8,12] The evaluation of the GIST treatment with imatinib mesylate is usually performed with CT, sometimes with ^{18}FDG-PET. The problem in the evaluation of the GIST treatment with imatinib mesylate is that they correlate poorly with currently internationally agreed classifications for the evaluation of response to the treatment of solid tumours like the World Health Organization criteria or the Response Evaluation Criteria in Solid Tumors (RECIST) criteria. It is suggested that changes in tumour density on CT scans are better modes of assessment of the response to the imatinib treatment than an internationally agreed guidelines. The minority of patients with GIST, less than 15%, have a primary resistance to imatinib mesylate. Half of the patients will develop resistance 2 years after the initiation of the

imatinib treatment, usually because of the secondary KIT mutation.[12] Generally, the median time of recurrence of GISTs after the surgery is 19 to 25 months with the 5-year survival rate about 50%.[11]

GIST may be statistically rare mesenchymal tumour of the gastrointestinal tract, but whenever the large heterogeneous, abdominal mass with higher attenuation on periphery and lower in the central parts is depicted on the contrast-enhanced CT scans, GIST must be firstly put on the differential diagnosis list. That is important because the transabdominal biopsy of the tumour is not recommended because of the possibility of seeding the tumour cells.[16]

References

1. Miettinen M, Lasota J. Gastrontestinal stromal tumors: review on morphology, molecular pathology and differential diagnosis. *Arch Pathol Lab Med* 2006; **130:** 1466-78.

2. Levy AD, Remotti HE, Thompson WM, Sobin LH, Miettinen M. Fronm the Archives of the AFIP Gastrointestinal stromal tumors: radiologic features with pathologic correlation. *Radiographics* 2003; **23:** 283-304.

3. Kachanov DY, Dobrenkov KV, Shamanskaya TV, Abdullaev RT, Inushkina EV, Savkova RF, et al. Solid tumors in young children in moscow Region of Russian Federation. *Radiol Oncol 2008;* **42:** *39-44.*

4. Miettinen M, Lasota J. Gastrointestinal stromal tumors – definition, clinical, histological, immunohistochemical, and molecular genetic features and differential diagnosis. *Virchows Arch* 2001; **438**: 1-12.

5. Suster S. Gastrointestinal stromal tumors. *Semin Diagn Pathol* 1996; **13:** 297-313.

6. Levy AD, Remotti HE, Thompson WM, Sobin LH, Miettien M. Gastrointestinal stromal tumors: radiologic features with pathologic correlation. *Radiographics* 2003; **23:** 283-304.

7. Kindblom LG, Remotti HE, Aldenborg F, Meis-Kindblom JM. Gastrointestinal pacemaker cell tumor (GIPACT): gastrointestinal stromal tumors show phenotypic characteristics of the interstitial cells of Cajal. *Am J Pathol* 1998; **152:** 1259-69.

8. Blay J-Y, Bonvalot S, Casali P, Choi H, Debiec-Richter M, Dei Tos AP, et al. Consensus meeting for the management of gastrointestinal stromal tumors. Report of the GIST Consensus Conference of 20-21 March 2004, under the auspices of ESMO. *Ann Oncol* 2005; **16**: 566-78.

9. Miettinen M, Sobin LH, Lasota J. Gastrointestinal stromal tumors of the stomach:a clinicopathologic, immunohistochemical, and molecular genetic studies of 1765 cases with long-term follow-up. *Am J Surg Pathol* 2005; **29:** 52-68.

10. Dematteo RP, Lewis JJ, Leung D, Mudan SS, Woodruf JM, Brennan MF. Two hundred gastrointestinal tumors: recurrence patterns and prognostic factors for survival. *Ann Surg* 200; **231:** 51-8.

11. Emory TS, Sobin LH, Lukes L, Lee DH, O'Leary TJ. Prognosis of gastrointestinal smooth-muscle (stromal) tumors: dependence on anatomical site. *Am J Surg Pathol* 1999; **23:** 82-87.

12. Gold JS, DeMatteo RP. Combined surgical and molecular therapy: the gastrointestinal stromal tumor model. *Ann Surg* 2006; **244:** 176-84.

13. Ludwig DJ, Traverso LW. Gut stromal tumors and their clinical behavior. *Am J Surg* 1997; **173:** 390-4.

14. Sharp RM, Ansel HJ, Keel SB. Best cases from the AFIP: gastrointestinal stromal tumor. Armed Forces Institute of Pathology. *Radiographics* 2001; **21:** 1557-60.

15. Pidhorecky I, Cheney RT, Kraybill WG, Gibbs JF. Gastrointestinal stromal tumors: current diagnosis, biologic behavior, and management. *Ann Surg Oncol* 2001; **8:**50-9.

16. Burkill GJ, Badran M, Al-Muderis O, Meirion Thomas J, Judson IR, Fisher C, et al. Malignant gastrointestinal stromal tumor: distribution, imaging features, and pattern of metastatic spread. *Radiology* 2003; **226:** 527-32.

17. Phongkitkarun S, Phaisanphrukkun C, Jatchavala J, Sirachainan E. Assesment of gastrointestinal stromal tumors with computed tomography following treatment with imatinib mesylate, *World J Gastroenterol* 2008; **14:** 892-8.

18. Hong X, Choi H, Loyer EM, Benjamin RS, Trent JC, Charnsangavej C. Gastrointestinal stromal tumors: role of CT in diagnosis and response evaluation and surveillance after treatment with imatinib. *Radiographics* 2006; **26:** 481-95.

19. Hama Y, Okizuka H, Odajima K, Hayakawa M, Kusano S. Gastrointestinal stromal tumor of the rectum. *Eur Radiol* 2001; **11:** 216-9.

20. Ghanem N, Altehoefer C, Furtwängler A, Winterer J, Schäfer O, Springer O, et al. Computed tomography in gastrointestinal stromal tumors. *Eur Radiol* 2003; **13:** 1669-78.

21. Miettinen M, Sarlomo-Rikala M, Sobin LH, Lasota J. Gastrointestinal stromal tumors and leiomyosarcomas in the colon: a clinicopathologic, immunohistochemical, and molecular genetic study of 44 cases. *Am J Surg Pathol* 2000; **24:** 1339-52.

22. Miettinen M, Lasota J. KIT(CD117): a review on expression in normal and neoplastic tissues, and mutations and their clinicopathologic correlation. *Appl Immunohistochem Mol Morph* 2005; **13:** 205-20.

23. Sarlomo-Rikala M, Tsujimura T, Lendahl U, Miettinen M. Patterns of nestin and other intermediate filament expression distinguish between gastrointestinal stromal tumors, leiomioma and scwannomas. *APMIS* 2002; **110:** 499-507.

Radiol Oncol 2008; 42(4): 196-206. *doi:10.2478/v10019-008-0016-2*

review

Time dependence of electric field effects on cell membranes. A review for a critical selection of pulse duration for therapeutical applications

Justin Teissié [1,2], Jean Michel Escoffre[1,2], Marie Pierre Rols[1,2], Muriel Golzio[1,2]

[1] *CNRS; IPBS (Institut de Pharmacologie et de Biologie Structurale); 205 route de Narbonne, F-31077 Toulouse, France;*
[2] *Université de Toulouse; UPS; IPBS; F-31077 Toulouse, France*

Background. *Electropulsation is one of the non-viral methods successfully used to transfer drugs and genes into living cells in vitro as in vivo. This approach shows promise in field of gene and cellular therapies. This presentation first describes the temporal factors controlling electropermeabilization to small molecules (< 4kDa) and then the processes supporting DNA transfer in vitro. The description of in vitro events brings our attention on the processes occurring before (s), during (ms) and after electropulsation (ms to hours) of DNA and cells. They all appear to be multistep events with well defined kinetics. They cannot be described as just punching holes in a lipid matrix in a two states process.*

Conclusions. *The faster events (may be starting on the ns time scale) appear to be under the control of the external field while the slower ones are linked to the cell metabolism. Investigating the associated collective molecular reorganization by fast kinetics methods and molecular dynamics simulation will help in their safe developments for the in vivo processes and their present and potential clinical applications.*

Key words: electropulsation; electropermeabilization; electrotransfection; electroporation

Introduction

The application of electric field pulses to cells leads to the transient permeabilization of the membrane (electropermeabilization).[1] This phenomenon brings new properties to the cell membrane: it becomes permeabilized, fusogenic and exogenous membrane proteins can be inserted. It has been used to introduce a large variety of molecules into many different cells *in vitro*.[2,3] Clinical applications of the electropermeabilization are now under development as a results of the EU Cliniporator and Esope programs. A local antitumoral drug delivery to patients (a method called electrochemotherapy) is under clinical trial.[4-8] Transdermal drug delivery is obtained *in vivo*.[9] More recently, electropermeabilization has been also used to transfer DNA *in vivo,* into the skin, liver, melanoma and skeletal muscle cells.[10-15] It

Received 27 August 2008
Accepted 13 October 2008

Correspondence to: Dr. Justin Teissié, IPBS Université de Toulouse UMR 5089 CNRS, 205 route de Narbonne, 31077 Toulouse, France. Phonel: +33(0)5 61 17 58 12; Fax: +33(0)5 61 17 59 94; Email: justin.teissie@ipbs.fr

has the main advantages of being easy to use, fast, reproducible and safe.

While during 30 years due to technological limits, pulse duration was always larger than 1 microsecond, the recent availability of high voltage (tens of kV) nanosecond long pulse generators opens the way to a new approach. Very fast perturbations under strong fields are induced in the membrane organization.[16,17] A new field of development is now present for electropermeabilization and promising results for clinical applications were reported.

One of the limiting problems remains that very few is known on the physicochemical mechanisms supporting the reorganisation of the cell membrane. The molecular target of the field effect remains unclear.

The present review focuses on the critical role played by the pulse duration in the electropermeabilization to small molecules (< 4kDa) and on its support to the processes associated to DNA transfer *in vitro*. Pulse durations are easy to adjust for an optimization of the clinical target: electrochemotherapy, irreversible electropermeabilization or gene therapy as suggested as a final conclusion.

Electropermeabilization

Theory of membrane potential difference modulation.

An external electric field modulates the membrane potential difference.[18] From the physical point of view, a cell can be described as a spherical capacitor which is charged by the external electrical field. The transmembrane potential difference induced by the electric field, $\Delta\Psi i$ is a complex function $g(\lambda)$ of the specific conductivities of the membrane (λ_m), the pulsing buffer (λ_{out}) and the cytoplasm (λ_{cyt}), the membrane thickness and the cell size. Thus,[1]

$$\Delta\Psi i = f.\ g(\lambda).\ r.\ E.\cos\theta \qquad [1]$$

in which θ designates the angle between the direction of the normal to the membrane at the considered point on the cell surface and the field direction, E the field intensity, r the radius of the cell and f, which is a shape factor (a cell being a spheroid). Therefore, $\Delta\Psi i$ is not uniform on the cell surface. It is maximum at the positions of the cell facing the electrodes. These physical predictions were checked experimentally by videomicroscopy by using the potential difference sensitive fluorescent probes.[19-21]

The pulse duration plays a critical role when shorter than the capacitive loading time of the membrane. In the previous part of the paper, it was considered that the pulse was long enough to bring the potential steady state value. The loading time τ_{load} brings a limit in this description.[1]

$$\Delta\Psi i = f.\ g(\lambda).\ r.\ E.\cos\theta\ (1 - \exp(-t / \tau_{load})) \qquad [2]$$

Assumming that the membrane is a true dielectric with no electric leak, the loading time. τ_{load}, is given by

$$\tau_{load} = rC_m\ (1/2\lambda_{out} + 1/\lambda_{cyt}) \qquad [3]$$

C_m is the membrane capacitance, λ_{out} and λ_{cyt}, respectively, the conductance of the external buffer and of the cytoplasm. τ_{load} is longer for larger cells in a heterogeneous population. Longer pulses are needed to reach the asymptotic electrically induced transmembrane voltage value (Eq. 1). A key assumption in this physical description is that the electric pulse is a sharp square wave.[22] This description is under the assumption that the cell is a sphere. A more complex description is needed for spheroidal cells and their orientation relative to the field has to be taken into account.[23,24]

The membrane leakiness affects the loading time of the membrane when the field is applied.[1] Its physical definition is given in [26] by:

$$\tau = r\,Cm\,(\lambda_{cyt} + 2\lambda_{out}) / (2\,\lambda_{cyt}\lambda_{out} + r\lambda_m\,(\lambda_{cyt} + 2\,\lambda_{out})/d) \qquad [4]$$

As λ_m is dependent on the membrane leakiness, the loading time of the membrane will decrease with an increase in the membrane leakiness. The pulse duration plays a more critical role in such a case. But under physiological conditions, where λ_{out} is larger than 10 mS/cm, as λ_{cyt} is about 4 mS/cm, τ_{load} is always of the order of 1 μs for mammalian cells

Critical parameters affecting electropermeabilization

Effects of the electric field parameters. When the resulting transmembrane potential difference $\Delta\Psi$(*i.e.* the sum between the resting value of cell membrane $\Delta\Psi o$ and the electroinduced value $\Delta\Psi i$) reaches threshold values close to 250 mV, membranes become permeable.[25-26]

Permeabilization is controlled by the field strength. Field intensity larger than a critical value (Ep) must be applied to the cell suspension. From Eq. [1], permeabilization is first obtained for θ close to 0 or π. Ep is such that:

$$\Delta\Psi perm = f\,g\,(\lambda)\,r\,Ep \qquad [5]$$

Parts of the cell surface facing the electrodes are affected. The extent of the permeabilized surface of a spherical cell, Aperm, is given by:

$$Aperm = Atot\,(1 - Ep/E)/2 \qquad [6]$$

where Atot is the cell surface and E is the applied field intensity. Increasing the field strength (decreasing Ep/E) will increase the part of the cell surface, which is brought to the electropermeabilized state. This critical value of the transmembrane potential will be reached after a longer delay for the edges of the cap due to the loading time. But this delay remains always in the μs time scale. This will affect the mechanism of electropermeabilization only for a very short pulse duration.

These theoretical predictions were assayed on cell suspension by measuring the leakage of metabolites (ATP)[27] or observed at the single cell level by digitised fluorescence microscopy.[28,29] The experimental results are in agreement with the predictions. The field strength must be larger than the threshold value Ep to induce permeabilization. The permeabilized part of the cell surface is a linear function of the reciprocal of the field intensity. Permeabilization, due to structural alterations of the membrane, remained restricted to a cap on the cell surface when short lived pulses (microseconds) are applied. The area affected by the electric field depends also on the shape (spheroid) and on the orientation of the cell with the electric field lines.[24] If a train of 10 pulses is applied at a frequency of 1 Hz, it is observed that long pulses (more than 1 ms) slightly larger than Ep bring a permeabilization on two caps on the cell surface, each facing one electrode.

Experimental results obtained either by monitoring conductance changes on cell suspension[34] or by fluorescence observation at the single cell level microscopy[28,29] shows that the local level of permeabilization is strongly controlled by the pulse duration.[27,28]

As an electrical current is flowing, Joule heating is taking place. The temperature of the sample increases as a linear function of the pulse duration and of the square of the field intensity. I*n vitro*, this deleterious by-effect is controlled by using a low ionic content pulsing buffer to deliver a limited amount of energy. This of course cannot be controlled by that means *in vivo* but the tissue can be considered as a heat sink.

Sieving of electropermeabilization

Electropermeabilization allows a post-pulse free-like diffusion of small molecules (up to 4 kDa) whatever their chemical nature. There is a size limit for permeabilization and the process for macromolecules is described in the second part of the text. Polar small compounds cross easily the electropermeabilized membrane. But the most important feature is that this membrane organisation is long-lived in cells. Diffusion is observed during the seconds and minutes following the ms pulse. Most of the exchange takes place after the pulse.[28,29] Resealing of the membrane defects and of the induced permeabilization is a first order process, which appears to be controlled by protein reorganisation. For a given cell, the resealing time (reciprocal of k) is a function of the pulse duration but not of the field intensity as checked by digitised videomicroscopy.[27] A precise analysis shows that several resealing processes are acting, two are very fast (ms, <s) while the last one remains present during several minutes at room temperature.[30] Resealing of membrane defects is a metabolic process under control of the energy reserves of the cell.[31] One can take advantage of this slow resealing to deliver the successive pulses at a 1kHz frequency to reduce the duration of the treatment in ECT.[32]

These observations are in agreement with a model where the target of the field is under the control of the pulse duration. Due to their internal flexibility (mainly at the level of the polar heads), phospholipids are sensitive to short pulses. Their change in configuration brings an effect on the membrane proteins. The transmembrane ionic exchange induces a secondary effect on the cell organization. When long pulses are applied, they can induce long range reorganization (an electrophoretic drift of polar membrane components) and a direct effect on more rigid dipoles such as those associated with membrane proteins. Long pulses are not acting only on phospholipids but may affect directly the organization of membrane proteins.[33] Of course, the transmembrane exchange will be larger as the density of membrane defects will be increased.

Loading of macromolecules is a more complex mechanism, that will be described in details later.

Associated transmembrane exchange

Molecular transfer of small molecules (<4kDa) across the permeabilized area is mostly driven by the concentration difference across the membrane. Electrophoretic contribution to the transmembrane exchange during the pulse affects the loading of polar compounds.[29,30] Free diffusion of low weight polar molecules after the pulse can be described by using the Fick equation on its electropermeabilized part.[27] It plays the most important contribution to the loading. This gives the following expression for a given molecule S and a cell with a radius r:

$$\Phi(S) = 2\pi r^2 P_S \Delta S X(N, T) (1 - Ep/E) \exp(-k(N, T) t) \quad [7]$$

where $\Phi(S)$ is the flow at time t after the N pulses of duration T (the delay between the pulses being short compared to t), P_S is the permeability coefficient of S across the permeabilized membrane and ΔS is the concentration gradient of S across the membrane. Ep depends on r (size). Permeabilization remains present for a longer time when cells are kept at low temperature. The cytoskeletal integrity plays also a major role.[33]

Cellular responses

Reactive oxygen species (ROS) are generated at the permeabilized loci, depending

on the electric field parameters.[35] These ROS can affect the viability. The amount of ROS is increased with an increase in pulse duration. Long pulses may therefore be toxic for cells.

When a cell is permeabilized, a transient osmotic swelling may result leading to an entrance of water into the cell. This increase of cell volume can lead to the rupture of the membrane.[36,37] This swelling is under the strong control of the pulse duration. Using μs pulse does not trigger swelling (with the exception of red blood cells, the so called osmotic swelling) [38] while a twofold increase in volume was reported when using ms pulses.

There is a loss of the bilayer membrane asymmetry of the phospholipids.[39]

Carry-home messages on permeabilization

When cells are submitted to short lived electric field pulses, a free exchange of hydrophilic molecules takes place across the membrane. A leakage of cytosolic metabolites into the cytoplasm is obtained. Nevertheless, cell viability can be preserved under controlled electric field conditions. More drastic electric conditions affect strongly the cell viability. This effect is cell specific and some strains are weakly resistant to the electric trauma. Bringing them to a reversible permeabilized state needs a careful tuning of the electric parameters. The exchange of the hydrophilic compounds is strongly controlled by the pulse duration. Indeed the pulse duration plays a decisive role in the level of loading as it controls i) the density of permeabilized defects (X in Eq. 7) ii) the life time of these defects (k in Eq. 4).[40] Short pulses will induce few short lived defects and a very limited loading (that cannot even be detected in many conditions). A larger loading (leakage) of the cytoplasmic content will occur with long pulses. The cell viability will be preserved more when using short pulses.

Clinical applications are supported either by the loading of therapeutic compounds (bleomycin)[5-7] or by irreversible permeabilization (IRE).[41.]Electrochemotherapy is obtained by a low number of successive short lived pulses (100 μs) while IRE requires a much longer treatment. A delay between pulses as short as 1 ms can be observed to reduce the pain of the patient.

DNA electrotransfer

Gene expression is obtained after applying electric pulses to a cell DNA mixture. No transfected cells were detected in absence of electric field, in absence of DNA, or when DNA was added after the pulses.[42,43]

Electrotransfection was only detected for electric field values leading to permeabilization. Transfection threshold values were the same as the ones for cell permeabilization when pulses lasting ms were applied.[44.]

Events during electropulsation: Membrane –DNA interaction

Field strength is observed to have a critical role. Cell membrane must be permeabilized for plasmid-membrane interaction to occur. Plasmids interact only with the permeabilized cell surface. It is accumulated by the field associated electrophoretic drag as shown by fluorescence microscopy.[45] But no free plasmid diffusion into the cytoplasm is detected while this was proposed in older works.[42] No plasmid membrane interaction occurs if the nucleic acids are added after electropermeabilizing cells as proposed in.[19,38] Negatively charged DNA molecules migrate when submitted to an electric field.[43,46] But, electrophoretic DNA accumulation by itself is not enough to

bring transmembrane transfer and gene expression whatever the pulse duration.

Under permeabilizing field conditions, the pulse duration plays a critical role in the formation of the plasmid-cell complex. The complex between the plasmid and the cell surface is detected only when the pulse duration is at least 1 ms. This suggests that the density of defects is critical in the interaction between DNA and the permeabilized membrane.

Furthermore, this interpretation is supported by the observation that the DNA content in the complex, determined by the local fluorescence emission, is under the control of the field strength and the pulse duration.[45]

The reaction time of the DNA pushed against the part of the cell surface under the permeabilizing stress of the external field is increased by a longer pulse duration. This again is involved in the positive role of the pulse duration in gene electrotransfer.

This contribution of the pulse duration to the plasmid-membrane interaction has already been illustrated by a complex dependence of the gene expression.[43] The associated gene expression Expr is shown to obey the following equation:

$$Expr = K\ N\ T^{2.3}\ (1 - Ep/E)\ f(DNA) \qquad [8]$$

as long as the cell viability is not affected to a large extent by the pulse duration.[45] All parameters are as described above, K being a constant. The dependence on the plasmid concentration (ADN) is rather complex as high levels of plasmids appear to be toxic.[47]

A very recent on line videomicroscopy study showed that plasmid DNA was trapped in the electropermeabilized membrane where it forms aggregates.

The practical conclusion is that *in vitro* an effective transfer is obtained by using long pulses in order to drive the DNA towards the permeabilized area of the membrane by electropermeabilization but with a low field strength to preserve the cell viability.[44,48] Nevertheless, the transfection was obtained with short strong pulses in the pioneering experiments [18] and with stem cells.[49]

Events after electropulsation

The main conclusion of the observations during the pulse is that plasmids do not cross the membrane during that step, even if the membrane is permeabilized (for small molecules). They form complexes at the permeabilized membrane level. More than 2 s appears to be needed to get a stable DNA membrane complex after a 5 ms pulse.[66]

Cell electroassociated DNA remains accessible to DNAaseI, a double–strand nucleic acid degrading enzyme, up to 60 s after the pulsation in the case of CHO cells.[3] The DNA aggregates, which are anchored in the membrane after the electric field application, remain sensitive to the degrading action of the externally post pulse added nucleases, which are known not to cross the membrane

High field nanosecond field pulses cellular effect

Under classical electropulsation conditions (micro-millisecond duration, a few kV/cm magnitude), the transmembrane voltage change is only present on the plasma membrane. The interior of the cell is shielded from the external field by the plasma membrane. The electrical behaviour of the cell is different under strong HV nanosecond lasting pulses. A fast charging capacitive effect is present.[50] Two membrane capacitances, C_1 for the outer cell plasma membrane and C_2 for the inner organelle membrane, are being charged by currents from the exter-

nal voltage source. Charging of the external capacitance induces a transient voltage across the cytoplasm.[52] It results a charging of the organelle capacitance. As the size of the organelle is very small and the conductivity of the cytoplasm is higher than that of the external buffer, the charging time of the organelle capacitor is much faster than that of the plasma membrane capacitor.[51] The electric field induced transmembrane permeabilizing voltage is reached for the organelle as well for the plasma membrane.[52] As soon as the plasma membrane is electropermeabilized, it is short circuited and only a fraction of the external field remains present on the organelles.[50,51]

Another consequence of ultrashort pulses is the induction of an electrodeformation of the cell (electrostretching). The magnitude of this stress is high under low conductivities conditions. It brings an electrostretching of the membrane. This is supposed to contribute to the expansion step in the electropermeabilization. The induction of the force is very fast and is transiently present in the nanosecond range when a low conductivity buffer is present. The effect is not present when the buffer conductivity is close to the one of the cytoplasm.[53,54] This stretching effect can be present only when the rise time of the electric pulse is very fast (ns). This is not the case with pulse generators routinely used nowadays. But this effect should be kept in mind with the new developments of ns HV pulse generators.

As a consequence, organelles can be electropermeabilized by nanosecond long pulses. This is indeed what is observed. Cytoplasmic stored Calcium pools are observed to be released by nanosecond pulses. Permeabilization of organelles can be used to trigger apoptosis and cell death without direct leak from the cytoplasm. This was proposed as an approach to destroy tumor cells.[52,55-58] Preclinical studies of drug free tumor eradication were reported.[59,60]

The nuclear enveloppe can be permeabilized. Therefore, a new strategy for plasmid transfer is present. In a first step, millisecond pulses are used to introduced plasmids in the cytoplasm as classically described. After a 30 min incubation, a nanosecond high strength field is applied to induce the destabilization of the nucleus membrane and to facilitate the nuclear transfer of the plasmid and its expression. A significant increase of expression can be apparently obtained.[61]

This new methodology is a "hot" field of investigations where encouraging results have been published. But it is not yet a mature field as "classical" electropulsation.

Conclusions

"Classical" Electropermeabilization processes can be followed from microseconds up to days. Kinetic studies of electropermeabilization led to a description in 5 steps:

1- "*Induction step*"- the field induced the membrane potential difference increase which gave local defects (may be due to kinks in the lipid chains) when it reached a critical value (about 200 mV). A mechanical stress was present with a magnitude that depends on the buffer composition. This can be detected in less than 1 nanosecond but a limit is given by the charging time of the membrane. Molecular dynamic simulation suggests that it is much faster [62] in agreement with the nanosecond experiments (μs to ns due to the pulse generator).

2- "*Expansion step*"- These defects expanded as long as the field was present and with a strength larger than a critical value. Again an electromechanical stress remained present. This may be due to a "coalescence" process (μs to ms)

3- "*Stabilisation step*"- As soon as the field intensity was lower than the threshold value, that is mentioned in step 1, stabilisa-

Table 1. Operating parameters for the *in vitro* applications of electropulsation on mammalian cells

Applications	Duration	Field strength	Number of pulses
Electrochemotherapy (ECT)	100 μs	1.3 kV/cm	8
Electrotransfection (EGT)	5 to 10 ms	0.5 to 0.8 kV/cm	8
Eradication (IRE)	300 μs	1.5 kV/cm	3 x 10
Nanopulse eradication (nsIRE)	60 ns	12 kV/cm	200

tion processes were taking place within a few milliseconds, which brought the membrane to the permeabilized state for small molecules (ms).

4- "*Resealing step*"- A slow resealing was then occurring on a scale of seconds and minutes. It was a first order process. It is driven by the cellular metabolism (s to min).

5- "*Memory effect* "- Some changes in the membrane properties remained present on a longer time scale (hours) but the cell behaviour was finally back to normal.

Experiments showed that the mechanism of DNA transfer was different from what was observed for electropermeabilization (transfer of small molecules). Indeed, experimental results led to the conclusion that plasmids had to be present during electropulsation but crossed the electropulsed membrane in the minutes following it. No gene transfer was detected with a post-pulse DNA addition. These results were obtained on bacteria, yeast and mammalian cells.[37,63,64]

We proposed a model in which Electrotransfection appears as a multistep process [43] and brought its direct experimental evidence.[45.]

During the pulse,

i- electropermeabilization takes place (μs)
ii- plasmids are electrophoretically driven into contacts with the cell surface (ms)
iii- a metastable complex is formed between plasmids and the localised electropermeabilized part of the cell membrane (ms).
iv- a stable complex results (s)
v- long after the pulse, plasmids left the complex and diffused in the cytoplasm (min)
vi- a small fraction crossed the nuclear envelope to be expressed (h).

This interaction between plasmids and electropermeabilized membrane is strongly controlled by the pulse duration (always on the ms time scale). Additive effects of successive pulses are obtained. Only the localised part of the cell membrane brought to the permeabilized state by the external field is competent for the transfer.[43]

Practical consequences

Electropermeabilization is one of the non-viral methods successfully used to transfer genes into living cells *in vitro* as *in vivo*. It has the main advantages of being easy to perform, fast, reproducible and safe. This approach appears promising for gene therapy and is a clinical routine for drug delivery. A careful choice of the pulse duration and delays between the successive steps of electropulsation is needed to get successful applications (Table 1).[65] This remains linked to phenomenological conclusions. Its further developments need a better understanding of the basic effects induced at the membrane, cellular and tissue levels by electrical events and the plasmid entry in the cell.

Acknowledgements

This work was supported by the CNRS, the AFM (Association française pour les myopathies), the région Midi Pyrénées and the Proteus Slovenia-CNRS exchange program.

The authors wish to thank their colleagues: L. Mir in Villejuif (France), D. Miklavcic, T. Kotnik, M. Cemazar, G. Sersa and G. Pucihar, all from Ljubljana (Slovenia) and E. Neumann in Bielefeld (Germany) for so many helpful discussions.

References

1. Neumann E, Sowers AE, Jordan CA. Electroporation and electrofusion in cell biology. York: Plenum press; 1989.

2. Orlowski S, Mir LM. Cell electropermeabilization: a new tool for biochemical and pharmacological studies. *Biochim Biophys Acta* 1993; **1154:** 51-63.

3. Eynard N, Rols MP, Ganeva V, Galutzov B., Sabri N, Teissié J. Electrotransformation pathways of procaryotic and eucaryotic cells: recents developments. *Bioelectrochem Bioenerg* 1997; **44:** 103-10.

4. Mir LM, Roth C, Orlowski S, Quintin Colonna F, Fradelizi D, et al. Systemic antitumor effects of electrochemotherapy combined with histoincompatible cells secreting interleukin-2. Systemic antitumor effects of electrochemotherapy combined with histoincompatible cells secreting interleukin-2. J Immunother Emphasis Tumor Immunol 1995; **17:** 30-8 .

5. Cemazar M, Sersa G. Electrotransfer of therapeutic molecules into tissues.*Curr Opin Mol Ther* 2007; **9:** 554-62.

6. Sersa G, Miklavcic D, Cemazar M, Rudolf Z, Pucihar G, Snoj M. Electrochemotherapy in treatment of tumours. *Eur J Surg Oncol* 2008; **34:** 232-40.

7. Mir LM, Gehl J, Sersa G, Collins CG, Garbay JR, Billard V, et al. Standard operating procedures of the electrochemotherapy: Instructions for the use of bleomycin or cisplatin administered either systemically or locally and electric pulses delivered by the CliniporatorTM by means of invasive or non-invasive electrodes *Eur J Cancer 2006;* **42(Suppl 4):** 14-25.

8. Mir LM, Glass LF, Sersa G, Teissie J, Domenge C, Miklavcic D, et al. Effective treatment of cutaneous and subcutaneous malignant tumours by electrochemotherapy. *Br J Cancer* 1998; **77:** 2336-42.

9. Prausnitz MR, Bose VG, Langer R, Weaver JC. Electroporation of mammalian skin: a mechanism to enhance transdermal drug delivery. *Proc Natl Acad Sci USA* 1993; **90:** 10504-8.

10. Titomirov A, Sukarev S, Kistanova E. In vivo electroporation and stable transformation of skin cells of newborn mice by plasmid DNA. *Biochim Biophys Acta* 1991; **1088:** 131-4.

11. Heller R, Jaroszeski M, Atkin A, Moradpour D, Gilbert R, Wands J, et al. In vivo gene electroinjection and expression in rat liver. *FEBS Lett* 1996; **389:** 225-8.

12. Rols MP, Delteil C, Golzio M, Dumond P, Cros S, Teissie J. In vivo electrically mediated protein and gene transfer in murine melanoma. *Nat Biotechnol* 1998; **16:** 168-71.

13. Aihara H, Miyazaki J. Gene transfer into muscle by electroporation in vivo. *Nat Biotechnology* 1998; **16:** 867-70.

14. Mir LM, Bureau MF, Rangara R, Schwartz B, Sherman D. Long-term, high level in vivo gene expression after electric pulse- mediated gene transfer into skeletal muscle. *C R Acad Sci III* 1998; **321:** 893-9.

15. Muramatsu T, Nakamura A, Park M. In vivo electroporation: A powerful and convenient means of nonviral gene transfer to tissues of living animals. [Review]. *Int J Mol Med* 1998; **1:** 55-62.

16. Pliquett U, Joshi RP, Sridhara V, Schoenbach KH. High electrical field effects on cell membranes. *Bioelectrochemistry* 2007; **70:** 275-82.

17. Pakhomov AG, Kolb JF, White JA, Joshi RP, Xiao S, Schoenbach KH. Long-lasting plasma membrane permeabilization in mammalian cells by nanosecond pulsed electric field (nsPEF). *Bioelectromagnetics* 2007; **28:** 655-63.

18. Neumann E, Schaefer-Ridder M, Wang Y, Hofschneider PH. Gene transfer into mouse lyoma cells by electroporation in high electric fields. *EMBO J* 1982; **1:** 841-5.

19. Gross D, Loew LM, Webb WW. Optical imaging of cell membrane potential changes induced by applied electric fields. *Biophys J* 1986; **50:** 339-48.

20. Lojewska Z, Farkas DL, Ehrenberg B, Loew LM. Analysis of the effect of medium and membrane conductance on the amplitude and kinetics of membrane potentials induced by externally applied electric fields. *Biophys J* 1989; **56:** 121-8.

21. Hibino M, Shigemori M, Itoh H, Nagayama K, Kinosita K jr. Membrane conductance of an electroporated cell analyzed by submicrosecond imaging of transmembrane potential. *Biophys J* 1991; **59:** 209-20.

22. Kotnik T, Pucihar G, Rebersek M, Miklavcic D, Mir LM. Role of pulse shape in cell membrane electropermeabilization. *Biochim Biophys Acta* 2003; **1614:** 193-200.

23. Pucihar G, Kotnik T, Valic B, Miklavcic D. Numerical determination of transmembrane voltage induced on irregularly shaped cells. *Ann Biomed Eng* 2006; **34:** 642-52.

24. Valic B, Golzio M, Pavlin M, Schatz A, Faurie C, Gabriel B, et al. Effect of electric field induced transmembrane potential on spheroidal cells: theory and experiment. *Eur Biophys J* 2003; **32:** 519-28.

25. Teissié J, Tsong TY. Electric field induced transient pores in phospholipid bilayer vesicles. *Biochemistry* 1981; **20:** 1548-54.

26. Teissié J, Rols MP. An experimental evaluation of the critical potential difference inducing cell membrane electropermeabilization. *Biophys J* 1993; **65:** 409-13.

27. Rols MP, Teissie J. Electropermeabilization of mammalian cells. Quantitative analysis of the phenomenon. *Biophys J* 1990; **58:** 1089-98.

28. Gabriel B, Teissie J. Direct observation in the millisecond time range of fluorescent molecule asymmetrical interaction with the electropermeabilized cell membrane. *Biophys J* 1997; **73:** 2630-7.

29. Gabriel B, Teissie J. Time courses of mammalian cell electropermeabilization observed by millisecond imaging of membrane property changes during the pulse. *Biophys J* 1999; **76:** 2158-65.

30. Pucihar G, Kotnik T, Miklavic D, Teissie J. Kinetics of transmembrane transport of small molecules into electropermeabilized cells. *Biophys J* 2008; **95:** 2837-48.

31. Rols MP, Delteil C, Golzio M, Teissie J. Control by ATP and ADP of voltage-induced mammalian-cell-membrane permeabilization, gene transfer and resulting expression. *Eur J Biochem* 1998; **254:** 382-8.

32. Pucihar G, Mir LM, Miklavcic D. The effect of pulse repetition frequency on the uptake into electropermeabilized cells in vitro with possible applications in electrochemotherapy. *Bioelectrochemistry* 2002; **57:** 167-72.

33. Teissie J, Rols MP. Manipulation of cell cytoskeleton affects the lifetime of cell membrane electropermeabilization. *Ann N Y Acad Sci* 1994; **720:** 98-110.

34. Kinosita K Jr, Tsong TY. Voltage-induced conductance in human erythrocyte membranes. *Biochim Biophys Acta* 1979; **554:** 479-97.

35. Gabriel B, Teissie J. Generation of reactive-oxygen species induced by electropermeabilization of Chinese hamster ovary cells and their consequence on cell viability. *Eur J Biochem* 1994; **223:** 25-33.

36. Kinosita K Jr,Tsong TY. Hemolysis of human erythrocytes by transient electric field. *Proc Natl Acad Sci USA* 1977; **74:** 1923-7.

37. Golzio M., Mora MP, Raynaud C, Deltei C, Teissie J, Rols MP. Control by osmotic pressure of voltage-induced permeabilization and gene transfer in mammalian cells. *Biophys J* 1998; **74:** 3015-22.

38. Tsong TY. Electroporation of cell membranes. *Biophys J* 1991; **60:** 297–306.

39. Haest CW, Kamp D, Deuticke B. Transbilayer reorientation of phospholipid probes in the human erythrocyte membrane. Lessons from studies on electroporated and resealed cells. *Biochim Biophys Acta* 1997; **1325:** 17-33.

40. Rols MP, Teissie J. Electropermeabilization of mammalian cells to macromolecules: control by pulse duration. *Biophys J* 1998; **75:** 1415-23.

41. Al-Sakere B, Andre F, Bernat C, Connault E, Opolon P, Davalos RV, et al. Tumor ablation with irreversible electroporation. *PLoS ONE* 2007; **2(11):** e1135.

42. Klenchin VA, Sukharev SI, Serov SM, Chernomordik LV, Chizmadzev YuA Electrically induced DNA uptake by cells is a fast process involving DNA electrophoresis. *Biophys J* 1991; **60:** 804-11.

43. Wolf H, Rols MP, Boldt E, Neumann E, Teissie J. Control by pulse parameters of electric field-mediated gene transfer in mammalian cells. *Biophys J* 1994; **66:** 524-31.

44. Rols MP, Teissie J. Electropermeabilization of mammalian cells to macromolecules: control by pulse duration. *Biophys J* 1998; **75:** 1415-23.

45. Golzio M, Teissie J, Rols MP. Direct visualization at the single-cell level of electrically mediated gene delivery. *Proc Natl Acad Sci U S A* 2002; **99:** 1292-7.

46. Neumann E, Werner E, Sprafke A, Kruger K. Electroporation phenomena. Electrooptics of plasmid DNA and of lipid bilayer vesicles. In: Jennings BR, Stoylov SP, editors. Colloid and molecular electro-optics. Bristol: IOP publishing LTD; 1992. p. 197-206.

47. Rols MP, Coulet D, Teissie J. Highly efficient transfection of mammalian cells by electric field pulses. Application to large volumes of cell culture by using a flow system. *Eur J Biochem* 1992; **206:** 115-21.

48. Kubiniec RT, Liang H, Hui SW. Effects of pulse length and pulse strength on transfection by electroporation. *Biotechniques* 1990; **8:** 16-20.

49. Ferreira E, Potier E, Logeart-Avramoglou D, Salomskaite-Davalgiene S, Mir LM, Petite H. Optimization of a gene electrotransfer method for mesenchymal stem cell transfection. *Gene Ther* 2008; **15:** 537-44.

50. Frey W, White JA, Price RO, Blackmore PF, Joshi RP, Nuccitelli R, et al. Plasma membrane voltage changes during nanosecond pulsed electric field exposure. *Biophys J* 2006; **90:** 3608-15.

51. Kotnik T, Miklavcic D. Theoretical evaluation of voltage inducement on internal membranes of biological cells exposed to electric fields. *Biophys J* 2006; **90:** 480-91.

52. Tekle E, Oubrahim H, Dzekunov SM, Kolb JF, Schoenbach KH, Chock PB. Selective field effects on intracellular vacuoles and vesicle membranes with nanosecond electric pulses. *Biophys J* 2005; **89:** 274-84.

53. Muller KJ, Sukhorukov VL, Zimmermann U. Reversible electropermeabilization of mammalian cells by high-intensity, ultra-short pulses of submicrosecond duration. *J Membr Biol* 2001; **184**: 161-70.

54. Sukhorukov VL, Mussauer H, Zimmermann U. The effect of electrical deformation forces on the electropermeabilization of erythrocyte membranes in low- and high-conductivity media. *J Membr Biol* 1998; **163:** 235-45.

55. Beebe SJ, Fox PM, Rec LJ, Willis LK, Schoenbach KH. Nanosecond high intensity pulsed electric fields induce apoptosis in human cells. *FASEB J* 2003; **30:** 286–292.

56. Vernier TP, Sun YH, Marcu L, Craft CM, Gundersen MA. Nanoelectropore-induced phosphatidylserine translocation. *Biophys J* 2004; **86:** 4040–8.

57. Brown FD, Rozelle AL, Yin HL, Balla T, Donaldson JG. Phosphatidylinositol 4,5-bisphosphate and Arf-regulated membrane traffic. *J Biol Chem* 2001; **154:** 1007–17.

58. White JA, Blackmore PF, Schoenbach KH, Beebe SJ. Stimulation of capacitative calcium entry in HL-60 cells by nanosecond pulsed electric fields. *J Biol Chem* 2004; **279:** 22964–72.

59. Nuccitelli R, Pliquet U, Chen X, Ford W, James Swanson R, Beebe SJ, et al. Nanosecond pulsed electric fields cause melanomas to self-destruct. *Biochem Biophys Res Commun* 2006; **343:** 351-60.

60. Garon EB, Sawcer D, Vernier PT, Tang T, Sun Y, Marcu L, et al. .In vitro and in vivo evaluation and a case report of intense nanosecond pulsed electric field as a local therapy for human malignancies. *Int J Cancer* 2007; **121:** 675-82.

61. Beebe SJ, White J, Blackmore PF, Deng Y, Somers K, Schoenbach KH. Diverse effects of nanosecond pulsed electric fields on cells and tissues. *DNA Cell Biol* 2003; **22:** 785-96.

62. Tarek M. Membrane electroporation: a molecular dynamics simulation. *Biophys J* 2005; **88:** 4045-53.

63. Eynard N, Sixou S, Duran N, Teissie J. Fast kinetics studies of Escherichia coli electrotransformation. *Eur J Biochem* 1992; **209:** 431-6.

64. Ganeva V, Galutzov B, Teissie J. Fast kinetic studies of plasmid DNA transfer in intact yeast cells mediated by electropulsation. *Biochem Biophys Res Commun* 1995; **214:** 825-32.

65. Lebar AM, Sersa G, Kranjc S, Groselj A, Miklavcic D. Optimisation of pulse parameters in vitro for in vivo electrochemotherapy. *Anticancer Res* 2002; **22:** 1731-6.

66. Phez E, Faurie C, Golzio M, Teissié J, Rols MP. New insights in the visualization of membrane permeabilization and DNA/membrane interaction of cells submitted to electric pulses. *Biochim Biophys Acta* 2005; **1724:** 248-54.

Radiol Oncol 2008; 42(4): 207-14. doi:10.2478/v10019-008-0019-z

research article

Quality of life in patients after combined modality treatment of rectal cancer: Report of a prospective phase II study

Vaneja Velenik, Irena Oblak, Franc Anderluh

Department of Radiotherapy, Institute of Oncology Ljubljana, Slovenia

Background. *The literature reports are unclear whether a permanent stoma reduces the quality of life (QOL) of patients with locally advanced rectal cancer (T3-4 and/or N+). Our aim was to compare the QLQ of patients with abdominoperineal resection and with restorative surgery, treated with preoperative radiochemotherapy in a prospective phase II clinical trial.*

Methods. *Fifty-seven patients were irradiated to 45 Gy in 25 fractions over 5 weeks to the pelvis concomitantly with oral capecitabine 825 mg/m^2, twice a day, including weekends. Surgery was scheduled 4-6 weeks after the completion of the chemoradiotherapy. Four courses of chemotherapy were planned postoperatively. Patients still alive and without recurrence of the disease, with a minimum follow up of 2 years, were surveyed with two self-rating questionnaires developed by the European Organisation for Research and Treatment of Cancer (EORTC): one was cancer specific (EORTC QLQ-C30) and one was site specific (EORTC QLQ-C38).*

Results. *QLQ was assessed in 28 of 32 patients eligible (87.5%). The median time from surgery to filling in the questionnaires was 35 months. For all scales of EORTC QLQ-C30 and EORTC QLQ-C38, no significant differences in median scores were observed between the two groups of patients.*

Conclusions. *QOL did not differ in patients with abdominoperineal resection from patients with sphincter-sparing surgery.*

Key words: preoperative radiochemotherapy; rectal cancer; quality of life

Introduction

The preoperative chemoirradiation has become a standard part of treatment protocols in stage II and III rectal cancer. Compared to postoperative chemoradiotherapy, the advantage of preoperative application of chemotherapeutics and irradiation includes improved compliance, reduced toxicity and down staging of the tumour in a substantial number of patients. The latter can potentially increase the feasibility of sphincter-saving resection in low-sited tumours.[1] The impairment of anorectal, voiding and sexual function is a frequent adverse effect of the multimodality treatment. Thus, the addition of radiotherapy (RT) to surgery

Received 13 October 2008
Accepted 5 November 2008

Correspondence to: Vaneja Velenik, PhD, MD, Department of Radiotherapy, Institute of Oncology Ljubljana, Zaloška c. 2, 1000 Ljubljana, Slovenia. Phone: +386 1 5879 661; Fax: +386 1 5879 304; E-mail: vvelenik@onko-i.si

improves the oncologic outcome but, potentially, adds morbidity to that associated with surgery.[2] A poor functional outcome after the restorative surgical technique may effect on the patient's quality of life (QOL). The construction of permanent colostomy following an abdominoperineal resection (APR) may be associated with one or more physical and psyhosociological problems as well. In the past, prospective studies with rectal cancer patients have focused on the tumour response, local control, survival and treatment related toxicity as primary end-points. Although these parameters remain central in the evaluation process, there is an increasing recognition of the need to assess more systematically the impact of cancer and its treatment on the functional, psychological and social health of the individual. As MRI has become incorporated in the diagnostic procedure of rectal disease,[3] the measurement of the functional outcome and QOL in rectal cancer patients, treated with preoperative radiochemotherapy and surgery has also become incorporated in clinical trials over the past decade.[4]

The aim of the present study was to assess QOL outcomes in patients treated with restorative procedures, compared with those in patients after APR by using a recommended and proven method.

Patients and methods

Patients

Between June 2004 and January 2005, fifty-seven patients with locally advanced resectable rectal cancer were treated with preoperative radiotherapy and concomitant capecitabine. Thirty-two patients, who were alive and without evidence of disease progression at a minimum follow-up of 2 years, were asked to participate in QOL study. Twenty-eight participated after having given informed consent. The characteristics of patients who answered the questionnaires are listed in Table 1.

Table 1. Characteristics of patients who answered the questionnaires

Characteristics	Number (%)
Number of responders/eligible patients	28/32 (87.5)
Median age (range) years	67 (37-81)
Gender	
Male	20 (71.4)
Female	8 (28.6)
WHO performance status	
Stage 0	27 (96.4)
Stage I	1 (3.6)
Tumour distance from the anal verge (cm)	6.5 (1-12)
Clinical TNM stage	
Stage II	14 (50.0)
Stage III	14 (50.0)
Permanent stoma	
Yes	9 (32.1)
No	19 (67.9)
Postoperative chemotherapy	
Yes	27 (96.4%)
No	1 (3.6%)
Median time (range) from surgery to answering (ra	35 (26-39)

Treatment

The details of both the patients and the treatment have been reported previously.[5] Briefly, the prospective phase II trial has been approved by the Republic Ethic Committee. The entry criteria included: histologically verified adenocarcinoma of the rectum, clinical stage II or III (IUCC TNM classification 2002); no prior radiotherapy and/or chemotherapy; World Health Organisation (WHO) performance

status <2; age at diagnosis of 18 or older; adequate bone marrow, liver, renal and cardiac function (no history of ischemic heart disease), and written informed consent.

Radiotherapy was delivered using 15 MV photon beams and four-field box technique, once per day, 5 days weekly. The small pelvis received 45 Gy in 25 fractions over 5 weeks. Three-dimensional CT-based treatment planning was performed. The clinical target volume (CTV) was defined to cover the small pelvis from the L5-S1 interspace to 5 cm below the primary tumour. The lateral borders were 5 mm outside the true bony pelvis. The posterior margin covered the sacrum, and the anterior margin encompassed the posterior one-third to one-half of the bladder and/or vagina. An additional 1 cm in all directions was added to the CTV to obtain the planning target volume (PTV). The dose was prescribed to cover the PTV with a 95% reference isodose (95% of the ICRU point dose). Patients were treated in the prone position. They were instructed to have a full bladder during irradiation, and no devices were used to displace the small bowel out of the irradiated volume. A multileaf collimator was used for shaping the fields and for the protection of normal tissues.

Chemotherapy was administered concomitantly with radiotherapy and consisted of capecitabine administered orally at a daily dose of 1650 mg/m^2, divided into two equal doses given 12 hours apart. One of the doses was taken 2 hours prior to irradiation. The chemotherapy started on the first day of radiotherapy and finished on the last day of radiotherapy (including weekends).

According to the protocol, surgery was planned for 4-6 weeks after the completion of the chemoradiotherapy. Although TME was the preferred surgical technique, it was not mandatory. Abdominoperineal resection (APR) was carried out in 17 (30.9%) patients, anterior resection (AR) in 4 (7.3%) patients, low anterior resection (LAR) in 32 (58.2%) patients, exenteration of the small pelvis in 1 (1.8%) patient and Hartmann's resection in 1 (1.8%) patient. As determined by the histopathological examination of surgical specimens, the resection was radical (R0) in 54 (98.2%) patients. A temporary colostomy was required in 32 (88.8%) patients.

Four courses of chemotherapy were planned postoperatively. It was administered in 44/55 (80%) of patients. Eighteen (40.9%) patients received adjuvant 5-Fluorouracil/Leukovorin and 26 (59.1%) patients received capecitabine.

QLQ assessment

QLQ was assessed using two validated questionnaires developed by European Organisation for Research and Treatment of Cancer (EORTC). One questionnaire assessed the cancer specific QOL (the third version of the Quality of life Questionnaire Core 30 items, i.e. QLQ-C30)[6] and the other site - specific (colorectal) QOL (Quality of life Questionnaire Core 38 items, *i.e.* QLQ-C38).7

The QLQ-C30 is a 30-items questionnaire. It includes a total of nine multi-item scales: five functional scales (physical, role, cognitive, emotional, and social); three symptom scales (fatigue, pain, and nausea and vomiting); and a global health and quality-of-life scale. Separate six single items are included to measure gastrointestinal symptoms (diarrhoea and constipation), dyspnoea, appetite loss, sleeping disturbances and economic consequences of the disease.

The QLQ-C38 questionnaire comprises 38 questions, of which 19 are completed by all patients and the remaining by a subset of the patients (men or women; patients with or without stoma). It incorporates two functional scales (body image and sexuality) and seven symptom scales (micturition

problems induced by irradiation, chemotherapy side effects, gastrointestinal general symptoms, defecation problems, stoma - related problems, and sexual dysfunction in men and women). The remaining single items assess future perspectives and weight loss.

Both questionnaires contain questions related to the previous week. Four response categories, from 1 (not at all) to 4 (very much), are possible.

Statistical analysis

The scoring was performed according to the EORTC QLQ-C30 scoring manual.[8] The principle of scoring was to estimate the average of the items that contributed to the scale; this was the raw score. A linear transformation was used to standardize the raw score, so that all scores ranged from 0 to 100. The higher scale score for the functional scale or the global health status/QOL represents a higher level of functioning, or higher QOL; whereas the higher level of symptoms/problems for the symptom/item scales represents a higher level of symptomatology, or dysfunction. Missing values were calculated such that if at least one-half the items from the scale had been completed, it was assumed that the missing items would have had values equal to the average of the items present.

Demographic and clinical data were calculated using descriptive statistics. Results of QOL information were expressed as means and medians. The nonparametric Mann-Whitney *U*-test was used to compare median scores of QOL scales between the two treatment groups of patients. A 5% level of statistical significance was used for variables ($P<0.05$). Data were analyzed using SPSS for Windows (version 13.0; SPSS, Chicago, IL, USA).

We hypothesized that at least some scores of various scales would vary between subgroups of patients in favour of patients with restorative type of surgery.

Results

Oncological outcome

Before the therapy, an abdominoperineal resection was planned in 24 out of 55 patients who had definitive surgery. After the completion of chemoradiotherapy, the sphincter-conserving surgery was successfully performed in 7 of these 24 patients. Among 31 patients in whom the sphincter-conserving surgery was planned before having had any therapy, this was not possible in two patients, which resulted in an ultimate sphincter preservation rate of 65.5% (36/55).

A local relapse has occurred in 1 (1.8%) patient and a dissemination in 13 (24.1%) out of 54 patients with a median time to progression of 23 months (range 3-23 months). Second malignancies have occurred in 2 patients. The median 2-year overall survival, disease-free survival and disease-specific survival rates were 84.2%, 72.5% and 92.4%, respectively, and local control was 98.2%.

QOL evaluation

Of 32 eligible patients from the prospective phase II trial, 28 (87.5%) completed the EORTC QLQ-C30 and QLQ-C38 questionnaires: 19 patients with sphincter conserving surgery and 9 patients with APR. Three patients refused to participate in the study and one was judged ineligible because of serious comorbidities. Surveys were completed a median of 35 (26-39) months after the surgery.

The general results of QLQ-C30 for all patients with or without stoma are given in Table 2. The global quality of life scores, representing the overall health and quality

Table 2. EORTC QLQ-C30 mean and median functional scale and single-item scores according to the type of surgery

	APR (8 patients)		Restorative surgery (20 patients)		
Item	Mean (s.d.)	Median (range)	Mean (s.d.)	Median (range)	*P*
Global QOL	69 (24)	71 (25-100)	65 (28)	71 (0-100)	0.86
Functional scale					
Social function	75 (28)	83 (33-100)	80 (24)	92 (17-100)	0.71
Cognitive function	67 (35)	75 (0-100)	82 (23)	83 (17-100)	0.26
Role function	69 (31)	67 (17-100)	83 (24)	100 (17-100)	0.30
Emotional function	73 (34)	83 (0-100)	81 (22)	88 (33-100)	0.64
Physical function	78 (19)	83 (47-100)	81 (24)	93 (20-100)	0.47
Symptom scale					
Pain	25 (24)	25 (0-50)	18 (29)	0 (0-100)	0.36
Fatigue	36 (37)	33 (0-100)	25 (23)	22 (0-67)	0.57
Nausea and vomiting	10 (15)	0 (0-33)	3 (6)	0 (0-17)	0.30
Single items					
Dyspnoea	21 (40)	0 (0-100)	8 (24)	0 (0-100)	0.64
Insomnia	21 (35)	0 (0-100)	33 (29)	33 (0-100)	0.22
Appetite loss	13 (25)	0 (0-67)	3 (10)	0 (0-33)	0.53
Diarrhoea	17 (36)	0 (0-100)	17 (25)	0 (0-100)	0.67
Constipation	17 (18)	17 (0-33)	15 (23)	0 (0-67)	0.71
Financial impact	29 (33)	17 (0-67)	17 (25)	0 (0-67)	0.41

of life of patients, were similar. There was no difference in medians for all other scale scores. Patients having had APR seem to have less sleep disturbances (0 versus 33; p=0.22) and they tended to report lower levels of role functioning (67 versus 100; p=0.3) and cognitive functioning (75 versus 83; p=0.26) than did patients having had restorative resection.

The results of QLQ-C38 for the two surgical groups are given in Table 3. No significant differences in median scores were observed between the two surgical groups for any of the scales. However, APR group of patients tended to report a lower body image score (61 versus 89; p=0.16). The sexual functioning score and sexual enjoyment score were very low in both groups, but in the APR group the sexual functioning score was higher (33 versus 17; p=0.11).

Discussion

The abdominoperineal resection (APR) was long considered the standard treatment of tumours lying in the lower third of the rectum, providing a good local control. A more precise understanding of tumour biology and of failure patterns, has lead to the acceptance of short distal resection margins. Advances in surgical stapling and coloanal anastomoses technique have made it possible to treat many low rectal cancers by the sphincter-saving low anterior resection in preference to an APR. The survival and lo-

Table 3. EORTC QLQ-C38 mean and median functional scale and single - item scores according to the type of surgery

	APR (8 patients)		Restorative surgery (20 patients)		
Item	Mean (s.d.)	Median (range)	Mean (s.d.)	Median (range)	*P*
Functional scale					
Body image	67 (23)	61 (33-100)	81 (20)	89 (44-100)	0.16
Future perspectives	46 (43)	50 (0-100)	56 (35)	67 (0-100)	0.56
Sexual functioning	40 (32)	33 (0-100)	19 (21)	17 (0-67)	0.11
Sexual enjoyment	44 (34)	33 (0-100)	29 (28)	33 (0-67)	0.49
Symptom scale					
Micturition problems	33 (28)	33 (0-78)	22 (22)	11 (0-56)	0.39
General gastrointestinal	17 (21)	7 (0-60)	19 (14)	20 (0-40)	0.48
Defecation problems			23 (17)	24 (0-57)	
Stoma- related problems	26 (20)	21 (5-67)			
Sexual dysfunction of males	0 (0)	0 (0-0)	0 (0)	0 (0-0)	1.0
Sexual dysfunction of females	17	17 (17-17)	17 (24)	17 (0-33)	1.0
Weight loss	8 (15)	0 (0-33)	5 (17)	0 (0-67)	0.62

cal recurrence rate was not compromised.[9]

There are many other factors, which impact the decision, which surgical procedure to undertake for low-lying cancers: patient gender, preoperative sphincter function, stage of the disease, potential distal resection margin and surgeon preference. The avoidance of permanent colostomy has been used to judge the quality of the rectal cancer surgery. Although the avoidance of a permanent stoma following rectal cancer excision is regarded as a favourable outcome measure, the bowel function after the sphincter-sparing procedures may be greatly altered, resulting in faecal urgency and incontinence.[10] Patients receiving preoperative radiochemotherapy for rectal cancer may develop also other unpleasant symptoms, such as micturition problems and sexual dysfunction. These symptoms, which occurred in a substantial proportion of patients, have been reported previously.[11] Our aim was to evaluate the effect of these symptoms on the health-related QOL as an important endpoint.

It is difficult to evaluate the QOL after the rectal cancer surgery. For that purpose, non-cancer-specific or nonstardized questionnaires with a different methodology for scoring were used, *i.e.* self-reported by patients or scored by physicians. Additionally, the authors provided different types of preoperative or postoperative treatment. The evaluations of QOL were mostly of retrospective nature with a different time for questionnaire administration and evaluated on small sample sizes. So, the heterogeneity in the evaluation of QOL after the rectal cancer surgery gave rise to inconsistent and conflicting findings. Any comparison between data reported by different authors might be misleading. The use of standardized questionnaires is necessary. In our study, the evaluation of health-related QOL of patients was assessed by using EORTC cancer and site specific questionnaires,

which are validated and preferred measures in recent clinical trials.

Some studies have suggested that patients with a colostomy have a poorer QOL when compared to those who had restorative resection.[12,13] In the present study no significant differences in median scores were observed in any of the function scales of QLQ-C30 questionnaire studied (physical, role, social, emotional, cognitive functions and overall QOL) between the two groups. Our finding is in agreement with the observation reported by Allal *et al*.[14] and Camilleri-Brennan *et al*.[4] In a prospective study, Grumann *et al.*[15] showed that following LAR patients had even a lower QOL than those who underwent APR. A recent analysis of eight studies in a Cochrane Database Systemic Review showed mixed results. Half of the studies revealed no difference with regard to QOL between APR and LAR, in one the QOL in patients with stoma was only slightly affected and others revealed that the formation of stoma significantly affected the patients QOL.[16] The similarities in QOL in stoma and non-stoma patients may be due to the adaptation and the phenomenon of "response shift",[17] in which patients who have survived life-threatening disease seem to have new internal standards and, thereby, often report good QOL. Even patients who have undergone pelvic exenteration report having good QOL.[18] In agreement with other authors, we found that APR was associated with a lower perception of body image (feeling less attractive) than LAR.

Defecation-related problems, such as urgency, incontinence and incomplete bowel emptying, are well-known side effects of sphincter-preserving surgery.[11] Interestingly, the assessment of gastrointestinal problems on the QLQ-C38 and constipation on the QLQ-C30 showed similarities in the two groups. Camilleri-Brennan *et al.* found that patients who had sphincter saving resection had more problems with constipation.[4] Scores for stoma-related problems in both studies were comparable low, probably due to better stoma care. Standardized training by the specialized nurse is performed in every stoma patient in our department. That might lead to a better perception of QOL in our study.[19]

While most of the studies have suggested that the sexual function was impaired in patients receiving permanent stomas,[15,20,21] in present study, no difference in this dimension of the QLQ-C38 was revealed. Unexpected, the sexual functioning score tended to be higher in patients with APR than in patients with LAR, although the difference was not significant. Because of a small sample size and older age of our patients than in other studies, no valid conclusion can be made regarding this issue. Urinary problems were more frequently encountered after APR than after LAR. These differences are probably surgeon dependent.

The present study is limited by a lack of control measurements before the treatment. In addition, the number of evaluated patients was small, as only patients without evidence of disease treated in one clinical trial were surveyed. So a lack of statistical power might also be relevant. To obtain a large, unselected patient sample, we started to evaluate the QOL of all patients with rectal cancer, treated with preoperative radiochemotherapy, prospectively: before preoperative treatment, 1 year and 3 years after the operation.

In conclusion, consequences of the multimodality treatment of rectal cancer have an important bearing on QOL. Patients after the combined modality treatment with restorative surgical procedures do not necessary have a better QOL, mainly due to the impairment of the bowel function. In addition to traditional endpoints, such a disease control and survival, assessing restrictions

in QOL are necessary to provide a comprehensive understanding of the outcome of the combined modality treatment.

References

1. Sauer R, Becker H, Hohenberger W, Rodel C, Wittekind C, Fietkau R, et al. Preoperative versus postoperative chemoradiotherapy for rectal cancer. *N Engl J Med* 2004; **351:** 1731-40.

2. Dahlberg M, Glimelius B, Graf W, P hlman L. Preoperative irradiation affects functional results after surgery for rectal cancer: Results from a randomised study. *Dis Colon Rectum* 1998; **41:** 543-49.

3. Sofić A, Šehović N, Bešlić Š, Prnjavorac B, Bilalović N, Čaluk J, et al. MR rectum imaging with ultra sound gel as instrumental contrast media in tubulovillous adenoma. *Radiol Oncol* 2008; **42:** 136-42.

4. Camilleri-Brennan J, Cteele RJC. Objective assessment of morbidity and quality of life after surgery for low rectal cancer. *Colorectal Dis* 2002; **4:** 61-6.

5. Velenik V, Anderluh F, Oblak I, Strojan P, Zakotnik B. Capecitabine as a radiosensitizing agent in neoadjuvant treatment of locally advanced resectable rectal cancer: prospective phase II trial. *Croat Med J* 2006; **47:** 693-700.

6. Aaronson NK, Ahmedzai S, Bergman S, Bullinger M, Cull A, Duez NJ, et al. The European Organisation for Research and Treatment of Cancer QLQ-C30; A quality of life instrument for the use in international clinical trials in oncology: *J Natl Cancer Inst* 1993; **85:** 365-76.

7. Sprangers MAG, te Velde A, Aaronson NK. The construction and testing of the EORTC Colorectal Cancer Specific Quality-of-life questionnaire Module (the QLQ-C38). *Eur J Cancer* 1999; **35:** 238-47.

8. Fayers P, Aaronson N, Bjordal K, Curran D, Groenvold M. EORTC QLQ-C30 Scoring Manual. 2nd edition. Brussels: EORTC Quality of Life Study Group; 1999.

9. Williams NS, Johnston D. Survival and recurrence after sphincter saving resection and abdominoperineal resection for carcinoma of the middle third of the rectum. *Br J Surg* 1984; **71:** 278-82.

10. Di Betta E, D'Hoore A, Filez L, Penninckx F. Sphincter saving rectum resection is the standard procedure for low rectal cancer. *Int J Colorectal Dis* 2003; **18:** 463-9.

11. Velenik V, Anderluh F, Oblak I, Strojan P, Segedin B, Zakotnik B. Preoperative capecitabine and concomitant radiotherapy in operable rectal cancer: a phase II study with 2 years follow-up. Science and multidisciplinary management of GI malignancies: Proceedings book 2008. p. 325. [Abstract No 516].

12. Williams NS, Johnston D. The quality of life after rectal excision for low rectal cancer. *Br J Surg* 1983; **70:** 460-2.

13. Frigell A, Ottander M, Stenbeck H, Pahlman L. Quality of life of patiemts treated with abdominoperineal resection or anterior resection for rectal carcinoma. *Ann Chir Gynaecol* 1990; **79:** 26-30.

14. Allal AS, Bieri S, Pelloni A, Spataro V, Anchisi S, Ambrosetti P, et al. Sphincter-sparing surgery after preoperative radiotherapy for low rectal cancers: feasibility, oncologic results and Quality of life outcomes. *Br J Cancer* 2000; **82:** 1131-7.

15. Grumann MM, Noack EM, Hoffmann IA, Schlag PM. Comparison of quality of life in patients undergoing abdominoperineal extirpation or anterior resection for rectal cancer. *Ann Surg* 2001; **233:** 149-56.

16. Pachler J, Wille-Jorgensson P. Quality of life after rectal resection for cancer, with or without permanent colostomy. *Cochrane Database Syst Revue* 2005; **18:** CD004323.

17. Sprangers MA, Schwartz CE. The challenge of response shift for quality-of-life-based clinical oncological research. *Ann Oncol* 1999; **10:** 747-9.

18. Guren MG, Wiig JN, Dueland S, Tveit KM, Fossa SD, Waehre H, et al. Quality of life in petients with urinary diversion after operation for locally advanced rectal cancer. *Eur J Surg Oncol* 2001; **27:** 645-51.

19. Comb J. Role of stoma care nurse: patients with cancer and colostomy. *Br J Nurs* 2003; **12:** 852-6.

20. Sprangers MAG, Taal BG, Aaronson NK, te Velde A. Quality of life in colorectal cancer. Stoma vs. nonstoma patients. *Dis Colon Rectum* 1995; **38:** 361-9.

21. Schmidt CE, Bestmann B, Kuchler T, Longo WE, Kremer B. Prospective evaluation of quality of life of patients receiving either abdominoperineal resection or sphincter-preserving procedure for rectal cancer. *Ann Surg Oncol* 2005; **12:** 117-23.

Radiol Oncol 2008; 42(4): 215-24. *doi:10.2478/v10019-008-0022-4*

research article

Management of cutaneous side effects of cetuximab therapy with vitamin K1 crème

Janja Ocvirk and Martina Rebersek

Department of Medical Oncology, Institute of Oncology Ljubljana, Ljubljana, Slovenia

Background. *Cetuximab is a chimeric human-murine monoclonal antibody against the epidermal growth factor receptor (EGFR). It has shown activities against multiple malignancies in clinical trials. EGFR-inhibitors often cause skin toxicity, most frequently acneiform eruption. Xerosis, eczema, fissures, teleangiectasias, nail changes and paronychia can be seen in some cases, rarely hyperpigmentation. The management of the skin toxicity helps patients to overcome cetuximab-associated skin toxicity and is of great importance for patients' compliance. It is generally manageable with standard topical or systemic antibiotics and anti-inflammatory agents. The education of patients prior to beginning the therapy and proactive intervention at the first signs of skin toxicity are keys to the successful management. The aim of our study was to investigate cutaneous side-effects of the treatment with cetuximab and to determine the efficacy of vitamin K1 crème.*

Methods. *From September 2006 to August 2007 30 patients with metastatic colorectal cancer were treated with cetuximab in combination with chemotherapy and suffered from acne-like rash. They were followed at least 3 months, once per week. Skin care was taken with crème with urea and 0.1% K1 vitamin (Reconval K1®) topically starting after first documented cutaneous toxicity, and was evaluated according to NCI CTCAE, ver.3.*

Results. *Of 30 patients 6 had grade 3 rash, 18 patients grade 2 and 6 patients grade 1. Reconval K1® was used twice daily. In all patients we observed the improvement of cutaneous toxicity. The median improvement was 8 days and 18 days to observe down-staging in rash at least for 1 grade. In only 3 of 6 patients with grade 3 toxicity the reduction of cetuximab dose was needed. In historical controls in all patients with grade 3 the reduction of cetuximab dose was recommended and performed. No dose reduction or delay of treatment was needed in group of patients with grade 1 and 2 cutaneous toxicity. We didn't observe any local or systemic toxicity of topical use of Reconval K1®.*

Conclusions. *To our knowledge this is the first documented effect of topical use of K1 vitamin crème for reducing cetuximab induced cutaneous toxicity in patients with metastatic colorectal cancer. We conclude that Reconval K1® is useful in skin care in patients treated with cetuximab. Further studies are needed to evaluate the impact on response rate of cetuximab and quality of life.*

Key words: cetuximab; cutaneous side-effects; vitamin K1 crème; colorectal cancer

Received 26 November 2008
Accepted 5 December 2008

Correspondence to: Janja Ocvirk, MD, PhD, Institute of Oncology Ljubljana, Zaloska 2, Ljubljana. Phone: +386 1 5879 220; Fax: +386 1 5879 305; E-mail: jocvirk@onko-i.si

Introduction

Cetuximab is a chimeric immunoglobulin G1 (IgG1) monoclonal antibody that binds to the extracellular domain of epidermal growth factor receptor (EGFR) with high specificity and a higher affinity than that of epidermal growth factors, thus blocking ligand-induced phosphorylation of EGFR. The affinity is approximately 5 to 10-fold higher than that of endogenous ligands.[1,2]

EGFR (c-erbB1 or HER1) is a member of the ErbB family of tyrosine kinase receptors. EGFR is a 170-kd cell surface protein composed of 3 regions: an extracellular ligand-binding domain, a hydrophobic transmembrane domain, and an intracellular domain with adenosine triphosphate (ATP)-dependent tyrosine kinase activity.[3] EGFR signalling pathways are involved in the control of cell survival, cell cycle progression, angiogenesis, cell migration and cellular invasion/metastasis.[4]

EGFR is found to be overexpressed in many of human tumours: colorectal, gastric, oesophageal, head and neck, lung, breast and prostate cancer, as well as glioblastoma, bladder and ovarian carcinoma.[2,5]

Binding of the antibody to EGFR prevents the stimulation of the receptor by endogenous ligands and results in inhibition of cell proliferation, enhanced apoptosis, and reduced angiogenesis, invasiveness and metastasizing. Binding of cetuximab to the receptor also results in internalization of the antibody-receptor complex which leads to an overall downregulation of EGFR expression.[6] Preclinical studies have demonstrated that cetuximab reduces the resistance to chemotherapy and radiotherapy of human tumour cell lines in vitro and of nude mice bearing xenografts of human tumours. In clinical and preclinical studies, cetuximab has been shown to induce a response to treatment when used in combination with chemotherapy in the patients previously refractory to chemotherapy.[6]

Clinical efficacy of cetuximab

Cetuximab in combination with irinotecan and oxaliplatin is approved for the treatment of patients with epidermal growth factor receptor (EGFR)-expression in metastatic colorectal cancer. In combination with radiation therapy, it is indicated for the treatment of patients with locally advanced squamous cell cancer of the head and neck (SCCHN).[4]

Metastatic colorectal cancer (CRC)

The approval of cetuximab followed the positive results of BOND trial; the combination of cetuximab plus irinotecan induced a response rate of 23% in the patients with irinotecan refractory EGFR-positive metastatic CRC and tumour stabilization in 33% of patients. The response rate after cetuximab alone in this trial was 11%.[7]

The data from the large study (MABEL) confirmed the activity of cetuximab in heavily pre-treated patients. The overall response rate was 20%, the disease control rate was 45% and the survival estimate was at that time 9.2 months.[8]

The EPIC study investigated the overall survival of the second-line irinotecan versus irinotecan plus cetuximab in metastatic CRC patients after the progression or intolerance of the first-line oxaliplatin based regimen. The addition of cetuximab to irinotecan led to a significant increase in RR (16.4 *vs* 4.2), a significant increase in disease control (61.4 *vs* 45.8), and a 30% reduction in the risk of disease progression.[9]

Cetuximab was used in the first-line therapy in several small trials and showed promising results.[2] There are also trials showing the effectiveness of cetuximab in

Table 1. Simplified classification of acneiform eruption caused by EGFR inhibitors

A/ NCI CTC v 3.0			
Rash/desquamation			
Gradus 1	Gradus 2	Gradus 3	Gradus 4
Lesions without symptoms	Lesions with symptoms	Lesions with symptoms	Exfoliative or ulcerative erythroderma
	<50% body surface	≥50% body surface	

B/ NCI CTCAE v3.0			
Rash/desquamation			
Gradus 1	Gradus 2	Gradus 3	Gradus 4
Lesions without symptoms	Lesions with symptoms	Lesions with symptoms	Exfoliative ulcerative or bullous erythroderma
	<50% body surface	≥50% body surface	
Rash: acne/acneiform			
Gradus 1	Gradus 2	Gradus 3	Gradus 4
Intervention not indicated	Intervention not indicated	Pain, disfigurement, ulceration or desquamation	-

the first-line treatment of mCRC: a phase III study (CRYSTAL trial) comparing standard FOLFIRI alone with cetuximab in combination with FOLFIRI proved the effectiveness of cetuximab. With the use of cetuximab, the median progression-free survival was significantly longer (8.9 months *vs* 8 month), and the response rate increased (46.9% *vs* 38.7%), thereby reducing the relative risk of progression by approximately 15%.[10]

The large phase II study comparing cetuximab plus FOLFOX-4 with FOLFOX-4 alone in the first-line treatment (OPUS trial) showed that the combination was effective and safe. The overall response rate increased by 10%.[11]

Cetuximab is also effective in combination with the angiogenesis inhibitor bevacizumab. The phase II trial (BOND-2 study) showed that the combination therapy with cetuximab, bevacizumab and irinotecan, compared to cetuximab and bevacizumab alone, improved the efficacy. After irinotecan failure, this combination increased the response rate and prolonged the time to progression (response rate was 37% *vs* 23% and median time to progression 7.9 months *vs* 5.6 months).[12]

The combination therapy with cetuximab after the failure of the conventional therapy increases resectability rates without increasing operative mortality or liver injury. Adam and colleagues showed that 7% of patients treated with cetuximab after the failure of the conventional therapy experienced a treatment response that allowed curative hepatectomy. These patients were unresectable after two or more lines of conventional treatment and prior to the initiation of the treatment with cetuximab.[13]

The results from phase I study[14] and phase II study showed that cetuximab could be safely administered every second week.[15]

Squamous cell carcinoma of the head and neck (SCCHN)

Cetuximab plus radiotherapy show a significant efficacy benefit over radiotherapy alone in the treatment of locally advanced SCCHN. The risk of the locoregional progression was 32% lower with the use of cetuximab plus radiotherapy than with radiotherapy alone. Cetuximab plus radiotherapy also demonstrated a significant improvement in the median overall survival versus radiotherapy alone. Also the risk of death was 26% lower with the use of cetuximab plus radiotherapy compared to radiotherapy alone.[16]

Cetuximab was investigated in the second-line and first-line settings for the patients with recurrent/metastatic SCCHN following the failure of surgery or radiotherapy. In the phase III randomized comparison of cisplatin plus cetuximab or cisplatin plus placebo, the addition of cetuximab to cisplatin increased the response rate to 26% and 10%, respectively, and was also associated with the trend towards a prolonged median overall survival (9.2 vs 8.0 months).[17]

The phase I study showed that the addition of cetuximab to a platinum/5-FU combination in the treatment of patients with recurrent and/or metastatic SCCHN was active and well tolerated in the first-line settings.[18]

Cetuximab was also effective in nasopharyngeal carcinoma: the combination of cetuximab plus carboplatin showed an important clinical benefit in the patients with recurrent and/or metastatic nasopharyngeal carcinoma failing chemotherapy with an overall response rate of 12% and median overall survival of 7.6 months.[19]

Other indications

In the phase I and II studies, it was shown that the combination of capecitabine plus cetuximab together with radiotherapy, as well as capecitabine, oxaliplatine plus cetuximab together with radiotherapy could be feasible and safe regimens for rectal cancer.[2]

Other phase II and III studies showed a significant response to treatment in variable proportions of patients with non-small cell lung cancer (NSCLC) when cetuximab was used as the first- or second-line in combination with chemotherapy.[6]

Safety profile and side effects

Cetuximab is well-tolerated in cancer patients both as a single agent and in combination with other anti-cancer agents or radiation. Skin reactions may develop in more than 80% of patients and mainly present as acne-like rash and/or, less frequently, as pruritus, dry skin, desquamation, hypertrichosis, or nail disorders (e.g. paronychia). Approximately 15% of the skin reactions are severe, including single cases of skin necrosis. The majority of skin reactions develop within the first three weeks of therapy. They generally resolve, without sequelae, over the course of the following weeks and months even when the treatment is continued.[2,7,20]

In combination with irinotecan, additional reported undesirable effects were those related to irinotecan (such as diarrhoea, nausea, vomiting, mucositis, stomatitis, fever, leukopenia, alopecia).

In combination with the local radiation therapy of the head and neck area, additional undesirable effects were those typical of the radiation therapy (such as mucositis, radiation dermatitis, dysphagia or leucopoenia, mainly presenting as lymphocytopenia).[4]

Anaphylactic hypersensitivity reactions, characterized by a rapid onset of airway obstruction, urticaria, and hypotension, occurred in 3% of patients. Approximately

90% of the reactions developed with the first cetuximab infusion, despite premedication with antihistamines.

Other serious adverse events during cetuximab monotherapy, with the incidence of 5% or less, included interstitial lung disease, fever, sepsis, kidney failure, pulmonary embolus, dehydration, and diarrhoea.[4] Progressively decreasing serum magnesium levels which, in some patients, developed into severe hypomagnesaemia, were also noted.[21]

The EGFR is important for the normal skin development and the function.[22] In normal adult human epidermis, EGFR is strongly expressed in keratinocytes, in the sebaceous glands, and also in the epithelium of hair follicles. The expression is higher in the basal layer of the epidermis and in the outer root sheath of hair follicles, where the keratinocytes are proliferating and are undifferentiated. After the therapy with EGFR inhibitor, histopathological findings of the skin showed a thinner and more compact stratum corneum as well as prominent keratin plugs.[23] Thus, blocking the EGFR pathway leads to a unique group of skin reactions dominated by an acne-like eruptions, eczema, xerosis, changes of the hair and nails.

Vitamin K is activator EGFR pathway. The use of vitamin K crème can reduce skin toxicity caused by EGFR inhibitors.[24] The aim of our study was to determine the efficacy of vitamin K1 crème.

Patients and methods

The treatment of metastatic colorectal cancer with cetuximab after the failure of the treatment with irinotecan was first performed in Slovenia in 2005. During the period from September 2006 to August 2007, thirty patients with metastatic colorectal cancer were treated with cetuximab in combination with chemotherapy and suffered from acne-like rash.

The patients with the typical acneiform rash skin reactions were included. They occurred from the sixth day after the first application of cetuximab to 14 days at the latest. They were followed once per week at least 3 months. For the clinical improvement was relevant the improvement of skin adverse reactions at each control. Skin care was taken with crème with urea and 0.1% K1 vitamin (Reconval K1®) topically twice per day starting after the first documented cutaneous toxicity, It was classified according to the National Cancer Institute Common Toxicity Criteria, Version 3.0 (NCI CTC v 3.0 (Table 1).[25]

Erbitux was administered at a loading dose of 400 mg/m^2 infused over 2 hours, followed by a weekly dose of 250 mg/m^2 infused over 1 hour. The patients were premedicated with a histamine$_1$ antagonist with or without corticosteroids.

Results

The treatment with cetuximab showed a great efficacy with the evident skin toxicity. The most common side effect seen with cetuximab was an acneiform skin rash. The following skin reactions were also observed: hair and nail changes, rhagades, paronychia, trichomegalia, and uveitis.

Acneiform rash skin reactions

Acneiform eruptions were more or less confined to the seborrhoea areas which are rich in sebaceous glands (face, neck, scalp, shoulders, upper trunk and chest in V-shaped patterns) (Figures 1-3). Occasionally, they affected lower parts of the back and abdomen, but rarely arms and legs.

Six out of 30 patients experienced grade 3, 18 patients grade 2, and 6 patients grade

Figure 1. Tipical acneiform eruption caused by EGFR inhibitors.

Figure 2. Tipical acneiform eruption caused by EGFR inhibitors.

1 acneiform rash skin reaction at the time we started to manage skin rash.

Acneiform eruptions compared to the acne vulgaris are different and are appearing on the changed skin which is very dry and disposed to cracks. The skin lesions consist of follicular papules, which may evolve into pustules and possibly dry out with the formation of yellow crusts. Skin lesions can be accompanied by pruritus and xerosis. The aetiology of acneiform eruptions differs from that of acne vulgaris; so, the treatment generally used for acne vulgaris is not helpful and we do not advise it (i.e. the treatment with benzoyl peroxide).

In all patients skin care with K1 crème twice per day was performed. For grade 2 acneiform eruptions, topical antibiotic preparations, mostly clindamycin (1%) and erythromycin, are used according to the antibiograms and experiences, concomitantly with vitamin K1 crème, when pustules were observed. We used systemic antibiotics in 4

Figure 3. Tipical acneiform eruption caused by EGFR inhibitors.

Figure 4a. Acneiform rash before treatment with vitamin K1 crème.

Figure 4b. The scin after 1 week of using vitamin K1 crème.

Figure 5a. Acneiform rash before treatment with vitamin K1 crème.

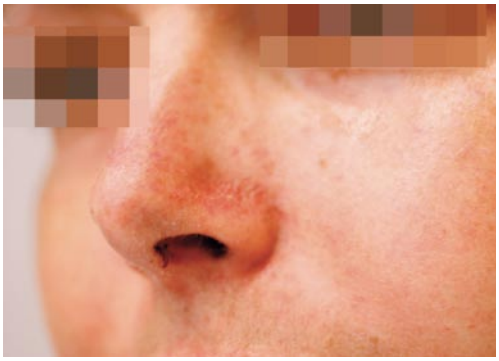

Figure 5b. The scin after 1 week of using vitamin K1 crème.

patients with G3 skin rash and topical antibiotics in 2 patients with G3 and 5 patients with G2 skin rash.

Median observed time for the improvement of skin toxicity was 8 days, but according to patients' report it was even shorter. We also recorded lowering of grade of skin rash. Median time for the improvement of skin rash of all grades was 18 days.

The results of the improvement of skin rash are presented in figures (Figures 4-7).

In case of grade 3 reaction, the treatment with cetuximab should be discontinued until the reactions resolve recording to SmPC of drug. The treatment can be restarted at a lower dose. We discontinued the treatment in only 3 patients with G3 skin rash; no case of grade 4 skin rash was reported.

Other less common reactions are nail changes (paronychia), hair modifications, xeroses trichomegalia, dry itchy skin, rhagades, uveitis and conjunctivitis, telangiectasias, hyperpigmentation, fissures in genital and anal region.

In a group of patients, where we used vitamin K1 crème, 3 and 6 months after the treatment we did not observe any xeroderma or telangiectasias, even they are frequently noticed in the cetuximab treatment; especially we observed them in patients before using vitamin K1 crème.

Figure 6a. Acneiform rash before treatment with vitamin K1 crème.

Figure 6b. The skin after 1 week of using vitamin K1 crème.

Figure 7a. Acneiform rash before treatment with vitamin K1 crème.

Figure 7b. The skin after 1 week of using vitamin K1 crème.

Discussion

Cetuximab is a monoclonal antibody which is registered for the treatment of metastatic colorectal cancer, head and neck cancers and lately also in the treatment of NSCLC. By blocking EGFR inhibits the proliferation of different types of tumour cells, as well as normal cells expressing EGFR, which are in skin, intestinal mucus and liver cells. The overexpression of EGFR in the epidermis, sweat glands, hair follicles and endotelium cells is reflected as an adverse reaction on the skin, mucus membranes, hair and nails.[20,26]

Skin toxicities are especially acneiform eruption, xerosis, fissures of palms and foot, paronychia and changes in hair growth. Aetiology and signs of skin reactions of patients in our study were very similar as described in many articles.[27-29]

Adverse events are related to the dose and are more intensive at high dose; by the lowering of the dose, the intensity of adverse events decreases, too. The correlation between the extent and/or severity of the acneiform eruption and anti-tumour efficacy of cetuximab, which was reported in literature, was observed also in our patients.[20]

Therapeutic methods for the management of skin adverse effects observed in the treatment with cetuximab are not standardized because there are no effective products to treat them and, above all, because published data are very contradictory.

In all patients with G1 acneiform rash we used only vitamin K1 crème. In patients with super-infections of skin presented as pustules, we used also topic or systemic antibiotics according to clinical references and the extent of infection (G2 and G3 side effects). We also used 1% topic antibiotic clindamicyn in 5 of 18 patients with G2 skin toxicity, namely, pustules and 2 with G3 skin toxicity. We often decided for the use of systemic antibiotic in such cases according to previous experiences. According to our experiences, we advise not to use benzoyl peroxide for the management of acneiform eruptions, as well as not to use corticosteriods.

For the patients who have grade 1 acneiform eruptions, the treatment with vitamin K1 crème alone was enough to manage skin toxicity. For the patients with grade 2 skin eruptions, the addition of topical antibiotics to the already mentioned therapy is recom-

mended for those with pustules; especially clindamycin is clinically proved and according to its antibiogram considered to be the most effective antibiotic. The appropriate treatment of the patients with grade 3 skin reactions is systemic treatment with antibiotic clindamycin and topically with vitamin K1 crème.

Conclusions

It is very important to recognize timely and accurately the skin adverse effects of EGFR inhibitors and to treat them promptly in order to assure a better quality of life to the patients during the treatment. In addition to traditional endpoints, such as disease control and survival, the quality of life became more and more important.[27,30] The proper management of skin reactions enables the longer treatment with cetuximab, without the dose reduction or drug discontinuation. The continuous treatment assures effective treatment, better response to treatment, and longer survival of patients, which is the most important goal to be achieved.

Patients have to be encouraged to follow physician's advice regarding the treatment of dermatological side effects. The appropriate treatment of side effects allows the patients to continue receiving the therapy without dose reduction or drug discontinuation and to have better outcome of the treatment.

The study performed at our clinic is the first documented effect of topical use of K1 vitamin crème for reducing cetuximab induced cutaneous toxicity in patients with metastatic colorectal cancer. We conclude that Reconval K1® is useful in skin care in patients treated with cetuximab. Further studies are needed to evaluate the impact on the response rate of cetuximab and quality of life.

References

1. Baselga J. Why the epidermal growth factor receptor? The rationale for cancer therapy. *Oncologist* 2002; **7(Suppl 4):** 2-8.
2. Moosmann N, Heinemann V. Cetuximab in the treatment of metastatic colorectal cancer. *Expert Opin Biol Ther* 2007; **7:** 243-56.
3. Frieze DA, McCune JS. Current status of cetuximab for the treatment of patients with solid tumors. *Ann Pharmacother* 2006; **40:** 241-50.
4. Summary of product characteristics. http://www.emea.europa.eu/humandocs/Humans/EPAR/erbitux/erbitux.htm; 25 November 2008.
5. Smrdel U, Kovač V. Erlotinib in previously treated non-small-cell lung cancer. *Radiol Oncol* 2006; **40:** 39-42.
6. Harding J, Burtness B. Cetuximab: an epidermal growth factor receptor chimeric human-murine monoclonal antibody. *Drugs Today* 2005; **41:** 107-127.
7. Cunningham D, Humblet Y, Siena S, Khayat D, Bleiberg H, Santoro A, et al. Cetuximab monotherapy and cetuximab plus irinotecan in irinotecan-refractory metastatic colorectal cancer. *N Eng J Med* 2004; **351:** 337-45.
8. Wilke H, Glynne-Jones R, Thaler J, Adenis A, Preusser P, Aguilar EA, et al. Cetuximab plus irinotecan in heavily pretreated metastatic colorectal cancer progressing on irinotecan: MABEL Study. *J Clin Oncol* 2008; **26:** 5335-43.
9. Scheiuthauer W, Sobrero A, Lenz HJ, Maurel J, Lutz M, Middleton G, et al. Cetuximab plus irinotecan in patients with mCRC who failed prior oxaliplatin-based therapy: the EPIC trial. [Abstract]. *Eur J Cancer* 2007; **5(4):** 235.
10. Van Cutsem E, Nowacki M, Lang I, Cascinu S, Schepotin I, Maurel J, et al. Randomized phase III study of irinotecan and 5-FU/FA with or without cetuximab in the first-line treatment of patients with metastatic colorectal cancer (mCRC): the CRYSTAL trial. ASCO 2007. *J Clin Oncol* 2007; **25(18 Suppl):** Abstract 4000.
11. Bokemeyer C, Staroslawska E, Makhson A, Bondarenko I, Hartmann JT, Shelygin Y, et al. Cetuximab plus 5-FU/FA/oxaliplatin (FOLFOX-4) versus FOLFOX-4 in the first-line treatment of metastatic colorectal cancer (mCRC): a large-scale phase II study, OPUS. [Abstract]. *Eur J Cancer* 2007; **5(4):** 236.

12. Salz LB, Lenz HJ, Kindler HL, Hochster HS, Wadler S, Hoff PM, et al. Randomized phase II trial of cetuximab, bevacizumab, and irinotecan compared with cetuximab and bevacizumab alone in irinotecan-refractory colorectal cancer. The BOND-2 study. *J Clin Oncol* 2007; **25:** 4516-8.

13. Adam R, Aloia T, Levi F, de Haas RJ, Paule B, Bralet MP, et al. Hepatic resection after rescue cetuximab treatment for colorectal liver metastases previously refractory to conventional systemic treatment. *J Clin Oncol* 2007; **25:** 4593-602.

14. Ciardiello F, Cervantes A, Vega-Villegas ME, Casado E, Rodriguez-Braun E, Martinelli E, et al. Optimal dose for an every 2 week (q2w) cetuximab (C) regimen in patients (pts) metastatic colorectal cancer (mCRC): a phase I safety, pharmacokinetics(PK) and pharmacodynamics (PD) study of weekly (q1w) add q2w schedules. [Abstract]. *Eur J Cancer* 2007; **5(4):** 247.

15. Pfeiffer P, Bjerregaard JK, Qvortrup C, Jensen BV, Yilmaz M, Nielsen D. Simplification of cetuximab (Cet) administration: double dose of every second week as a 60 minute infusion. *J Clin Oncol* 2007; **25(18 Suppl):** Abstract 4133.

16. Bonner JA, Harari PM, Giralt J, Azarnia N, Shin DM, Cohen RB, et al. Radiotherapy plus cetuximab for squamous-cell carcinoma of the head and neck. *N Eng J Med* 2006; **354:** 567-78.

17. Burtness B, Goldwasser MA, Flood W, Mattar B, Forrastiere AA. Phase III randomized trial of cisplatin plus cetuximab in metastatic/recurrent head and neck cancer: An eastern Cooperative Oncology Group study. *J Clin Onc*ol 2005; **23:** 8646-54.

18. Bourhis J, Rivera F, Mesia R, Awada A, Geoffrois L, Borel C, et al. Phase I/II study of cetuximab in combination with cisplatin or carboplatin and fluorouracil in patients with recurrent or metastatic squamous cell carcinoma of the head and neck. *J Clin Oncol* 2006; **24:** 2866-72.

19. Bernier J. Cetuximab in the treatment of head and neck cancer. *Expert Rev Anticancer Ther* 2006; **6:** 1539-52.

20. Saltz LB, Meropol NJ, Loehrer PJ Sr, Needle MN, Kopit J, Mayer RJ. Phase II trial of cetuximab in patients with refractory colorectal cancer that expresses the epidermal growth factor receptor. *J Clin Oncol* 2004; 22: 1201-8.

21. Carson EJ, Novak AM, Stella PJ. Hypomagnesemia in patients with stage IV colorectal cancer treated with cetuximab as a single agent. [Abstract 3655]. *Proc Am Soc Clin Oncol* 2005; **24:** 248-54.

22. Vallbohmer D, Lenz HJ. Epidermal growth factor receptor as a target for chemotherapy. *Clin Colorectal Cancer* 2005; **5(Suppl 1):** S19-27.

23. Damjanov N, Meropol NJ. Epidermal growth factor receptor inhibitors for the treatment of colorectal cancer: a promise fulfilled? *Oncology* 2004; **18:** 479-88.

24. Perez- Soler R, Zou Y, Li T, Tornos C, Ling Y. Topical vitamin K3 (Vit K3, Menadione) prevents erlotinib and cetuximab-induced EGFR inhibition in the skin. *J Clin Oncol* 2006; **24(18 Suppl):** Abstract 3036.

25. National Cancer Institute. Common terminology criteria for adverse events v.3.0 http:// ctep.cancer.gov/reporting/ctc.html.

26. Busam KJ, Capodieci P, Motzer R, Kiehn T, Phelan D, Halpern AC. Cutaneous side-effects in cancer patients treated with the epidermal growth factor receptor antibody C225. *Br J Dermatol* 2001; **144:** 1169-76.

27. Segaert1 S, Van Cutsem E. Clinical signs, pathophysiology and management of skin toxicity during therapy with epidermal growth factor receptor inhibitors *Ann Oncol* 2005; **16:** 1425-33.

28. Agero ALC, Dusza SW, Benvenuto-Andrade C, Busam KJ, Myskowski P, Halpern AC. Dermatological side-effects associated with the epidermal growth factor receptor inhibitors. *J Am Acad Dermatol* 2006; **55:** 657-70.

29. Galimont-Collen AFS, Vos LE, Lavrijsen APM, Ouwrkerk J, Gelderblom H. Classification and management of skin, hair, nail and mucosal side-effects of epidermal growth factor receptor (EGFR) inhibitors. *Eur J Cancer* 2007; **43:** 845-51.

30. Velenik V, Oblak I, Anderluh F. Quality of life in patients after combined modality treatment of rectal cancer: Report of a prospective phase II study. *Radiol Oncol* 2008: **42:** 207-14.

case report

Pituitary metastasis of renal cell carcinoma: a case report

Vesna Bišof[1], Antonio Juretić[1], Nera Šarić[1], Ante Melada[2], Zdravko Perković[3], Marko Radoš[4], Ranka Padovan Štern[4]

[1]Department of Oncology, [2]Department of Neurosurgery, [3]Department of Endocrinology, [4]Clinical Institute for Diagnostic and Interventional Radiology, University Hospital Centre "Zagreb", Zagreb, Croatia

Background. *Solitary metastasis of renal cell carcinoma in the pituitary gland is extremely rare and only in 7% of cases it is symptomatic.*

Case report. *We report the case of a 52 year old man presenting with visual disturbance and headache after three years of treatment due to the metastatic renal cell carcinoma. Magnetic resonance imaging (MRI) showed tumour mass in supraselar region compressing optic chiasm with no other brain metastatic lesions. The trans-sphenoidal reduction of the tumour was performed. Pathology and imunohistology revealed metastasis of clear cell renal carcinoma.*

Conclusions. *This is the 25th case of symptomatic pituitary metastases of renal cell carcinoma reported in literature.*

Key words: pituitary gland; renal cell carcinoma; metastasis

Introduction

Renal cell carcinoma is the most common primary tumour of the kidney accounting 1 - 3% of all adult malignancies.[1] Although brain is the fourth most common site of metastasis after lung, bone and liver with approximately 5%[1], solitary metastasis of renal cell carcinoma in the pituitary gland is extremely rare.[1-6] The frequency of pituitary metastases from systemic malignant tumours ranged from 1% to 25% at autopsy.[7] Only 7% of pituitary metastases are symptomatic.[2] Pituitary metastases occur usually in patients with highly disseminated disease. Breast and lung cancer are the most common diseases that metastasize to the pituitary gland.[2,6]

Received 14 October 2008
Accepted 28 October 2008

Correspondence to: Vesna Bišof, MD, Department of Oncology, University Hospital Centre "Zagreb", Kišpatićeva 12, Zagreb, Croatia. Phone: +385 1 2388 035; Fax: +385 1 2388 583; E-mail: vesna.bisof@zg.t-com.hr

Case report

We present the case of a patient diagnosed with a pituitary gland metastatic renal cell carcinoma after three years of treatment due

Figure 1a. Tumour mass in supraselar region presented by magnetic resonance imaging (MRI), sagittal image.

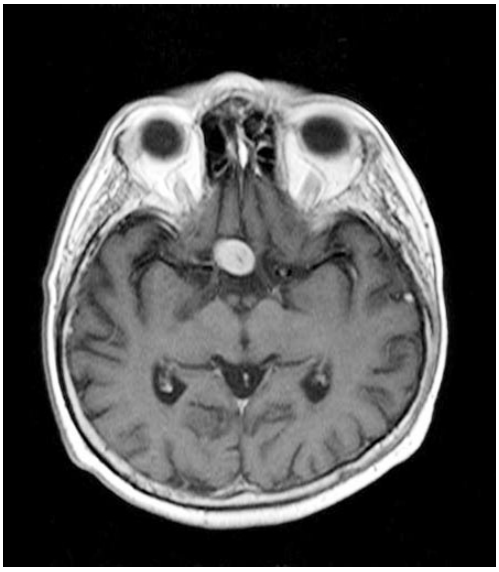

Figure 1b. Tumor mass in supraselar region presented by magnetic resonance imaging (MRI), axial image.

to the metastatic disease. In August 2003, a 49 year old man presented with tumour of the lower part of the left kidney. Left nephrectomy was performed. Pathology confirmed clear cell carcinoma, tumour stage T3bN0M0. During his first postoperative visit to the oncological department multiple bilateral lung metastases smaller than 1 cm in diameter were found along with osteolysis of the posterior part of the forth right rib. Patient ECOG score was 0. Since interferon and interleukin-2 were not registered for the treatment of metastatic renal cell carcinoma in Croatia, his treatment was started with chemotherapy – vinblastin 6 mg/m^2 every two weeks from December 2003 until June 2004.

Control examinations performed during the treatment revealed a stable disease. However, on control computed tomography (CT) in September 2004 the progression of the forth posterior rib lesion measuring now 3.5 x 6.8 cm in diameter with protrusion in intratoracic space was found. Lung metastatic disease was stable. There was no sign of other metastatic site. The palliative radiotherapy treatment to the progressed lesion of the forth posterior rib was performed; dose 30 Gy in 10 fractions. The second line chemotherapy was lomustin (CCNU) 160 mg every 5 weeks, 7 cycles, from October 2004 until May 2005.

CT scan done in May 2005 revealed the progression of lung metastases *i.e*. enlargement in size and number of lung lesions. On the contrary, the lesion of the forth rib was smaller than on the previous CT scan. Since June 2005 until September 2005 the patient was treated with 5-fluorouracil (5-FU) once a week and with an interferon A 2α 3 mil IU sc. three times a week (purchased by the patient). Due to the fatigue of the patient and enlargement of the fourth rib lesion, along with stable disease of other metastatic lung lesions, it was decided to perform reirradiation to enlarged lesion, total dose 30 Gy in 10 fractions. From December 2005 until April 2006, 5 - FU and interferon A 2α therapy was continued. Due to the progression of the lung lesions from April 2006 un-

Table 1. Reported cases of pituitary metastasis from renal cell carcinoma

Author	Age/Sex	Interval from primary diagnosis to pituitary metastasis	Endocrinological finding	Visual involvement	Treatment
Anniko *et al.* (1981)[8]	59/M	9 years	hypopituitarism	yes	surgery
Bounaguidi *et al.* (1983)[9]	53/M	0 year	hypopituitarism, diabetes insipidus	yes	surgery, RT to pituitary fossa
James *et al.* (1984)[3]	75/M	9 years	normal	yes	surgery
Eick *et el.* (1985)[10]	66/M	0 year	hypopituitarism	no	surgery, RT to pituitary fossa and whole brain
Horikoshi *et al.* (1988)[11]	51/M	0 year	hypopituitarism	yes	surgery, RT to pituitary fossa
McCormic *et al.* (1989)[5]	35/F	0 year	hypopituitarism	yes	surgery, RT to sella and parasellar region
Nishio *et al.* (1992)[12]	63/F	4 years	hypopituitarism	yes	surgery, RT to pituitary fossa
Koshiyama *et al.* (1992)[4]	57/M	0 year	hypopituitarism	yes	surgery, RT to pituitary fossa
Weiss *et al.* (1993)[13]	59/M	0 year	hypopituitarism	yes	surgery, RT to pituitary fossa
Uchino *et al.* (1996)[14]	63/F	4 year	NA	NA	surgery
Beckett *et al.* (1998)[15]	56/M	0 year	hypopituitarism	no	surgery, RT to pituitary fossa, interferon-α
Marar *et al.* – 2 cases (1998)[16]	54/M	3 years	hypopituitarism	yes	surgery
	73/M	8 years	hypopituitarism	no	surgery
Weber *et al.* (2003)[17]	62/M	4 years	diabetes insipidus	yes	surgery
Basaria *et al.* (2004)[18]	77/F	3 months	hypopituitarism	yes	surgery, stereotactic RT
Yokoyama *et al.* (2004)[1]	63/M	8 years	hypopituitarism, diabetes insipidus	yes	stereotactic RT
Pallud *et al.* (2005) [19]	70/M	6 years	NA	yes	surgery, RT to pituitary fossa
Liu et al. (2005)[7]	54/M	NA	hypopituitarism	yes	surgery, RT to pituitary fossa, interferon-α
Gopan *et al.* (2007) – five cases[20]	67/M	27 years	hypopituitarism, diabetes insipidus	yes	surgery, whole brain RT with boost to the pituitary fossa
	51/M	12 years	hypopituitarism	yes	surgery, whole brain RT , interferon-α, thalidomide, sunitinib
	53/M	0 year	hypopituitarism, diabetes insipidus	yes	surgery, RT to the sella
	67/F	11 years	hypopituitarism	no	stereotactic RT, sorafenib
	61/F	1 year	hypopituitarism	no	stereotactic RT, AG 013736*
Bisof *et al.* (2008) – this report	49/M	3 years	hypopituitarism	yes	surgery, whole brain RT

* phase II clinical trial with tyrosine kinase inhibitor AG-013736

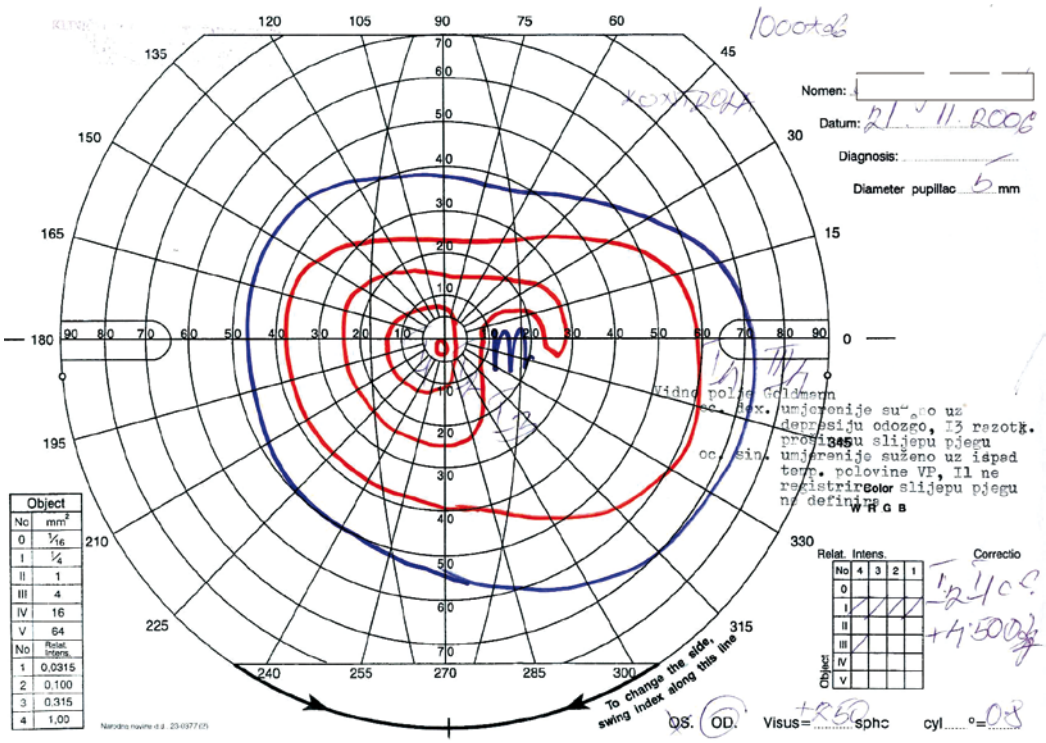

Figure 2a. Disturbances in visual function presented by Goldmann test, right eye.

til August 2006 the patient was treated with gemcitabin 600 mg/m^2, days 1 and 8, every 28 days (purchased by the patient).

In August 2006 vision disturbances and headache had been first reported. Magnetic resonance imaging (MRI) showed tumour mass in supraselar region 30 x 13 mm in diameter compressing optic chiasm. A radiological examination did not demonstrate other possible brain metastatic lesions. Based on the radiological imaging it was difficult to differentiate pituitary macroadenoma, meningeoma and metastasis of tumour (Figures 1a, 1b).

Since visual function deteriorated progressively, a trans-sphenoidal surgery was performed. Pathology and imunohistology revealed metastasis of clear cell renal carcinoma.

The visual function was quickly improved but Goldmann test (Figures 2a, 2b) showed still disturbances in the visual function. Endocrinological findings were almost consistent with panhypopituitarism: T4 = 80.8 nml/L (normal range 70 - 165), TSH < 0.05 mIJ/L (0.40 - 4.2), testosteron < 0.03 nmol/L (3 - 22, for > 50 yrs), SHBG 7 nmol/L (15 -100), cortisol = 13 nmol/L (138 - 690), aldosteron = 879 pmol/L (20 - 410). A replacement hormone therapy was introduced to the patient.

Postoperative control MRI after two months showed residual tumour 20x13x12 mm in diameter but now along with multiple brain metastases. The palliative brain photon beam radiotherapy was performed, total dose 30 Gy in 10 fractions. CT scan of thorax and abdomen revealed the progression of the lung metastases and the occur-

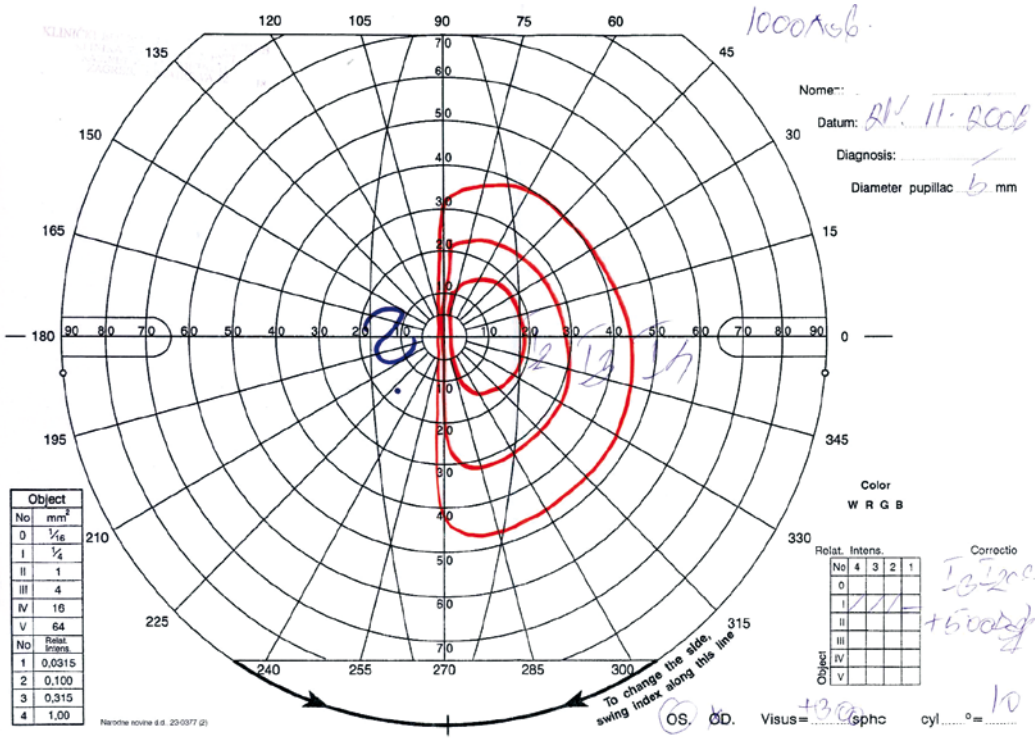

Figure 2b. Disturbances in visual function presented by Goldmann test, left eye.

rence of new bone metastases. Surprisingly, the patient was without respiratory disturbances but he reported fatigue. His general appearance was Cushingoidal. He died ten months after the operation of the pituitary gland.

Discussion

Up to our knowledge only 24 cases of symptomatic pituitary metastasis of renal cell carcinoma has been reported in the literature (Table 1). Only six of them were female, while 18 were men. The majority *i.e.* 19 patients presented with hypopituitarism, while 17 patients presented with visual field defect like our patient. Our patient has not experienced symptoms of *diabetes insipidus* which is reported to be more frequent in pituitary metastasis than in pituitary adenomas.[7,21] It is very difficult to differentiate pituitary metastasis from adenoma based on radiological and clinical findings.[2,3,10,12,22] But Liu *et al.*[7] found out that the strong enhancement of the tumour and the strong bone destruction without marked sellar enlargement are characteristic radiological features of pituitary metastasis. Fassett *et al.*[2] stated that thickening of the pituitary stalk, invasion of the cavernous sinus and sclerosis of the surrounding *sella turcica* could indicate pituitary metastasis. Tumour invasiveness usually makes the resection difficult. There was no significant survival benefit in surgical series.[2] The treatment of pituitary metastasis is multimodal, consisting of surgery, radiotherapy and chemotherapy. The long-term benefit of postoperative radiotherapy is not known

due to the rarity of such cases. The applied dose ranged in the literature from 9 to 60 Gy, with median dose 36 Gy.[6] Our patient was treated with 30 Gy in ten fractions due to the occurrence of brain metastases although first it was intended to apply a higher dose. Stereotactic radiotherapy can be beneficial in sparing the optic nerves. The primary aim of treating pituitary metastasis is to improve the quality of life through symptomatic relief and to prevent the neurological deterioration.

The overall median length of the patient's survival after the diagnosis of pituitary metastasis is only 180 days.[6] However, the paper recently published by Gopan *et al*.[20] reported the overall survival ranging from 6 to 46 months from the initial diagnosis of pituitary metastasis. This can be explained by the application of new chemotherapeutic agents like sorafenib and sunitinib. Stereotactic radiotherapy with or without whole brain radiotherapy was performed in all five reported patients.

In our case, whole brain radiotherapy was performed due to the brain dissemination. Sorafenib and sunitinib were not registered for the treatment of metastatic renal cell carcinoma in our country at the time.

Symptomatic pituitary metastasis of renal cell carcinoma is a rare case, occurring usually in highly disseminated renal cell carcinoma. Palliative surgery and radiotherapy treatment can contribute essentially to the improvement of the quality of life of such patients.

References

1 Yokoyama T, Yoshino A, Katayama Y, Watanabe T, Kashima Y, Yoshikawa T, et al. Metastatic pituitary tumour from renal cell carcinoma treated by fractionated stereotactic radiotherapy (Case report). *Neurol Med Chir (Tokyo)* 2004; **44:** 47-52.

2 Fassett DR, Couldwell WT. Metastases to the pituitary gland. *Neurosurg Focus* 2004; **16:** E8.

3 James RL Jr, Arsenis G, Stoler M, Nelson C, Baran D. Hypophyseal metastatic renal cell carcinoma and pituitary adenoma. Case report and review of the literature. *Am J Med* 1984; **76:** 337-40.

4 Koshiyama H, Ohgaki K, Hida S, Takasu K, Yumitori K, Shimatsu A, Koh T. Metastatic renal cell carcinoma to the pituitary gland presenting with hypopituitarism. *J Endocrinol Invest* 1992; **15:** 677-81.

5 McCormick PC, Post KD, Kandji AD, Hays AP. Metastatic carcinoma to the pituitary gland. *Br J Neurosurg* 1989; **3:** 71-9.

6 Morita A, Meyer FB, Laws ER Jr. Symptomatic pituitary metastases. *J Neurosurg* 1998; **89:** 69-73.

7 Liu H, Ymaki T, Oka S-I, Koyanagi I, Houkin K. Metastatic renal cell carcinoma mimicking pituitary adenoma: case report. *Neurol Med Chir (Tokyo)* 2005; **45:** 418-22.

8 Anniko M, Lundquist PG, Silfversward C, Wersall J. Hypernephroma metastasis in the pituitary gland. A case report. *Arch Otorhinolaryngol* 1981; **232:** 227-32.

9 Buonaguidi R, Ferdeghini M, Faggionato F, Tusini G. Intrasellar metastasis mimicking a pituitary adenoma. *Surg Neurol* 1983; **20:** 373-8.

10 Eick JJ, Bell KA, Stephan MT, Fuselier HA Jr. Metastatic renal cell carcinoma presenting as an intrasellar mass on computerizes tomography. *J Urol* 1985; **134:** 128-30.

11 Horikoshi T, Mitsuka S, Kimura R, Fukamachi A, Nukui H. Renal cell carcinoma metastatic to the hypophysis, case report. *Neurol Med Chir (Tokyo)* 1988; **28:** 78-82.

12 Nishio S, Tsukamoto H, Fukui M, Matsubara T: Hypophyseal metastatic hypernephroma mimicking a pituitary adenoma. Case report. *Neurosurg Rev* 1992; **15:** 319-22.

13 Weiss RE, Corvalan AH, Dillon RW. Metastatic renal cell carcinoma presenting as impotence. *J Urol* 1993; **149:** 821-2; discussion 823.

14 Uchino A, Hasuo K, Mizushima A, Matsumoto S, Mihara F, Jimi M et al. Intracranial metastasis of renal cell carcinoma: MR imaging. *Radiat Med* 1996; **14:** 71-6.

15 Beckett DJ, Gama R, Wright J, Ferns GA. Renal carcinoma presenting with adrenocortical insufficiency due to a pituitary metastasis. *Ann Clin Biochem* 1998; **35(Pt 4):** 542-4.

16 Marar IE, Kandil H, Kanal E, Marion D, Inman M, Amico JA. Renal cell carcinoma metastatic to the pituitary gland: clinical manifestations and successful treatment with transsphenoidal resection. *Endocr Pract* 1998; **4:** 204-7.

17 Weber J, Gassel AM, Hoch A, Spring A. Concomitant renal cell carcinoma with pituitary adenoma. *Acta Neurochir (Wein)* 2003; **145:** 227-31.

18 Basaria S, Westra WH, Brem H, Salvatori R. Metastatic renal cell carcinoma to the pituitary presenting with hyperprolactinemia. *J Endocrinol Invest* 2004; **27:** 471-4.

19 Pallud J, Nataf F, Roujeau T, Roux FX. Intraventricular haemorrhage from a renal cell carcinoma pituitary metastasis. *Acta Neurochir (Wein)* 2005; **147:** 1003-4.

20 Gopan T, Toms SA, Prayson RA, Suh JH, Hamrahian AH, Weil RJ. Symptomatic pituitary metastases from renal cell carcinoma. *Pituitary* 2007; **10:** 251-9.

21 Mäurer J, Busch M, Matthaei D, Helwig A, Dühmke E. Diabetes insipidus and breast carcinoma – the importance of NMR tomography planning. *Strahelenther Onkol* 1993; **169:** 126-8.

22 Sioutos P, Yen V, Arbit E. Pituitary gland metastases. *Ann Surg Oncol* 1996; **3:** 94-9.

Radiol Oncol 2008; 42(4): 232-9. *doi:10.2478/v10019-008-0015-3*

research article

A phantom to assess the accuracy of tumor delineation using MRSI

Amr A. Heikal, Keith Wachowicz, Steven D. Thomas, Biagio Gino Fallone

Department of Medical Physics, Cross Cancer Institute; Departments of Oncology and Physics, University of Alberta, Edmonton, Alberta, Canada

Background. *Studies have demonstrated that magnetic resonance spectroscopic imaging (MRSI) can detect regions of abnormal activity (tumor) that would not have been covered using conventional imaging and contouring methods. With increased interest in MRSI it is important that its accuracy in tumor delineation be investigated. While some effort has been made to design phantoms to examine the performance of MRSI sequences, most phantoms rely on using traditional glass or acrylic as the phantom building material.*

Material and methods. *In this work, a gel-based detail phantom has been developed to assess the ability of the spectroscopic imaging sequences to accurately represent the geometry of tumors. The gel-based phantom is used as an alternative to conventional acrylic or glass based phantoms for use with MRSI.*

Results. *Gel-based phantoms have the advantage of having a magnetic susceptibility close to that of water. In addition, we demonstrate the benefits of having no finite wall thickness separating phantom compartments. The utility of the phantom was illustrated in comparisons between different MRSI sequences of the same nominal resolution as well as different filtering parameters.*

Conclusions. *Due to their ease of construction and the reduced artifacts, gel phantoms are a reliable tool for assessing the performance of MRSI sequences.*

Key words: MR spectroscopic imaging; tumor; phantoms; brain; 3 T

Introduction

The advantages that spectroscopic imaging can offer cancer therapy are significant. By measuring different metabolite levels – effectively a means of non-invasive biopsy – magnetic resonance spectroscopic imaging (MRSI) can detect tissue abnormalities that may not yet be visible in conventional MRI. Pirzkall *et al*. and Pallud *et al.* have shown that tumor extent as shown by MRSI may differ greatly from the extent shown on conventional MRI scans.[1,2] Moreover, Walecki *et al.* have shown that MRSI may help in identifying patients who have a high risk of recurrence.[3] This has led to an increase in interest in incorporating MRSI into treatment planning by adding a biological target volume in the contouring process. More recently, several methods of

Received 23 September 2008
Accepted 1 October 2008

Correspondence to: Amr A. Heikal, Department of Medical Physics, Cross Cancer Institute; Departments of Oncology and Physics, University of Alberta, 11560 University Avenue, Edmonton, Alberta T6G 1Z2, Canada; Phone: +1 780 989 4342; Fax: +1-780 432 8615; E-mail: aheikal@phys.ualberta.ca

tumor identification and registration techniques have been used to integrate MRSI results into the radiotherapy process.[4;5] Such studies have demonstrated that MRSI can detect regions of abnormal activity (tumor) that would not have been covered using conventional imaging and contouring methods.[5] As such, the delineation of the tumor volume in treatment plans for radiotherapy has changed when MRSI metabolite information was considered.

In the midst of the move to improve the spatial resolution of MRSI, it is important to remember that the ability to properly visualize detailed tumor boundaries is influenced by many imaging and processing parameters, not just the nominal resolution of the scan. Also, with the increased importance of spatial definition of the tumor site for radiotherapy, it is of great importance to have a method of evaluating the accuracy of the boundaries derived from an MRSI sequence under development for use in radiotherapy planning.

While some effort has been made to design phantoms to examine the performance of MRSI sequences; most phantoms have relied on using traditional glass or acrylic as the phantom building material.[6,7] Detail phantoms utilizing acrylic or glass containers are vulnerable to susceptibility artifacts arising from the interface of the compartment wall material and the solution used to fill the phantom.[8] Those artifacts are more pronounced in high-detail and irregularly shaped phantoms.

Moreover, detail phantoms rely on a sharply defined boundary between two regions of the phantom. The amount of detail an imaging sequence can reproduce is measured by how accurately it can reproduce that boundary. Having a finite wall containing no metabolites causes a pronounced partial volume artifact in the spectral data. Those artifacts enhance that boundary in a way that is not representative of a human brain. This is demonstrated in the results and discussion section.

In this work, a gel-based detail phantom has been developed to assess the ability of the spectroscopic imaging sequences to accurately represent the detailed geometry of tumors. The gel-based phantom is used as an alternative to conventional acrylic or glass based phantoms for use with MRSI because it avoids susceptibility and compartment wall-related partial volume artifacts. The use of the phantom is demonstrated by comparing the performance of three MRSI sequences.

Material and methods

Gelatin detail phantom design

A phantom designed to simulate tumors was constructed using 5% by weight porcine gel containing clinically relevant concentrations of choline chloride (3 mM) and creatine hydrate (10 mM).[9] A cast acrylic wedge (base: 3.8 cm, height: 9 cm, width: 3.8 cm) was inserted in the liquid gel and later removed when the gel hardened. The void left by the wedge was filled with a solution containing elevated levels of choline chloride (10 mM), and the same concentration of creatine as in the background (Figure 1). The higher concentration of choline inside

Figure 1. A photograph and a T2 weighted transverse image of the porcine gel detail phantom.

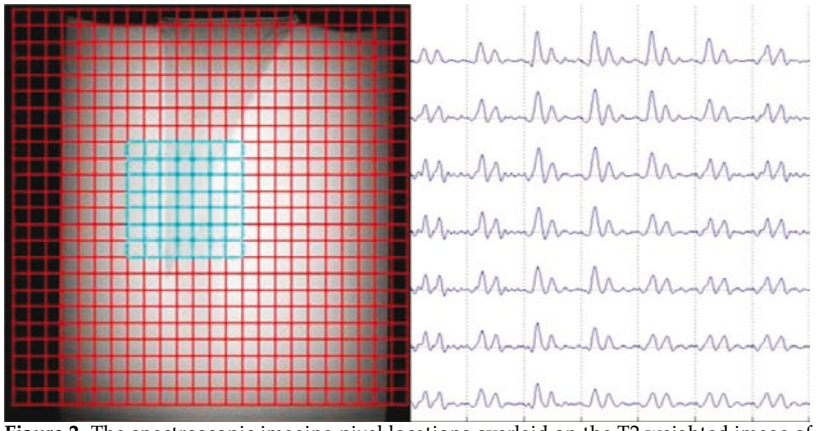

Figure 2. The spectroscopic imaging pixel locations overlaid on the T2 weighted image of the phantom. The spectra on the right correspond to the highlighted pixels. The peaks shown are Choline (left) and Creatine (right). The change in the Choline concentration inside the wedge-shaped compartment is clearly noticeable on the spectra.

the wedge-shaped void was used to simulate the presence of a malignancy.

Comparison of MRSI sequences

The phantom is designed to assess the ability of the spectroscopic imaging sequences to accurately represent the detailed geometry of tumors. The utility of this phantom was demonstrated by comparing the output of different MRSI sequences with the same nominal resolution. The phantom was scanned with 3 MRSI sequences: 2-D Point Resolved Spectroscopy (PRESS), 2-echo Spin Echo Spectroscopic Imagine (SESI), and 4-echo SESI, all of nominal voxel size 5×5×10 mm^3. A 10 mm thick single-slice T2-weighted image of the phantom was acquired at a position coinciding with the spectroscopic scans (Figure 2). This allowed a proper comparison of the spectroscopic results to the phantom geometry. Cho/Cr ratio maps were calculated for each of the spectroscopic scans.

Comparison of k-space filters

The phantom can also be used to optimize filter parameters. Such use is demonstrated by comparing the Cho/Cr maps resulting from the same 2-D PRESS sequence using different k-space filters. Since 2-D cosine k-space filters are routinely used on our system to reduce ringing, it was the type of filter chosen for this demonstration. The phantom was scanned with 2-D PRESS of nominal voxel size 5×5×10 mm^3. The data was reconstructed twice; once using no k-space filter and once using a 2-D cosine k-space filter shown in Figure 3. Similar to the previous comparison, a 10 mm thick single-slice T2-weighted image of the phantom was acquired at a position coinciding with the spectroscopic scans to allow for a proper comparison of the spectroscopic results to the phantom geometry.

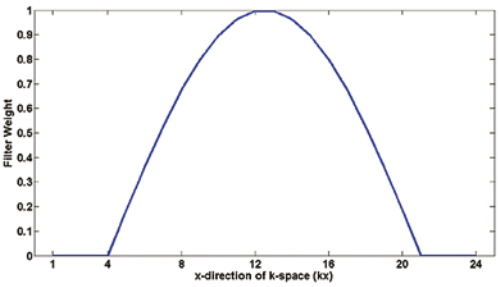

Figure 3. The profile of the 2-D cosine filter in one k-space direction.

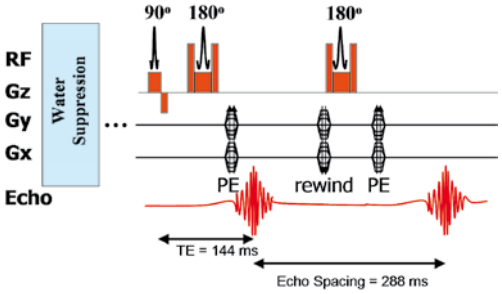

Figure 4. A schematic of a 2-echo SESI MRSI sequence.

Spectroscopic imaging scan parameters

All scans were performed on a Philips Intera 3 T MRI (Philips Medical Systems, Bothell, WA) unit together with a transmit/receive birdcage head coil. In this work two types of sequences were used: 2-D PRESS and SESI. The PRESS sequence is a standard sequence used for many in-vivo MRSI studies, especially those interested in high signal-to-noise.[10,11]

SESI offers the choice of acquiring more than one echo per repetition, hence decreasing the overall scan time.[11] The SESI sequence consists of 2 RF pulses applied on the same plane. The first 90° pulse excites the slice of interest and then a 180° refocusing pulse generates an echo at TE_1. More echoes can be generated by applying subsequent 180° refocusing pulses on the same plane each with a different phase encoding (Figure 4). This is analogous to a fast spin echo sequence in imaging.

In the multi-echo SESI sequences the centre of k-space is filled with the first echoes while the edges are filled with data from the later echoes. This produces a T2 weighting artifact in the form of decreased contrast at high spatial resolution compared to 2-D PRESS or single-echo SESI.

For all sequences the TR was set to 1500 ms, and the TE to 144 ms. The number of phase encodes and FOV was set to 24×24 and 120 mm, respectively, yielding a nominal voxel size of 5×5×10 mm^3 for all sequences. For the SESI sequences the inter-echo spacing was set to 288 ms.

Prior to running the MRSI scans, second order shimming was established over the volume-of-interest (VOI).[12] Water suppression was achieved by a mix of chemical shift selective (CHESS) suppression and inversion recovery.[13; 14] First, a CHESS excitation pulse for water is applied followed by crusher gradients. This yielded a dephased negative water signal that tends to return to equilibrium through T1 relaxation. The measurement is then acquired at the zero crossing of the water signal in a fashion similar to inversion recovery.

Processing

The raw data acquired from the MRSI scans were processed on the scanner console using MR Systems Intera (release 1.5.4.3) (Philips Medical Systems, Bothell, WA). First, a cosine filter was applied to the raw k-space data to reduce ringing. The data was then reconstructed to xy-space and adopized by a Lorentzian – Gaussian filter to reduce noise. Zero-order phase, inhomogeneities, and eddy currents were corrected using unsuppressed water measurements collected during the scans. Finally, the frequency domain data was exported to Matlab (The MathWorks, Inc., Natick, MA) where it was further analyzed using in-house developed software that calculates the area under different metabolite peaks.

Peak fitting

The in-house developed peak fitting algorithm fitted a sum of Lorentzians to the complex spectra based on seeding values for the chemical shift, estimated peak heights, and full width half maxima (FWHM).[15] A Levenberg-Marquardt algorithm was used to minimize the sum of squares of the difference between the raw spectrum and the

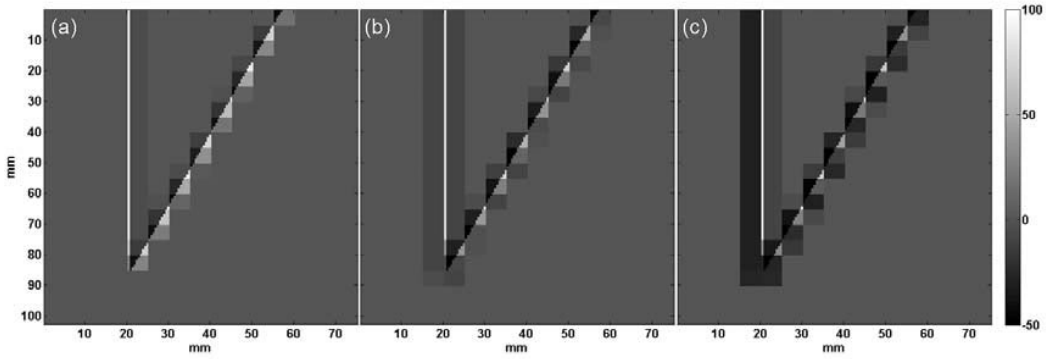

Figure 5. Percentage difference images between simulated 5×5 mm^2 pixel images and the phantom geometry using: (a) no compartment wall, (b) 1 mm wall, (c) 2 mm wall.

Lorentzians to achieve the best fit.[16]

The Lorentzian parameters (peak heights, chemical shift, and FWHM) resulting from the peak fitting algorithm were used in the software to analytically calculate the area under the peaks from each spectrum. Since phase was corrected in the processing stage, the real spectrum is assumed to be equal to the absorption spectrum. Hence the area under the peak is calculated as (π/2×FWHM×peak height). Finally, the software produced metabolite area maps, as well as a choline-to-creatine ratio map.

In-plane interpolation of the metabolite maps has been routinely used in the literature to correlate MRSI with CT and MRI images for treatment planning.[17] The interpolation smoothes the appearance of the metabolite maps and allows for better comparison with CT and MRI images. In this work, the metabolite maps were linearly interpolated to 0.5 mm pixels in-plane.

Results and discussion

Effects of the phantom wall material

The rationale behind the choice of the phantom material was to minimize magnetic susceptibility artifacts and partial volume artifacts caused by the presence of compartment walls of finite thickness. While it has been suggested in the literature that the use of water equivalent glass can solve problems of magnetic susceptibility, the problem of wall-related partial volume artifacts would still persist.[8]

The use of porcine gel as the phantom's building material can remedy both these issues. The magnetic susceptibility of the porcine gel is very close to that of water making susceptibility differences negligible. Furthermore, the lack of a physical compartment wall in this design eliminates the issue of its related partial volume artifacts.

In a simple demonstration conducted in Matlab (The MathWorks, Inc., Natick, MA), the two-dimensional geometry of the phantom was modeled using pixel dimensions of 0.5 mm. Derived from a 2-D PRESS scan of a choline filled phantom, the wedge shaped compartment was assigned arbitrary pixel values of 4000 while the pixels outside the wedge were assigned a value of 1500. A compartment wall was included in the geometric simulation whose thickness was varied between 0 mm and 2 mm and was assigned a pixel value of 0. The pixel values of the 0.5 mm model were then averaged to 5 mm pixels, a resolution achievable by MRSI. Figures 5(a), 5(b), and 5(c) show that with a thickness as small as 1 mm, compartment walls can produce visible artifacts

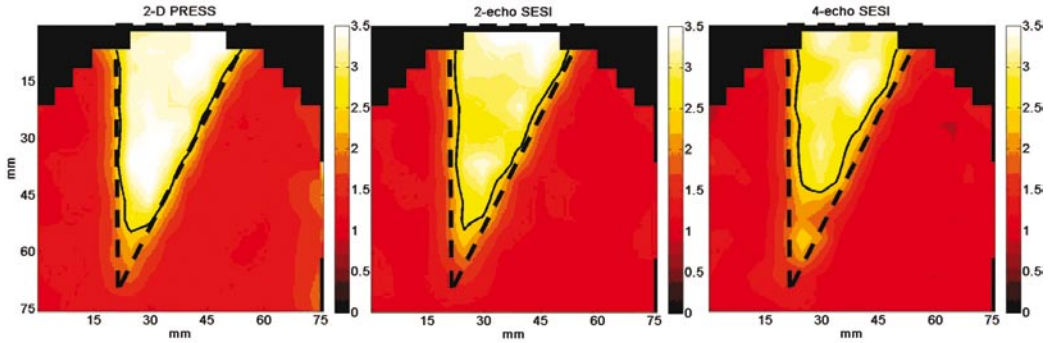

Figure 6. Comparison of the Cho/Cr ratio map and the phantom geometry. The scale represents the Cho/Cr value. The dashed line represents the phantom geometry and the solid line represents the contour at Cho/Cr ≥ 2.5. The sequences left to right are 2-D PRESS sequence, 2-echo SESI sequence and 4-echo SESI sequence.

that degrade the accuracy and performance of the phantom.

Comparison of MRSI sequences

Three MRSI sequences of the same nominal resolution were used to illustrate the utility of the gel detail phantom. Figure 6 shows the Cho/Cr ratio maps of a 2-D PRESS, a 2-echo SESI, and a 4-echo SESI sequence compared to phantom geometry.

The tip of the wedge forming the high-detail region of the phantom is intended to show differences in high-detail accuracy between the three sequences. From Figure 6, it is apparent that the 2-D PRESS and the 2-echo SESI ratio maps reveal a higher choline-to-creatine ratio extending further into the high detail region of the phantom than in the case of 4-echo SESI. Overall, 2-D PRESS and 2-echo SESI show better conformance to the phantom geometry than 4-echo SESI.

One can quantitatively compare the different sequences by analyzing the deviation between of area of the wedge as shown by the T2 weighted image and the metabolite map. For this purpose the user can choose the suitable tumor contouring criterion for the metabolite maps whether it is a specific metabolite ratio (e.g. Cho/Cr, or Cho/NAA) or z-score (e.g choline-to-NAA index).[5;18;19] In this demonstration an arbitrary Cho/Cr ≥ 2.5 was chosen as the tumor contouring criterion. The metabolite maps of the three sequences were automatically contoured at that value and the percentage difference of the areas was found to be 13.7%, 24.4%, and 38.3% for 2-D PRESS, 2-echo SESI, and 4-echo SESI, respectively. Due to the lack of T2 weighting, 2-D PRESS exhibits the smallest deviation from the phantom geometry. The larger deviations shown by multi-echo SESI can be attributed to T2 losses accumulated in acquiring more than one echo per excitation. Such losses are progressively more evident with the increasing number of echoes per excitation.

Comparison of k-space filters

The ability of MRSI to accurately detect tumor boundaries is sensitive to factors such as k-space sampling and filtering. Like the T2 weighting artifacts discussed earlier, the k-space filter parameters can greatly deteriorate tumor boundary accuracy in MRSI. The phantom was used to reveal differences in tumor delineation resulting from changing k-space filtering. Figure 7 shows the Cho/Cr ratio maps of a 2-D PRESS scan of the phantom reconstructed using unfiltered and 2-D cosine filtered k-space respectively. While the filtered dataset produces fewer noise fluctuations in the ratio map, there

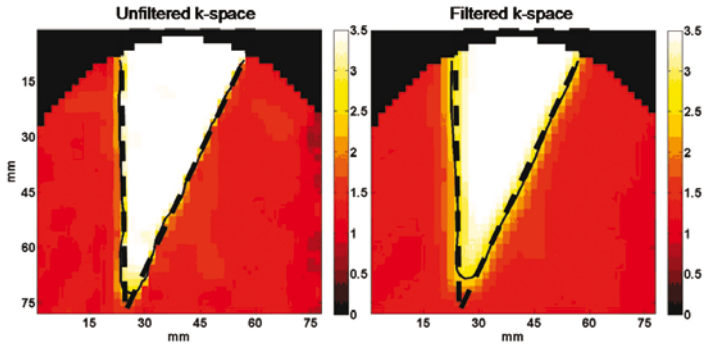

Figure 7. Comparison of the effects of k-space filtering on tumor delineation. The scale represents the Cho/Cr value. The dashed line represents the phantom geometry and the solid line represents the contour at Cho/Cr ≥ 2.5.

is a much more prominent transition zone visible along the wedge margin. The difference in tumor delineation between the two reconstructions is clear in the lower high-detail region of the wedge shape.

The phantom can be used to evaluate how the detected tumor volume is influenced by different combinations of k-space sampling and filtering during the development phase of a new MRSI sequence. Furthermore, it is useful as a quality assurance tool to ensure the preservation or improvement of the quality of tumor delineation when developing an MRSI sequence or signal processing methods.

Conclusions

Studies have shown that MRSI has the potential of detecting areas of tumors growth that were otherwise undetectable using conventional imaging. However the ability of MRSI to accurately represent tumor geometry is not always clearly defined by its nominal voxel size, which is influenced by many imaging and processing parameters. It is therefore important to understand and quantify such ability if MRSI is to be used with radiotherapy planning. In this work a detail phantom has been introduced to assist in the process of improving the ability of the spectroscopic imaging sequences to accurately represent the geometry of tumors.

The phantom was developed for assessing the performance of MRSI sequences. Traditionally, MRSI phantoms are susceptible to magnetic susceptibility artifacts and wall-related partial volume artifacts arising from their building material. The use of a porcine gel phantom minimizes the susceptibility artifacts, and the lack of a physical compartmental wall eliminates the associated partial volume artifacts.

The phantom was shown to be successful in demonstrating the differences in tumor boundary definition shown by three MRSI sequences of the same nominal resolution. It was also used to show the differences resulting from applying different k-space filters to the same sequence. There are a number of imaging and filtering parameters that can influence high-resolution contrast of an MRSI sequence. For example, harsh k-space filtering parameters tend to minimize the signal at the edges of k-space. Similarly, increasing the number of echoes acquired per excitation will produce a T2 weighted k-space, resulting in decreased contrast at high spatial-resolution in the metabolite maps. While a sequence may be designed to achieve a desired nominal resolution, the above mentioned factors can influence the spatial accuracy of tumor boundary delineation to an extent which may not be intuitive to the user. The phantom introduced in this work can be used as a development tool to investigate the effects of those im-

aging and filtering parameters on the accuracy of tumor delineation before applying the developed sequences clinically. Finally, the reduced artifacts associated with using porcine gel coupled with its relative ease of construction make this kind of phantom a viable option for evaluating the performance of MRSI sequences in both clinical and scientific settings.

Acknowledgements

Discussion with Dr. Burkhard Maedler from Philips Medical Systems, are appreciated. We acknowledge the financial support of the Canadian Institutes of Health Research, Translational Research Training in Cancer, Canada Foundation for Innovation, and the Alberta Science and Research Investments Program.

References

1. Pallud J, Devaux B, Nataf F, Roux FX, Daumas-Duport C. Spatial delimitation of low grade oligodendrogliomas. *Neurochirurgie* 2005; **51:** 253-9.

2. Pirzkall A, Li X, Oh J, Chang S, Berger MS, Larson DA, et al. 3D MRSI for resected high-grade gliomas before RT: tumor extent according to metabolic activity in relation to MRI. *Int J Radiat Oncol Biol Phys* 2004; **59:** 126-37.

3. Walecki J, Tarasow E, Kubas B, Czemicki Z, Lewko J, Podgorski J, et al. Hydrogen-1 MR spectroscopy of the peritumoral zone in patients with cerebral glioma: assessment of the value of the method. *Acad Radiol* 2003; **10:** 145-53.

4. Chang J, Thakur S, Perera G, Kowalski A, Huang W, Karimi S, et al. Image-fusion of MR spectroscopic images for treatment planning of gliomas. *Med Phys* 2006; **33:** 32-40.

5. McKnight TR, Noworolski SM, Vigneron DB, Nelson SJ. An automated technique for the quantitative assessment of 3D-MRSI data from patients with glioma. *J Magn Reson Imaging* 2001; **13:** 167-77.

6. Hunjan S, Adalsteinsson E, Kim DH, Harsh GR, Boyer AL, Spielman D, et al. Quality assurance of magnetic resonance spectroscopic imaging-derived metabolic data. *Int J Radiat Oncol Biol Phys* 2003; **57:** 1159-73.

7. Woo DC, Kim BS, Jung SL, Park HJ, Rhim HS, Jahng GH, et al. Develpment of a cone-shaped phantom for multi-voxel MR scpectroscopy. *J Neurosci Methods* 2007; **162:** 101-7.

8. Rice JR, Milbrandt RH, Madsen EL, Frank GR, Boote EJ, Blenchinger JC. Anthromorphic ^{1}H MRS head phantom. *Med Phys* 1998; **25:** 1145-56.

9. Barker PB, Hearshen DO, Boska MD. Single-voxel proton MRS of the human brain at 1.5T and 3.0T. *Magn Reson Med* 2001; **45:** 765-9.

10. Drost DJ, Riddle WR, Clarke GD. Proton magnetic resonance spectroscopy in the brain: Report of AAPM Task Group #9. *Med Phys* 2002; **29:** 2177-97.

11. Nishimura DG. *Principles of magnetic resonance imaging*: Stanford: Stanford University; 1996.

12. Haacke EM. *Magnetic resonance imaging, physics principles and sequence design.* New York: John Wiley & Sons; 1999.

13. Doddrell DM, Galloway G, Brooks W, Filed J, Bulsing J, Irving M, et al. Water signal elimination in vivo, using suppression by mistimed echo and repetitive gradient episodes. *J Magn Reson* 1986; **70:** 176-80.

14. Hasse A, Frahm J, Hanicke W, Mattaei W. 1H NMR chemical shift selective (CHESS) imaging. *Phys Med Biol* 1985; **30:** 341-4.

15. Mierisova S, Ala-Korpela M. MR spectroscopy quantitation: a review of frequency domain methods. *NMR Biomed* 2001; **14:** 247-59.

16. Moré JJ. *The Levenberg-Marquardt algorithm: implementation and theory*. In: GA Watson, editor. Lecture notes in mathematics. Heidelberg: Springer Verlag; 1977. p. 105-16.

17. Nelson SJ, Graves E, Pirzkall A, Li X, Chan AA, Vigneron DB, et al. In vivo molecular imaging for planning radiation therapy of gliomas: an application of 1H MRSI. *J Magn Reson Imaging* 2002; **16:** 464-76.

18. Narayana A, Chang J, Thakur S, Huang W, Karimi S, Hou B, et al. Use of MR spectroscopy and functional imaging in the treatment planning of gliomas. *Br J Radiol* 2007; **80:** 347- 54.

19. Jeun SS, Kim MC, Kim BS, Lee JM, Chung ST, Oh CH, et al. Assessment of malignancy in gliomas by 3T 1H MR spectroscopy. *J Clin Imaging* 2005; **29:** 10-5.

Radiol Oncol 2008; 42(4): 173-80.

Kakšen je najpogostejši mamografski videz T1a in T1b invazivnih rakov dojk?

Podkrajšek M, Žgajnar J, Hočevar M

Izhodišče. Podatki o mamografskem videzu pod 1 cm velikih invazivnih rakov dojk (RD) so skopi. Avtorji uporabljajo različna merila. Namen naše raziskave je bil ugotoviti najpogostejši mamografski videz majhnih invazivnih RD (T1a in T1b).

Bolniki in metode. V raziskavo je bilo vključenih 100 žensk s 102 invazivnim RD, manjše velikosti (1-10 mm), ki smo jih našli pri mamografiji na Onkološkem inštitutu v 16 mesecih. Mamografski videz smo opisali kot: tumor, tumor s mikrokalcinacijami, samo mikrokalcinacije in drugo (asimetrična zgostitev, arhitekturni nemir).

Rezultati. Najpogosteje smo našli tumor brez kalcinacij (60/102; 59%). Pri 12/102 (11%) je bil viden tumor s kalcinacijami. Samo mikrokalcinacije so bile ugotovljene pri 12/102 (11%) ter asimetrična zgostitev in arhitekturni nemir pri 18 invazivnih RD (18%). Največ invazivnih RD (44/60) je imelo videz zvezdastega tumorja. Odstotek tipa razvejanih mikrokalcinacij je bil višji pri ženskah pod 50. letom starosti.

Zaključek. Najpogostejše mamografski videz majhnih invazivnih RD je ne glede na starost bolnic zvezdast tumor. Kalcinacije z/brez tumorja so pogostejše pri ženskah pod 50. letom starosti.

Radiol Oncol 2008; 42(4): 181-6.

Obliterativna hepatokavopatija – ultrazvočna in kavografska diagnostika – prikaz primera

Kutlu R

Izhodišča. Obliterativna hepatokavopatija je relativno nov pojem, ki definira primarno trombozo spodnje votle vene in membranozno obstrukcijo spodnje votle vene pri Budd-Chiari sindromu.
Prikaz primera. Prikazan je primer kavografskih in ultrazvočnih sprememb pri popolni zapori spodnje votle vene pri 36 letni bolnici, ki je bila pregledovana zaradi diagnostike posledic B hepatitisa.
Zaključki. Ta bolezen je bila dosedaj prvenstveno zdravljena s kiriurškimi posegi, npr. z portalno-mezenteričnim sistemskim odvodom (shuntom) ali s presaditvijo jeter. V zadnjem času pa se v takih primerih enako uspešni tudi interventni radiološki posegi, kot sta transjugularni intrahepatični portosistemski odvod in perkutana angioplastika jetrnih ven s postavitvijo žilnih opornic.

Radiol Oncol 2008; 42(4): 187-95.

Gastrointestinalni stromalni tumor želodca

Žokalj I, Čulinović-Čaić R, Magaš Z, Pavčec Z, Saghir H, Igrec J, Marotti M

Izhodišča. Gastrointestinalni stromalni tumorji (GIST-i) so najbolj pogosti mezenhimalni tumorji prebavnega trakta. Ne moremo jih preprosto deliti na benigne in maligne, ker je veliko vmesnih oblik. Na potek bolezni znatno vpliva njihova velikost in mitotska aktivnost, prav tako mesto, kjer se pojavijo. Najdemo jih kjerkoli vzdolž prebavnega trakta, v mezenteriju ali omentumu. GIST-i so največkrat benigni tumorji, v 70-80% pa se pojavijo v želodčni steni. V članku predstavljamo primer 70-letne bolnice z želodčno obliko GIST-a.

Prikaz primera. Pri bolnici smo naredili ultrazvočno preiskavo trebuha zaradi tipljive zatrdline v epigastriju. Videli smo večinoma hiperehogeno okroglo maso z majhnimi hipoehogenimi areali v centralnem delu. Preiskava z računalniško tomografijo pa je pokazala veliko ekspanzivno maso, heterogene strukture v želodčni steni. Tumor je kazal večji atenuacijski koeficient na periferiji in nižji v centralnem delu. Med operativnim zdravljenjem smo odstranili velik ekzofitičen tumor želodčne stene. Diagnozo GIST želodca smo postavili po patohistološkem in imunohistokemičnem pregledu tumorja.

Zaključki. GIST-i so statistično redki tumorji (0,1%-0,3% vseh gastrointestinalnih tumorjev), a ko najdemo bolnika z okroglo, večinoma ekzofitično tumorsko maso na steni gastrointestinalnega trakta ali peritoneja, moramo pomisliti tudi na GIST. Z ultrazvokom in računalniško tomografijo lahko postavimo klinično predoperativno diagnozo in opredelimo razširjenost bolezni.

Radiol Oncol 2008; 42(4): 196-206.

Časovna odvisnost učinkov električnih polj na celično membrano. Kritični pregled pomena trajanja električnih pulzov in njihova terapevtska uporabnost

Teissié J, Escoffre JM, Rols MP, Golzio M

Izhodišča. Elektroporacija je ena od nevirusnih metod vnosa molekul v celice tkiva in tumorje. Uspešno se uporablja za dostavljanje kemoterapevtikov in tudi genov. Metoda je uporabna pri zdravljenju tumorjev kot tudi pri genski terapiji. Prispevek obravnava časovno komponento elektroporacije pri vnosu malih molekul (< 4 kDa) in procese, ki vplivajo na vnos DNA v celice *in vivo*. Opisani so procesi, ki se dogajajo pred elektroporacijo, med njo (ms) in po njej (ms in h), pri prenosu DNA v celico. Ta proces je sestavljen iz več dogodkov, ki imajo dobro definirano kinetiko. Ne moremo ga opisati kot dogodek, ki tvori luknje v celični membrani, ne kot samo dvostopenjski proces.

Zaključki. Hitri dogodki so v času ns, in so pod vplivom zunanjega električnega polja, medtem ko so počasnejši dogodki povezani z metabolizmom membrane. Zato je nadaljne raziskovanje dogodkov na membrani pod vplivom električnih polj pomembno za varno uporabo elektroporacije v kliniki.

Radiol Oncol 2008; 42(4): 207-14.

Prospektivna raziskava kakovosti življenja bolnikov po kombiniranem zdravljenju raka danke

Velenik V, Oblak I, Anderluh F

Izhodišča. Iz poročil v literaturi ni razvidno, da bi trajna stoma poslabšala kakovost življenja bolnikov z lokalno napredovalim rakom danke (T3-4 in/ali N+). Naš namen je bil primerjati kakovost življenja bolnikov z abdominoperinealno amputacijo danke in bolnikov z ohranjeno kontinuiteto črevesa, zdravljenjih s predoperativno radiokemoterapijo v prospektivni raziskavi faze II.

Bolniki in metode. 57 bolnikov je bilo obsevanih 5-krat tedensko in z dnevnim odmerkom 1,8 Gy do skupne doze 45 Gy. Sočasno z obsevanjem so prejemali peroralno kemoterapijo s kapecitabinom v odmerku 825 mg/m^2/12 ur. Operacijo smo načrtovali 4-6 tednov po zaključeni predoperativni radiokemoterapiji. Po operaciji so bolniki prejeli 4 kroge kemoterapije. Pri ocenjevanju kakovosti življenja so bolniki, ki so bili po ≥ 2 letih sledenja brez znakov ponovitve bolezni, izpolnili vprašalnika, ki ju je razvila European Organisation for Research and Treatment of Cancer (EORTC): prvi je bil specifičen za bolnike z rakom (EORTC QLQ-C30) in drugi za bolnike z rakom debelega črevesa in danke (EORTC QLQ-C38).

Rezultati. Vprašalnik je izpolnilo 28 od 37 primernih bolnikov (87,5 %). Srednji čas od operacije do izpolnjevanja vprašalnikov je bil 35 mesecev. Pri nobenem vprašanju iz vprašalnikov EORTC QLQ-C30 in EORTC QLQ-C38 med skupinama ni bilo statistično pomembnih razlik v srednjem številu zbranih točk.

Zaključki. Razlike v kakovosti življenja med bolniki s trajno stomo in bolniki z ohranjenim analnim sfinktrom nismo zasledili.

Radiol Oncol 2009; 43(1): 215-24.

Obvladovanje neželenih učinkov na kožo s kremo z vitaminom K1 pri bolnikih zdravljenih s cetuksimabom

Ocvirk J, Rebersek M

Izhodišča. Cetuksimab je človeško-mišje monoklonalno protitelo proti receptorju za epidermalni rastni dejavnik (EGFR). V kliničnih raziskavah se je izkazal za učinkovitega pri številnih malignih obolenjih. Ob uporabi inhibitorjev EGFR so pogosti neželeni učinki na koži, med katerimi je najpogostejši akniformni izpuščaj. Pri nekaterih bolnikih opazimo tudi kserozo, ekcem, fisure, teleangiektazije, spremembe nohtov in paranihijo, hiperpigmentacija pa je bolj redka. Z dobrim obvladovanjem neželenih učinkov na kožo pomagamo bolnikom in izboljšamo kakovost življenja. V večini primerov je učinkovita standardna uporaba topičnih ali sistemskih antibiotikov ter protivnetnih zdravil. Ključnega pomena pri obvladovanju kožne toksičnosti sta edukacija bolnikov pred pričetkom zdravljenja ter hitro in učinkovito ukrepanje ob prvih znakih neželenih učinkov na kožo.
Namen pričujoče raziskave je bil ocenjevanje neželenih učinkov na kožo med zdravljenjem s cetuksimabom in ugotavljanje učinkovitosti kreme z vitaminom K1.
Metode. Od septembra 2006 do avgusta 2007 smo zdravili 30 bolnikov z razsejanim rakom debelega črevesa in danke s cetuksimabom in kemoterapijo, ki so imeli tudi akniformni izpuščaj zaradi zdravljenja. Sledili smo jih vsaj tri mesece, enkrat tedensko. Za obvladovanje akniformnega izpuščaja smo uporabljali kremo z vitaminom K1 in ureo (Reconval K1®). Bolniki so jo pričeli uporabljati neposredno po ugotovljenem pojavu kožne toksičnosti. Kožne neželene učinke smo ocenjevali glede na NCI CTCAE, ver. 3.
Rezultati. Šest od 30 bolnikov je imelo akniformni izpuščaj tretje stopnje, 18 druge in 6 prve stopnje. Reconval K1® smo uporabljali dvakrat dnevno. Pri vseh bolnikih smo opazili izboljšanje neželenih učinkov na koži. Srednji čas do izboljšanja je bil 8 dni in 18 dni do znižanja stadija neželenih učinkov vsaj za eno stopnjo.
V nasprotju s podatki o do sedaj zdravljenih bolnikih s cetuksimabom, pri katerih je nastopila 3. stopnja kožne toksičnosti ter je bilo pri vseh priporočeno in tudi nujno znižanje odmerka cetuksimaba, pa pri nekaterih naših bolnikih to ni bilo potrebno. Pri samo 3 od 6 bolnikov s 3. stopnjo kožne toksičnosti smo morali znižati odmerek cetuksimaba.
Pri bolnikih s 1. in 2. stopnjo kožne toksičnosti ni bilo potrebno znižati odmerka ali odložiti zdravljenja. Ob topični uporabi kreme Reconval K1® nismo opazili nobenih lokalnih ali sistemskih neželenih učinkov.
Zaključki. Po naših podatkih je to prva objavljena raziskava o učinkovitosti kreme z vitaminom K1 pri zmanjševanju neželenih učinkov na kožo ob zdravljenju s cetuksimabom pri bolnikih z razsejanim rakom debelega črevesa in danke. Reconval K1® je učinkovit v obvladovanju kožne toksičnosti pri bolnikih zdravljenih s cetuksimabom. Potrebne bodo nadaljne raziskave za ugotavljanje vpliva na kvaliteto življenja in odgovore na zdravljenje.

Radiol Oncol 2008; 42(4): 225-31.

Metastaza ledvičnega raka v hipofizi: prikaz primera

Bišof V, Juretić A, Šarić N, Melada A, Perković Z, Radoš M, Padovan Štern R

Izhodišča. Solitarna metastaza ledvičnega raka v hipofizije je zelo redka in le v 7% povzroča simptome bolezni.
Prikaz primera. Opisujemo 52-letnega bolnika, ki je imel motnje vida in glavobole 3 leta po zdravljenju metastatskega ledvičnega raka. Preiskava z magnetno resonanco je pokazala tumor v supraselarnem področju, ki je pritiskal na optično hiasmo. Drugih metastatskih sprememb pa nismo videli. Bolniku smo naredili transsfenoidalno redukcijsko operacijo. Patohistološki pregled, ki je obsegal tudi imunohistološko priskavo, je pokazal, da smo odstranili metastazo svetloceličnega ledvičnega raka.
Zaključki. Naš primer je petindvajseti, ki je opisan v literaturi kot bolnik s simptomatsko metastazo ledvičnega raka v hipofizi.

Radiol Oncol 2008; 42(4): 232-9.

Fantom za ocenjevanje natančnosti obrisovanja tumorjev z magnetno resonančno spektroskopijo (MRS)

Heikal AA, Wachowicz K, Thomas SD, Fallone BG

Izhodišča. Raziskave so pokazale, da lahko z magnetnoresonančne spektroskopije (MRS) zaznamo področja nenormalne aktivnosti (kot so v tumorju), ki bi jih z običajnimi metodami spregledali. Zaradi vse večjega zanimanja za MRS je pomembno raziskati njeno natančnost pri obrisovanju tumorjev. Kljub temu, da je bilo v izdelavo fantomov za preučevanje učinkovitosti MRS zaporedij vloženega že precej truda, so jih večino izdelali iz običajnega ali akrilnega stekla.

Material in metode. V članku predstavljamo fantom iz nehomogene želatine, ki smo ga razvili za ocenjevanje zmogljivosti spektroskopskih slikovnih zaporedij pri določanju geometrijskih oblik tumorjev. Fantom uporabljamo kot alternativo konvencionalnim fantomom iz običajnega in akrilnega stekla namenjenim MRS.

Rezultati. Fantomi iz želatine imajo prednost, ker je njihova magnetna susceptibilnost blizu magnetni susceptibilnosti vode. Poleg tega v članku dokažemo prednosti fantoma brez predelnih sten med deli z različno homogenostjo. Uporabnost fantoma prikažemo s primerjavami med različnimi MRS zaporedji pri isti nazivni ločljivosti ter s primerjavami med različnimi parametri filtriranja.

Zaključki. Zaradi enostavne izdelave in zmanjšanih artefaktov, so fantomi iz želatine zanesljivo orodje za ocenjevanje uspešnosti MRS zaporedij.

Notices

*Notices submitted for publication should contain a mailing address, phone and/or fax number and/or e-mail of a **Contact** person or department.*

Radiation oncology

January 22-24, 2009
The symposium "Advances in Technology: Practical Aspects on IMRT and Proton Therapy" will be offered in Chandler, Arizona, USA.
Contact ASTRO, 8280 Willow Oaks Corporate Dr., Suite 500, Fairfax, VA 22031; or call +1 703 502-1550; see http://www/astro.org

Prostate cancer

February 1-5, 2009
The ESTRO multidisciplinary teaching course on prostate cancer will take place in Seville, Spain.
Contact ESTRO office, Avenue E. Mounierlaan, 83/12, B-1200 Brussels, Belgium; or call +32 2775 93 40; or fax 32 2779 5494; or e-mail events@estro.org; or see http://www/estro-events.org

Radiation oncology

February 20-22, 2009
The international symposium " Stereotactic Body Radiation Therapy and Stereotactic Radiosurgery" will be offered in Lake Buena Vista, Florida, USA.
Contact ASTRO, 8280 Willow Oaks Corporate Dr., Suite 500, Fairfax, VA 22031; or call +1 703 502-1550; see http://www/astro.org

PET in radiation oncology

February 21-22, 2009
The ESTRO / EANM educational seminar on PET in radiation oncology will take place in Brussels, Belgium.
Contact ESTRO office, Avenue E. Mounierlaan, 83/12, B-1200 Brussels, Belgium; or call +32 2775 93 40; or fax 32 2779 5494; or e-mail events@estro.org; or see http://www/estro-events.org

Head and neck oncology

February 26-28, 2009
The "2nd International Conference on Innovative Approaches in Head and Neck Oncology" will take place in Barcelona, Spain.
See http:// www.estro.be

Lung cancer

March 6-7, 2009
The 10th European Congress: Perspectives in Lung Cancer will be held in Brussels, Belgium.
See http:// www.perspectivesinlungcancer.com

Interventional radiology

March 7-12, 2009
The 34th Annual Meeting of Society of Interventional Radiology will be held in Lake Buena Vista, Florida, USA.
Contact ASTRO, 8280 Willow Oaks Corporate Dr., Suite 500, Fairfax, VA 22031; or call +1 703 502-1550; see http://www/astro.org

Cancer therapy

March 11-15, 2009
The NCCN 14th Annual Conference: "Clinical Practice Guidelines & Quality Cancer Care" will be offered in Hollywood, Florida, USA.
Contact National Comprehensive Cancer Network, 275 Commerce Drive, Suite 300, Fort Washington, PA 19034; or phone +1 215 690 0300; or fax +1 215 690 0280; or see http:// www.nccn.org

Brachytherapy

March 22-26, 2009
The ESTRO teaching course ''Modern Brachytherapy Techniques'' will take place in Cairo, Egypt.
Contact ESTRO office, Avenue E. Mounierlaan, 83/12, B-1200 Brussels, Belgium; or call +32 2775 93 40; or fax 32 2779 5494; or e-mail events@estro.org; or see http://www/estro-events.org

Radiotherapy

March 23-27, 2009
The ESTRO teaching course ''Radiotherapy Treatment Planning, Principles and Practice" will be held in Dublin, Ireland.
Contact ESTRO office, Avenue E. Mounierlaan, 83/12, B-1200 Brussels, Belgium; or call +32 2775 93 40; or fax 32 2779 5494; or e-mail events@estro.org; or see http://www/estro-events.org

Oncology

March 28-31, 2009
The ESTRO teaching course on combined drug-radiation treatment: biological basis, current applications and perspectives will be offered in Berlin, Germany.
Contact ESTRO office, Avenue E. Mounierlaan, 83/12, B-1200 Brussels, Belgium; or call +32 2775 93 40; or fax 32 2779 5494; or e-mail events@estro.org; or see http://www/estro-events.org

Targeted therapies

April 1-5, 2009
The "4th IASLC/ASCO/ESMO International Meeting on Targeted Therapies on Lung Cancer" will be offered in Saint Paul de Vence, France.
E-mail: pia.hirsch@uchsc.edu

Breast cancer

April 2-4, 2009
The ESTRO multidisciplinary teaching course on breast cancer will take place in Lisbon, Portugal.
Contact ESTRO office, Avenue E. Mounierlaan, 83/12, B-1200 Brussels, Belgium; or call +32 2775 93 40; or fax 32 2779 5494; or e-mail events@estro.org; or see http://www/estro-events.org

Molecular oncology

April 26-30, 2009
The ESTRO teaching course ''Molecular Oncology for the Radiation Oncologist'' will take be offered in Santorini, Greece.
Contact ESTRO office, Avenue E. Mounierlaan, 83/12, B-1200 Brussels, Belgium; or call +32 2775 93 40; or fax 32 2779 5494; or e-mail events@estro.org; or see http://www/estro-events.org

Radiation oncology

April 27-29, 2009
The international IAEA's conference "Advances in Radiation Oncology (ICARO)" will be held in Vienna, Austria.
Contact ASTRO, 8280 Willow Oaks Corporate Dr., Suite 500, Fairfax, VA 22031; or call +1 703 502-1550; see http://www/astro.org

Thoracic oncology

May 1-3, 2009
The European Multidisciplinary Conference in Thoracic Oncology (EMCTO) will take place from in Lugano, Switzerland.
Contact EMCTO Conference Secretariat, c/0 ESMO Congress Department, Via Luigi Taddei 4, CH-6962 Viganello-Lugano, Switzerland; or fax +41 (0)91 973 19 18, or see www.emcto.org

Rectal cancer

May 10-12, 2009
The ESTRO multidisciplinary teaching course on evidence and research in rectal cancer will take place in Rome, Italy.
Contact ESTRO office, Avenue E. Mounierlaan, 83/12, B-1200 Brussels, Belgium; or call +32 2775 93 40; or fax 32 2779 5494; or e-mail events@estro.org; or see http://www/estro-events.org

Radiotherapy

May 10-14, 2009
The ESTRO teaching course on radiotherapy with protons and ions will be offered in Villingen, Switzerland.
Contact ESTRO office, Avenue E. Mounierlaan, 83/12, B-1200 Brussels, Belgium; or call +32 2775 93 40; or fax 32 2779 5494; or e-mail events@estro.org; or see http://www/estro-events.org

Radiotherapy

May 17-21, 2009
The ESTRO teaching course on IMRT and other conformal techniques in practice will be held in Milan, Italy.
Contact ESTRO office, Avenue E. Mounierlaan, 83/12, B-1200 Brussels, Belgium; or call +32 2775 93 40; or fax 32 2779 5494; or e-mail events@estro.org; or see http://www/estro-events.org

Thyroid cancer

May 27-31, 2009
The "World Congress on Thyroid Cancer'' will be held in Toronto, Canada.
Contact ASTRO, 8280 Willow Oaks Corporate Dr., Suite 500, Fairfax, VA 22031; or call +1 703 502-1550; see http://www/astro.org

Clinical oncology

May 29 – June 2, 2009
The American Society of Clinical Oncology Conference (ASCO 2009) will be offered in Orlando, USA.
E mail enews@asco.org; or see http://www/asco.org

Clinical trial statistics

June 9-12, 2009
The EORTC course "Clinical Trial Statistics for Non Statisticians" will be held in Brussels, Belgium.
See http://www.eortc.be/Seminar/Educationpgm/Stats2009/Default.htm

Oncology

June 20-26, 2009
The ECCO-AACR-ASCO workshop "Methods in Clinical Cancer Research" will be offered in Flims, Switzerland.
Contact the Workshop Coordinator Mrs. Kaat Cumps at kaat.cumps@ecco-org.eu; or see http://www.ecco-org.eu (go to the section Eduction/Flims/Flims11)

Radiotherapy

June 21-25, 2009
The ESTRO teaching course ''Imaging for Target Volume Determination in Radiotherapy'' will be held in Tours, France.
Contact ESTRO office, Avenue E. Mounierlaan, 83/12, B-1200 Brussels, Belgium; or call +32 2775 93 40; or fax 32 2779 5494; or e-mail events@estro.org; or see http://www/estro-events.org

Radiation oncology

June 25-27, 2009
The "MASCC/ISOO 2009 International Symposium of Supportive Care in Cancer: Multinational Association of Supportive Care of Cancer/International Society of Oral Oncology" will be held in Rome, Italy.
Contact ASTRO, 8280 Willow Oaks Corporate Dr., Suite 500, Fairfax, VA 22031; or call +1 703 502-1550; see http://www/astro.org

Paediatric oncology

June 28-30, 2009
The ESTRO teaching course on paediatric oncology will be offered in Brussels, Belgium.
Contact ESTRO office, Avenue E. Mounierlaan, 83/12, B-1200 Brussels, Belgium; or call +32 2775 93 40; or fax 32 2779 5494; or e-mail events@estro.org; or see http://www/estro-events.org

Prostate cancer

June 28-30, 2009
The ESTRO teaching course on brachytherapy for prostate cancer will take place in Istanbul, Turkey.
Contact ESTRO office, Avenue E. Mounierlaan, 83/12, B-1200 Brussels, Belgium; or call +32 2775 93 40; or fax 32 2779 5494; or e-mail events@estro.org; or see http://www/estro-events.org

Radiotherapy

June 28 – July 2, 2009
The ESTRO teaching course on 2D-3D planning and imaging will be offered in St Petersburg, Russia.
Contact ESTRO office, Avenue E. Mounierlaan, 83/12, B-1200 Brussels, Belgium; or call +32 2775 93 40; or fax 32 2779 5494; or e-mail events@estro.org; or see http://www/estro-events.org

Oncology

July 2-5, 2009
The Educational Cancer Convention (ECCLU) will be held in collaboration with European Society for Medical Oncology in Lugano, Switzerland.
E-mail www.cmelcher@eso.net; or see www.eso.net

Lung cancer

July 31 - August 4, 2009
The "13th World Conference on Lung Cancer" will be offered in San Francisco, USA.
Contact Conference Secretariat International Conference Services Ltd., Suite 2101 - 1177 West Hastings Street, Vancouver, BC Canada V6E 2K3; or call +1 604 681 2153; or e-mail wclc2009@meet-ics.com; or see http://www.2009worldlungcancer.org/

Radiotherapy

August 30 – September 3, 2009
The 19th Biennial ESTRO Conference" will be held in Maastricht, the Netherlands.
Phone +32 2775 93 40; or fax 32 2779 5494; or e-mail events@estro.org; or see http://www/estro-events.org

Oncology

September 4-8, 2009
The "34th ESMO Congress" will take place in Vienna, Austria.
Contact ESMO Head Office, Congress Department, Via La Santa 7, CH-6962 Viganello-Lugano, Switzerland; or +41 (0)91 973 19 19; or fax +41 (0)91 973 19 18; or e-mail congress@esmo.org; or see http://www.esmo.org

Medical physics

September 7-12, 2009
The "World Congress 2009 – Medical Physics and Biomedical Engineering" will take place in Munich, Germany.
See http://www. wc2009.org/world-congress-2009

Brachytherapy

September 10-12, 2009
The ESTRO teaching course ''3D Image-Based Brachytherapy for Gynaecological Malignancies'' will be offered in Amsterdam, The Netherlands.
Contact ESTRO office, Avenue E. Mounierlaan, 83/12, B-1200 Brussels, Belgium; or call +32 2775 93 40; or fax 32 2779 5494; or e-mail events@estro.org; or see http://www/estro-events.org

Radiation oncology

September 13-16, 2009
The "8th International Conference on Dose, Time and Fractionation in Radiation Oncology" will be held in Madison, Wisconsin, USA.
Contact ASTRO, 8280 Willow Oaks Corporate Dr., Suite 500, Fairfax, VA 22031; or call +1 703 502-1550; see http://www/astro.org

Oncology

September 20-24, 2009
The "15th ECCO and 34th ESMO Multidisciplinary Congress" will be offered in Berlin, Germany.
See http://www.ecco-org.eu

Nuclear medicine

October 10-14, 2009
The "EANM'09 Annual Congress of the European Association of Nuclear Medicine" will take place in Barcelona, Spain.
Contact EANM Executive Secretariat and call +43 1 212 80 30; or fax +43 1 212 80 309; or e-mail office@eanm.org; or see http://www. eanm.org

Radiation oncology

October 11-16, 2009
The ESTRO teaching course Evidence Based Radiation Oncology: Methodological Basis and Clinical Application '' will be offered in Vienna, Austria.
Contact ESTRO office, Avenue E. Mounierlaan, 83/12, B-1200 Brussels, Belgium; or call +32 2775 93 40; or fax 32 2779 5494; or e-mail events@estro.org; or see http://www/estro-events.org

Lung Cancer

October 15-17, 2009
The ESTRO multidisciplinary teaching course on lung cancer will be held in Prague, Czech Republic.
Contact ESTRO office, Avenue E. Mounierlaan, 83/12, B-1200 Brussels, Belgium; or call +32 2775 93 40; or fax 32 2779 5494; or e-mail events@estro.org; or see http://www/estro-events.org

Radiobiology

October 18-23, 2009
The ESTRO teaching course on basic clinical radiobiology will be offered in Toledo, Spain.
Contact ESTRO office, Avenue E. Mounierlaan, 83/12, B-1200 Brussels, Belgium; or call +32 2775 93 40; or fax 32 2779 5494; or e-mail events@estro.org; or see http://www/estro-events.org

Therapeutic radiology and oncology

November 1-5, 2009
The "American Society for Therapeutic Radiology and Oncology Annual Meeting ASTRO" will take place in Chicago, USA.
Contact ASTRO, 8280 Willow Oaks Corporate Dr., Suite 500, Fairfax, VA 22031; or call +1 703 502-1550; or see http://www.astro.org

Radiotherapy

November 15-19, 2009
The ESTRO teaching course on IMRT and other conformal techniques in practice will take place in Gliwice, Poland.
Contact ESTRO office, Avenue E. Mounierlaan, 83/12, B-1200 Brussels, Belgium; or call +32 2775 93 40; or fax 32 2779 5494; or e-mail events@estro.org; or see http://www/estro-events.org

PET in radiation oncology

November 21-22, 2009
The ESTRO / EANM educational seminar on PET in radiation oncology will take place in Vienna, Austria.
Contact ESTRO office, Avenue E. Mounierlaan, 83/12, B-1200 Brussels, Belgium; or call +32 2775 93 40; or fax 32 2779 5494; or e-mail events@estro.org; or see http://www/estro-events.org

PET in radiation oncology

December 13-17, 2009
The ESTRO teaching course on image-guided radiotherapy in clinical practice will take place in Brussels, Belgium.
Contact ESTRO office, Avenue E. Mounierlaan, 83/12, B-1200 Brussels, Belgium; or call +32 2775 93 40; or fax 32 2779 5494; or e-mail events@estro.org; or see http://www/estro-events.org

Head and neck cancer

February 25-27, 2010
The multidisciplinary symposium on head and neck cancer will be offered in Chandler, Arizona, USA.
Contact ASTRO, 8280 Willow Oaks Corporate Dr., Suite 500, Fairfax, VA 22031; or call +1 703 502-1550; see http://www/astro.org

Clinical oncology

June 4-8, 2010
The American Society of Clinical Oncology Conference (ASCO 2010) will be offered in Chicago, USA.
E mail enews@asco.org; or see http://www/asco.org

Oncology

October 8-12, 2010
The "35th ESMO Congress" will take place in Milan, Italy.
Contact ESMO Head Office, Congress Department, Via La Santa 7, CH-6962 Viganello-Lugano, Switzerland; or call +41 (0)91 973 19 19; or fax +41 (0)91 973 19 18; or e-mail congress@esmo.org; or see http://www.esmo.org

Nuclear medicine

October 9-13, 2010
The "EANM'10 Annual Congress of the European Association of Nuclear Medicine" will take place in Vienna, Austria.
Contact EANM Executive Secretariat and call +43 1 212 80 30; or fax +43 1 212 80 309; or e-mail office@eanm.org; or see http://www. eanm.org

Therapeutic radiology and oncology

October 31 – November 4, 2010
The "American Society for Therapeutic Radiology and Oncology Annual Meeting ASTRO" will take place in San Diego, California, USA.
Contact ASTRO, 8280 Willow Oaks Corporate Dr., Suite 500, Fairfax, VA 22031; or call +1 703 502-1550; or see http://www.astro.org

Clinical oncology

June 3-7, 2011
The American Society of Clinical Oncology Conference (ASCO 2010) will be offered in Chicago, USA.
E mail enews@asco.org; or see http://www/asco.org

Lung cancer

July 3-7, 2011
The "14th World Conference on Lung Cancer" will be offered in Amsterdam, The Netherlands.
See http://www.iaslc.org

Oncology

September 23-27, 2011
The "16th ECCO and 36th ESMO Multidisciplinary Congress" will be offered in Stockholm, Sweden.
See http://www.ecco-org.eu

Nuclear medicine

October 15-19, 2011
The "EANM'11 Annual Congress of the European Association of Nuclear Medicine" will take place in Birmingham, United Kingdom.
Contact EANM Executive Secretariat and call +43 1 212 80 30; or fax +43 1 212 80 309; or e-mail office@eanm.org; or see http://www. eanm.org

Oncology

September 27 – October 1, 2013
The "17th ECCO and 38th ESMO Multidisciplinary Congress" will be offered in Amsterdam, The Netherlands.
See http://www.ecco-org.eu

Lung cancer

2013
The "15th World Conference on Lung Cancer" will be offered in Sydney, Australia.
See http://www.iaslc.org

As a service to our readers, notices of meetings or courses will be inserted free of charge.
Please send information to the Editorial office, Radiology and Oncology, Zaloška 2, SI-1000 Ljubljana, Slovenia.

Authors Index 2008

Subject Index 2008

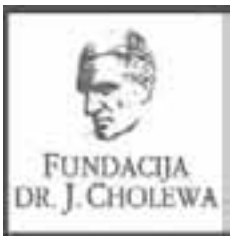

Fundacija "Docent dr. J. Cholewa"
je neprofitno, neinstitucionalno in nestrankarsko
združenje posameznikov, ustanov in organizacij, ki želijo
materialno spodbujati in poglabljati raziskovalno
dejavnost v onkologiji.

Dunajska 106
1000 Ljubljana

ŽR: 02033-0017879431

Activity of "Dr. J. Cholewa" Foundation for Cancer Research and Education – a report for the final quarter of 2008

Docent Dr. J. Cholewa Foundation for Cancer Research and Education continues to support the activities and advancement of oncology related sciences and is of opinion that excellent and unorthodox ideas must not be prevented to succeed for the simple lack of funding. It primarily supports cancer research and education activities in Slovenia, it continues to assess carefully the requests for research grants and scholarships submitted by Slovenian experts in oncology and other associated scientific activities, and helps putting resulting advances in cancer therapy in practice.

The "Docent Dr. L. Cholewa Foundation for Cancer Research and Education« continues to support the regular publication of "Radiology and Oncology" international medical scientific journal, that is edited, published and printed in Ljubljana, Slovenia. This support emphasizes the need for the spread of information advances in experimental and clinical cancer research to professionals and interested individuals in public in Slovenia and elsewhere. "Radiology and Oncology" is an open access journal, available free of charge on its own website, thus allowing its users and readers to access without hindrance.

The Foundation considers the support of the publication of the results from cancer research in Slovenia and from Slovenian authors in international scientific journals and other means of communication worldwide as one of its main activities. Its careful assessment of requests and proposals for research grants and scholarships submitted by experts in oncology and other associated scientific activities serves this goal in accordance with the spread of advanced knowledge of therapy and education in cancer.

Borut Štabuc, MD, PhD
Andrej Plesničar, MD, MSc
Tomaž Benulič, MD

SIEMENS

SiemensMedical.com/oncology

SEEK-FIND-ACT-FOLLOW - the Continuum of Oncology Care™

Siemens oncology portfolio comprises comprehensive workflow solutions integrating the full spectrum of care from screening/early detection and diagnosis through therapy and follow-up. All from one provider — with over 100 years history of innovation in medical technology.

Siemens proven clinical methods can help you to achieve more successful outcomes. How? Through industry-leading technology, increased productivity measures for maximized utilization potential, and patient-friendly design and features.

Every day in the United States alone, 29,000 cancer patients receive radiation therapy delivered by Siemens linear accelerators. As clinical protocols transition to include IMRT and IGRT, Siemens seamlessly integrates the diagnostic and treatment modalities. That's what we call **Best Practice Oncology Care**.

Siemens medical
Solutions that help

Vse za rentgen

dobite pri nas!

- rentgenski filmi in kemikalije
- rentgenska kontrastna sredstva
- rentgenska zaščitna sredstva
- aparati za rentgen, aparati za ultrazvočno diagnostiko in vsa ostala oprema za rentgen

Sanolabor, d.d., Leskoškova 4, 1000 Ljubljana
tel: 01 585 42 11, fax: 01 524 90 30
www. sanolabor.si

Sanolabor

LABORMED

ZASTOPA PODJETJA:

MENTOR

Prsni vsadki napolnjeni s silikonskim gelom, ekspanderji in drugi pripomočki pri rekonstrukciji dojk

Köttermann (Nemčija):
laboratorijsko pohištvo, varnostne omare za kisline, luge, topila, pline in strupe, ventilacijska tehnika in digestorji

Angelantoni scientifica (Italija):
hladilna tehnika in aparati za laboratorije, transfuzijo, patologijo in sodno medicino

Corning (Amerika):
specialna laboratorijska plastika za aplikacijo v imunologiji, mikrobiologiji, virologiji, ipd., mehanske eno- in večkanalne pipete in nastavki

Micronic (Nizozemska):
sistemi za shranjevanje vzorcev, pipete, nastavki za pipete

Implantech (Amerika):
obrazni in glutealni vsadki

Biomerica (Amerika):
hitri testi za diagnostiko, EIA /RIA testi

Ehret (Nemčija):
Laminar flow tehnika, inkubatorji, sušilniki, suhi sterilizatorji in oprema za laboratorijsko vzrejo živali - kletke

Dako (Danska):
testi za aplikacijo v imunohistokemiji, patologiji, mikrobiologiji, virologiji, mono- in poliklonalna protitelesa

Sakura finetek (Evropa):
aparati za pripravo histoloških preparatov: mikrotomi, zalivalci, tkivni procesorji, barvalci, pokrivalci

Integra Biosciens (Švica):
laboratorijska oprema za mikrobiologijo, biologijo celic, molekularno biologijo in biotehnologijo

SpectrumDesigns MEDICAL (Amerika):
moški pektoralni vsadki

Byron (Amerika):
liposuktorji in kanile za liposukcijo

LABORMED d.o.o.
Bežigrajski dvor
Peričeva 29, Ljubljana
Tel.: (0)1 436 49 01
Fax: (0)1 436 49 05

info@labormed.si

www.labormed.si

Merck Serono Onkologija / biološko zdravljenje za boljšo kakovost življenja

Erbitux 5 mg/ml raztopina za infundiranje (skrajšana navodila za uporabo)

Cetuksimab je rekombinirano IgG, protitelo, usmerjeno proti receptorju za epidermalni rastni faktor (EGFR). **Terapevtske indikacije:** Zdravilo Erbitux je indicirano za zdravljenje bolnikov z metastatskim kolorektalnim rakom in metastatskim tipom KRAS: v kombinaciji s kemoterapijo in kot samostojno zdravilo pri bolnikih, pri katerih zdravljenje z oksaliplatinom in irinotekanom ni bilo uspešno. Zdravilo Erbitux je v kombinaciji z radioterapijo indicirano za zdravljenje bolnikov z lokalno napredovalim rakom skvamoznih celic glave in vratu. **Odmerjanje in način uporabe:** Zdravilo Erbitux pri vseh indikacijah infundirajte enkrat na teden. Začetni odmerek je 400 mg cetuksimaba na m^2 telesne površine. Vsi naslednji tedenski odmerki so vsak po 250 mg/m^2. **Kontraindikacije:** Zdravilo Erbitux je kontraindicirano pri bolnikih z znano hudo preobčutljivostno reakcijo (3. ali 4. stopnje) na cetuksimab. **Posebna opozorila in previdnostni ukrepi:** Če pri bolniku nastopi blaga ali zmerna reakcija, povezana z infundiranjem, lahko zmanjšate hitrost infundiranja. Priporočljivo je, da ostane hitrost infundiranja na nižji vrednosti tudi pri vseh naslednjih infuzijah. Če se pri bolniku pojavi huda kožna reakcija (≥ 3. stopnje po kriterijih US National Cancer Institute, Common Toxicity Criteria: NCI-CTC), morate prekiniti terapijo s cetuksimabom. Z zdravljenjem smete nadaljevati le, če se je reakcija povrnila do 2. stopnje. Priporoča se določanje koncentracije elektrolitov v serumu pred zdravljenjem in periodično med zdravljenjem s cetuksimabom. Po potrebi se priporoča nadomeščanje elektrolitov. Posebna previdnost je potrebna pri oslabljenih bolnikih in pri tistih z obstoječo srčno-pljučno boleznijo. Neželeni učinki: Zelo pogosti (≥ 1/10): dispneja, blago do zmerno povečanje jetrnih encimov, kožne reakcije, blage ali zmerne reakcije povezane z infundiranjem, blag do zmeren mukozitis. Pogosti (≥ 1/100, < 1/10): konjunktivitis, hude reakcije povezane z infundiranjem. Pogostost ni znana: Opazili so progresivno zniževanje nivoja magnezija v serumu, ki pri nekaterih bolnikih povzroča hudo hipomagnezijemijo. Glede na resnost so opazili tudi druge elektrolitske motnje, večinoma hipokalciemijo ali hipokaliemijo. **Posebna navodila za shranjevanje:** Shranjujte v hladilniku (2 °C – 8 °C). Ne zamrzujte. **Vrsta ovojnine in vsebina:** 1 viala po 20 ml ali 100 ml. Imetnik dovoljenje za promet: Merck KGaA, 64271 Darmstadt, Nemčija. Podrobne informacije o zdravilu so objavljene na spletni strani Evropske agencije za zdravila (EMEA) http://www.emea.europa.eu.

Dodatne informacije so vam na voljo pri: Merck d.o.o., Dunajska cesta 119, 1000 Ljubljana, tel.: 01 560 3810, faks: 01 560 3831, el. pošta: info@merck.si

www.oncology.merck.de

MERCK SERONO

Arimidex®
anastrozol

Posodobili smo slovar

Skrajšan povzetek glavnih značilnosti zdravila Arimidex® 1 mg filmsko obložene tablete

Sestava zdravila: Ena tableta vsebuje 1 mg anastrozola.

Indikacije: Adjuvantno zdravljenje žensk po menopavzi, ki imajo zgodnji invazivni rak dojke s pozitivnimi estrogenskimi receptorji. Adjuvantno zdravljenje zgodnjega raka dojke s pozitivnimi estrogenskimi receptorji pri ženskah po menopavzi, ki so se dve do tri leta adjuvantno zdravile s tamoksifenom. Zdravljenje napredovalega raka dojke pri ženskah po menopavzi. Učinkovitost pri bolnicah z negativnimi estrogenskimi receptorji ni bila dokazana razen pri tistih, ki so imele predhodno pozitiven klinični odgovor na tamoksifen.

Odmerjanje in način uporabe: Odmerek (tudi starejše bolnice): 1 tableta po 1 mg peroralno, enkrat na dan. Odmerka zdravila ni treba prilagajati pri bolnicah z blago ali zmerno ledvično odpovedjo ali blagi in jetrni odpovedovanjem. Pri zgodnjem raku je priporočljivo trajanje zdravljenja 5 let.

Glavni neželeni učinki: Zelo pogosti (≥ 10 %): navali vročine, običajno blagi do zmerni. Pogosti: (≥ 1 % in < 10 %): astenija, bolečine/otekanost v sklepih, suhost vagine, razredčenje las, izpuščaji, slabost, driska, glavobol (vsi stopnjine blagi do zmerni)

Posebna opozorila in previdnostni ukrepi: Uporabe Arimidexa ne priporočamo pri otrocih, ker njegova varnost in učinkovitost pri njih še nista raziskani. Menopavzo je potrebno biokemično dokazati pri vseh bolnicah, kjer obstaja dvom o hormonskem statusu. Ni podatkov o varni uporabi Arimidexa pri bolnicah z znano ali nujno jetrno okvaro ali hudo ledvično odpovedjo (očistek kreatinina manj kakor 20 ml/min (oziroma 0,33 ml/s)). Pri ženskah z osteoporozo ali pri ženskah s povečanim tveganjem za razvoj osteoporoze je treba oceniti njihovo mineralno gostoto kosti z densitometrijo, na primer z aparatom DEXA na začetku zdravljenja, pozneje pa v rednih intervalih. Po potrebi je treba začeti z zdravljenjem ali preprečevanjem osteoporoze in to skrbno nadzorovati. Ni podatkov o uporabi anastrozola z analogi LHRH. Arimidex zmanjša nivo estrogena v obtoku, zato lahko pozroči zmanjšanje mineralne kostne gostote. Trenutno ni na voljo ustreznih podatkov o učinku bifosfonatov na izgubo mineralne kostne gostote, povzročene z anastrozolom, ali njihovi koristi, če se uporabijo preventivno. Zdravila vsebujejo laktozo.

Kontraindikacije: Arimidex je kontraindiciran pri ženskah pred menopavzo, nosečnosti in dojenju materam, bolnicah s hudo ledvično odpovedjo (očistek kreatinina manj kot 20 ml/min (oziroma 0,33 ml/s)), bolnicah z znanim do hudim jetrnim okvarjenjem, bolnicah, ki imajo znano preobčutljivost za anastrozol ali za katerokoli pomožno snov. Zdravila, ki vsebujejo estrogen, ne smete dajati sočasno z Arimidexom, ker bi se njegovo farmakološko delovanje izničilo. Sočasno zdravljenje s tamoksifenom.

Medsebojno delovanje z drugimi zdravili in druge oblike interakcij: Klinične raziskave o interakcijah z antipirinom in cimetidinom kažejo, da pri sočasni uporabi Arimidexa in drugih zdravil klinično pomembne interakcije, povzročene s citokromom P450, niso verjetne. Pregled baze podatkov o varnosti v kliničnih preskušanjih pri bolnicah, ki so se zdravile z Arimidexom in sočasno jemale drugo pogosto predpisana zdravila, ni pokazal klinično pomembnih interakcij.

Imetnik dovoljenja za promet: AstraZeneca UK Limited, 15 Stanhope Gate, London, W1K 1LN, Velika Britanija

Način predpisovanja zdravila: Rp/Spec

Datum priprave informacije: april 2007

Pred predpisovanjem, prosimo, preberite celoten povzetek glavnih značilnosti zdravila.

Dodatne informacije in literatura so na voljo pri:
AstraZeneca UK Limited
Podružnica v Sloveniji
Verovškova ulica 55
1000 Ljubljana

in na spletnih strneh:
www.arimidex.net
www.bcs.org
www.breastcancercare.org.uk

AstraZeneca
ONKOLOGIJA

APR 05/07 P

*adjuvant [ae´džuv*nt]*

1. adjective pomagljiv, koristen; – treatment with Arimidex: Adjuvantno zdravljenje žensk po menopavzi, ki imajo zgodnji invazivni rak dojke s pozitivnimi estrogenskimi receptorji.

*advanced [*dva:nst]*

1. adjective napreden; zvišan (cene); to be – napredovati; – in years visoke starosti; treatment of – breast cancer with Arimidex: Zdravljenje napredovalega raka dojke pri ženskah po menopavzi. Učinkovitost pri bolnicah z negativnimi estrogenskimi receptorji ni bila dokazana razen pri tistih, ki so imele predhodno pozitiven klinični odgovor na tamoksifen.

switch [swič]

1. transitive verb udariti, bičati s šibo (z repom); šibati z, hitro mahati z; naglo pograbiti; railway ranžirati, zapeljati (usmeriti) (vlak) na drug tir; electrical vključiti, vklopiti; spremeniti (pogovor), obrniti drugam (tok misli); to – back to figuratively (v mislih) vrniti se na;

– to Arimidex: Adjuvantno zdravljenje zgodnjega raka dojke s pozitivnimi estrogenskimi receptorji pri ženskah po menopavzi, ki so se dve do tri leta adjuvantno zdravile s tamoksifenom.

SKRAJŠAN POVZETEK GLAVNIH ZNAČILNOSTI ZDRAVILA

Gemcitabin Lek 200 mg in 1 g prašek za raztopino za infundiranje

lek

član skupine Sandoz

Lek farmacevtska družba d.d., Verovškova 57, 1526 Ljubljana, Slovenija • www.lek.si

Temodal 20 mg, 100 mg, 140mg, 180 mg, 250 mg.
Sestava zdravila: Vsaka kapsula zdravila Temodal vsebuje 20 mg, 100 mg, 140 mg, 180 mg ali 250 mg temozolomida.
Terapevtske indikacije Temodal kapsule so indicirane za zdravljenje bolnikov z:
- za zdravljenje novo diagnosticiranega glioblastoma multiforme, sočasno z radioterapijo in kasneje kot monoterapija
- malignim gliomom, na primer multiformnim glioblastomom ali anaplastičnim astrocitomom, ki se po standardnem zdravljenju ponovi ali napreduje.

Odmerjanje in način uporabe Temodal smejo predpisati le zdravniki, ki imajo izkušnje z zdravljenjem možganskih tumorjev. **Odrasli bolniki z novo diagnosticiranim glioblastomom multiforme** Temodal se uporablja v kombinaciji z žariščno radioterapijo (faza sočasne terapije), temu pa sledi do 6 ciklov monoterapije z temozolomidom. **Faza sočasne terapije** Zdravilo Temodal naj bolnik jemlje peroralno v odmerku 75 mg/m² na dan 42 dni, sočasno z žariščno radioterapijo (60 Gy, danih v 30 dnevnih odmerkih). Odmerka ne boste zmanjševali, vendar se boste vsak teden odločili o morebitni odložitvi jemanja temozolomida ali njegovi ukinitvi na podlagi kriterijev hematološke in nehematološke toksičnosti. Zdravilo Temodal lahko bolnik jemlje vse čas 42-dnevnega obdobja sočasne terapije do 49 dni, če so izpolnjeni vsi od naslednjih pogojev: absolutno število nevtrofilcev ≥ 1,5 x 10⁹/l, število trombocitov ≥ 100 x 10⁹/l, skupni kriterij toksičnosti (SKT) za nehematološko toksičnost ≤ 1. stopnje (z izjemo alopecije, slabosti in bruhanja). Med zdravljenjem morate pri bolniku enkrat na teden pregledati celotno krvno sliko. **Faza monoterapije** Štiri tedne po zaključku faze sočasnega zdravljenja z zdravilom Temodal in radioterapijo naj bolnik jemlje zdravilo Temodal do 6 ciklov monoterapije. V 1. ciklu (monoterapija) je odmerek zdravila 150 mg/m² enkrat na dan 5 dni, temu pa naj sledi 23 dni brez terapije. Na začetku 2. cikla odmerek povečajo na 200 mg/m², če je SKT za nehematološko toksičnost za 1. ciklel stopnje ≤ 2 (z izjemo alopecije, slabosti in bruhanja), absolutno število nevtrofilcev (ASN) ≥ 1,5 x 10⁹/l in število trombocitov ≥ 100 x 10⁹/l. Če odmerka niste povečali v 2. ciklusu, ga v naslednjih ciklusih ne smete povečevati. Ko pa odmerek enkrat povečate, naj ostane na ravni 200 mg/m² na dan v prvih 5 dneh vsakega naslednjega ciklusa, razen če nastopi toksičnost. Med zdravljenjem morate pregledati celotno krvno sliko na 22. dan (21 dni po prvem odmerku zdravila Temodal). **Ponavljajoči se ali napredujoči maligni gliom Odrasli bolniki** Posamezen ciklus zdravljenja traja 28 dni. Bolniki, ki še niso bili zdravljeni s kemoterapijo, naj jemljejo Temodal peroralno v odmerku 200 mg/m² enkrat na dan prvih 5 dni, temu pa naj sledi 23-dnevni premor (skupaj 28 dni). Pri bolnikih, ki so že bili zdravljeni s kemoterapijo, je začetni odmerek 150 mg/m² enkrat na dan, v drugem ciklusu pa se poveča na 200 mg/m² enkrat na dan 5 dni, če ni bilo hematoloških toksičnih učinkov (glejte poglavje 4.4). **Pediatrični bolniki** Pri bolnikih starih 3 leta ali starejših, posamezen ciklus zdravljenja traja 28 dni. Temodal naj jemljejo peroralno v odmerku 200 mg/m² enkrat na dan prvih 5 dni, potem pa naj sledi 23-dnevni premor (skupaj 28 dni). Otroci, ki so že bili zdravljeni s kemoterapijo, naj prejmejo začetni odmerek 150 mg/m² enkrat na dan 5 dni, s povečanjem na 200 mg/m² enkrat na dan 5 dni v naslednjem ciklusu, če ni bilo hematoloških toksičnih učinkov (glejte poglavje 4.4). **Bolniki z motnjami v delovanju jeter ali ledvic** Pri bolnikih z blagimi ali zmernimi motnjami v delovanju jeter je farmakokinetika temozolomida podobna kot pri tistih z normalnim delovanjem jeter. Podatki o uporabi zdravila Temodal pri bolnikih s hudimi motnjami v delovanju jeter (razred III po Child-ij ali motnjami v delovanju ledvic niso na volju. Na podlagi farmakokinetičnih lastnosti temozolomida obstaja majhna verjetnost, da bo pri bolnikih s hudimi motnjami v delovanju jeter ali ledvic potrebno zmanjšanje odmerka zdravila. Kljub temu je potrebna previdnost pri uporabi zdravila Temodal pri teh bolnikih. **Starejši bolniki:** Analiza farmakokinetike je pokazala, da starost ne vpliva na očistek temozolomida. Kljub temu je potrebna posebna previdnost pri uporabi zdravila Temodal pri starejših bolnikih. **Način uporabe** Temodal mora bolnik jemati na tešče. Temodal kapsule mora bolnik pogoltniti cele s kozarcem vode in jih ne sme odpirati ali zvečiti. Predpisani odmerek mora vzeti v obliki najmanjšega možnega števila kapsul. Pred jemanjem zdravila Temodal ali po njem lahko bolnik vzame antiemetik. Če po zaužitju odmerka bruha, ne sme še isti dan vzeti drugega odmerka. **Kontraindikacije** Temodal je kontraindiciran pri bolnikih, ki imajo v anamnezi preobčutljivostne reakcije na sestavine zdravila ali na dakarbazin (DTIC). Temodal je kontraindiciran tudi pri bolnikih s hudo mielosupresijo. Temodal je kontraindiciran pri ženskah, ki so noseče ali dojijo. **Posebno opozorila in previdnostni ukrepi** Pilotno preskušanje podajšanih 42-dnevne sheme zdravljenja je pokazalo, da imajo bolniki, ki so sočasno prejemali zdravilo Temodal in radioterapijo, še posebej veliko tveganje za nastanek pljučnice zaradi okužbe s Pneumocystis carinii (PCP). Profilaksa proti tovrstni pljučnici je torej potrebna pri vseh bolnikih, ki sočasno prejemajo zdravilo Temodal in radioterapijo v okviru 42-dnevne sheme zdravljenja (do največ 49 dni), ne glede na število limfocitov. Če nastopi limfopenija, mora bolnik nadaljevati s profilakso, dokler se limfopenija ne povrne na stopnjo ≤ 1. Antiemetična terapija: Z jemanjem zdravila Temodal sta zelo pogosto povezana slabost in bruhanje. **Laboratorijske vrednosti**: Pred jemanjem zdravila morata biti izpolnjena naslednja pogoja za laboratorijske izvide: ANC mora biti ≥ 1,5 x 10⁹/l in število trombocitov ≥ 100 x 10⁹/l. Na 22. dan (21 dni po prvem odmerku) ali v roku 48 ur od naslednega dne, morate pregledati celotno krvno sliko in jo nato spremljati vsak teden, dokler ni ANC nad 1,5 x 10⁹/l in število trombocitov nad 100 x 10⁹/l. Če med katerimkoli ciklusom ANC pade na < 1,0 x 10⁹/l ali število trombocitov na < 50 x 10⁹/l, morate odmerek zdravila v naslednjem ciklusu zmanjšati za eno odmerno stopnjo. Odmerne stopnje so 100 mg/m², 150 mg/m² in 200 mg/m². Najmanjši priporočeni odmerek je 100 mg/m². **Moški bolniki** Temozolomid lahko deluje genotoksično, zato morate moškim, ki se zdravijo z temozolomidom svetovati, da naj ne zaplodijo otroka še šest mesecev po zdravljenju. **Interakcije** Sočasna uporaba zdravila Temodal in ranitidina ni povzročila spremembe obsega absorpcije temozolomida ali monometiltriazenoimidazol karboksamida (MTIC). Jemanje zdravila Temodal s hrano je povzročilo 33 % zmanjšanje Cmax in 9 % zmanjšanje površino pod krivulijo (AUC). Kar ne moremo izključiti možnosti, da bi bila sprememba Cmax lahko klinično pomembna, naj bolniki jemljejo zdravilo Temodal brez hrane. Analiza populacijske farmakokinetike v preskušanjih druge faze je pokazala, da sočasna uporaba deksametazona, proklorperazina, fenitoina, karbamazepina, ondansetrona, antagonistov receptorjev H2 ali fenobarbitala ne spremeni očistka temozolomida. Sočasno jemanje z valprojsko kislino je bilo povezano z majhnim, a statistično značilnim zmanjšanjem očistka temozolomida. Uporaba zdravila Temodal v kombinaciji z drugimi mielosupresivnimi učinkovinami la hko poveča verjetnost mielosupresije. **Nosečnost** Študij na nosečih ženskah ni bilo. Predklinične študije na podganah in kuncih z odmerkom 150 mg/m² so pokazale teratogenost in/ali toksičnost za plod. Zato naj nosečе ženske načeloma ne bi jemale zdravila Temodal. Če pa je uporaba v času nosečnosti nujna, morate bolnico opozoriti na možne nevarnosti zdravila za plod. Ženskam v rodni dobi svetujte, naj med zdravljenjem z zdravilom Temodal preprečijo zanositev. **Dojenje** Ni znano, ali se temozolomid izloča v materino mleko, zato ženske, ki dojijo ne smejo jemati zdravila Temodal. **Neželeni učinki** V kliničnih preskušanjih so bili najpogostejši neželeni učinki, povezani z zdravljenjem, prebavne motnje, naključnje slabost (43 %) in bruhanje (26 %). Oba učinka sta bila ponavadi 1. ali 2. stopnje (od 0 do 5 epizod bruhanja v 24 urah) in sta prenehala sama, ali pa ju je bilo mogoče hitro obvladati s standardnim antiemetičnim zdravljenjem. Incidenca hude slabosti in bruhanja je bila 4 %. Laboratorijski izvidi: Trombocitopenija in. nevtropenija 3. in. 4. stopnje sta se pojavili pri 19 % in. 17 % bolnikov, zdravljenih zaradi malignega glioma. Zaradi njiju je bila potrebna hospitalizacija in/ali prekinitev zdravljenja z zdravilom Temodal pri 8 % in. 4 % bolnikov. Mielosupresija je bila predvidljiva (ponavadi se je pojavila v prvih nekaj ciklusih in je bila najizrazitejša med 21. in 28. dnevu, okrevanje pa je bilo hitro, ponavadi v 1 do 2 tednih. Opazili niso nobenih dokazov kumulativne mielosupresije. Trombocitopenija lahko poveča tveganje za pojav krvavitev, nevtropenija ali levkopenija pa tveganje za okužbe. **Imetnik dovoljenja za promet** SP Europe 73, rue de Stalle B-1180 Bruxelles Belgija. **Način in režim izdaje** Zdravilo se izdaja samo na recept, uporablja pa se pod posebnim nadzorom zdravnika specialista ali od njega pooblaščenega zdravnika. **Datum priprave informacije** oktober 2007.

Schering-Plough

Temodal®
temozolomid

Resnični napredek

Pri na novo odkritem glioblastomu multiforme in malignih gliomih, ki se ponovijo ali napredujejo.

Poenostavljeno zdravljenje

Z dvema novima jakostima
140 mg in 180 mg Temodal

- Možnost prejemanja manjšega števila kapsul
- Boljša sprejemljivost in sodelovanje bolnika
- Natančno odmerjanje
- Barvne kapsule za enostavnejšo dnevno uporabo

Schering-Plough

Temodal®
temozolomid

SKRAJŠAN POVZETEK GLAVNIH ZNAČILNOSTI ZDRAVILA

Ime zdravila: Tarceva 25 mg/100 mg/150 mg filmsko obložene tablete

Kakovostna in količinska sestava: Ena filmsko obložena tableta vsebuje 25 mg, 100 mg ali 150 mg erlotiniba (v obliki erlotinibijevega klorida).

Terapevtske indikacije: Nedrobnocelični rak pljuč: Zdravilo Tarceva je indicirano za zdravljenje bolnikov z lokalno napredovalim ali metastatskim nedrobnoceličnim rakom pljuč po neuspehu vsaj ene predhodne kemoterapije. Pri predpisovanju zdravila Tarceva je treba upoštevati dejavnike, povezane s podaljšanim preživetjem. Koristnega vpliva na podaljšanje preživetja ali drugih klinično pomembnih učinkov zdravljenja niso dokazali pri bolnikih z EGFR-negativnimi tumorji. Rak trebušne slinavke: Zdravilo Tarceva je v kombinaciji z gemcitabinom indicirano za zdravljenje bolnikov z metastatskim rakom trebušne slinavke. Pri predpisovanju zdravila Tarceva je treba upoštevati dejavnike, povezane s podaljšanim preživetjem. Koristnega vpliva na podaljšanje preživetja niso dokazali za bolnike z lokalno napredovalo boleznijo.

Odmerjanje in način uporabe: Zdravljenje z zdravilom Tarceva mora nadzorovati zdravnik z izkušnjami pri zdravljenju raka. Zdravilo Tarceva vzamemo najmanj eno uro pred zaužitjem hrane ali dve uri po tem. Kadar je potrebno odmerek prilagoditi, ga zmanjšujemo v korakih po 50 mg. Pri sočasnem jemanju substratov in modulatorjev CYP3A4 bo morda potrebna prilagoditev odmerka. Pri dajanju zdravila Tarceva bolnikom z jetrno okvaro je potrebna previdnost, če se pojavijo hudi neželeni učinki pride v poštev zmanjšanje odmerka ali prekinitev zdravljenja z zdravilom Tarceva. Uporaba zdravila Tarceva pri bolnikih s hudo jetrno ali ledvično okvaro ter pri otrocih ni priporočljiva. Nedrobnocelični rak pljuč: Priporočeni dnevni odmerek zdravila Tarceva je 150 mg. Rak trebušne slinavke: Priporočeni dnevni odmerek zdravila Tarceva je 100 mg, v kombinaciji z gemcitabinom. Pri bolnikih, pri katerih se kožni izpuščaj v prvih 4 do 8 tednih zdravljenja ne pojavi, je treba ponovno preštehati nadaljnje zdravljenje z zdravilom Tarceva.

Kontraindikacije: Huda preobčutljivost za erlotinib ali katero koli pomožno snov.

Posebna opozorila in previdnostni ukrepi: Močni induktorji CYP3A4 lahko zmanjšajo učinkovitost erlotiniba, močni zaviralci CYP3A4 pa lahko povečajo toksičnost. Sočasnemu zdravljenju s temi zdravili se je treba izogibati. Bolnikom, ki kadijo, je treba svetovati, naj prenehajo kaditi, saj so plazemske koncentracije erlotiniba pri kadilcih zmanjšane v primerjavi s plazemskimi koncentracijami pri nekadilcih. Verjetno je, da je velikost zmanjšanja klinično pomembna. Pri bolnikih, pri katerih se akutno pojavijo novi in/ali poslabšajo nepojasnjeni pljučni simptomi, kot so dispneja, kašelj in vročina, je zdravljenje z zdravilom Tarceva treba prekiniti, dokler ni znana diagnoza. Bolnike, ki se sočasno zdravijo z erlotinibom in gemcitabinom, je treba skrbno spremljati zaradi možnosti pojava toksičnosti, podobni intersticijski pljučni bolezni. Če je ugotovljena intersticijska pljučna bolezen, zdravilo Tarceva ukinemo in uvedemo ustrezno zdravljenje. Pri približno polovici bolnikov, ki so se zdravili z zdravilom Tarceva, se je pojavila driska. Zmerno do hudo drisko zdravimo z loperamidom. V nekaterih primerih bio morda potrebno zmanjšanje odmerka. V primeru hude ali dolgotrajne driske, navzeje, anoreksije ali bruhanja, povezanih z dehidracijo, je zdravljenje z zdravilom Tarceva treba prekiniti in dehidracijo ustrezno zdraviti. O hipokaliemiji in ledvični odpovedi so poročali redko. Posebno pri bolnikih z dejavniki tveganja (sočasno jemanje drugih zdravil, simptomi, bolezni ali drugi dejavniki, vključno z visoko starostjo) moramo, če je driska huda ali dolgotrajna oziroma vodi v dehidracijo, zdravljenje z zdravilom Tarceva prekiniti in bolnikom zagotoviti intenzivno intravensko rehidracijo. Dodatno je treba pri bolnikih s prisotnim tveganjem za razvoj dehidracije spremljati ledvično delovanje in serumske elektrolite, vključno s kalijem. Pri uporabi zdravila Tarceva so poročali o redkih primerih jetrne odpovedi. K njenemu nastanku je lahko pripomogla predhodno obstoječa jetrna bolezen ali sočasno jemanje hepatotoksičnih zdravil. Pri teh bolnikih je treba zato premisliti o rednem spremljanju jetrnega delovanja. Dajanje zdravila Tarceva je treba prekiniti, če so spremembe jetrnega delovanja hude. Tablete vsebujejo laktozo in jih ne smemo dajati bolnikom z redkimi dednimi stanji: intoleranco za galaktozo, laponsko obliko zmanjšane aktivnosti laktaze ali malabsorpcijo glukoze/galaktoze.

Medsebojno delovanje z drugimi zdravili in druge oblike interakcij: Erlotinib se pri ljudeh presnavlja v jetrih z jetrnimi citokromi, primarno s CYP3A4 in v manjši meri s CYP1A2. Presnova erlotiniba zunaj jeter poteka s CYP3A4 v črevesju, CYP1A1 v pljučih in CYP1B1 v tumorskih tkivih. Z zdravilnimi učinkovinami, ki se presnavljajo s temi encimi, jih zavirajo ali pa so njihovi induktorji, lahko pride do interakcij. Erlotinib je srednje močan zaviralec CYP3A4 in CYP2C8, kot tudi močan zaviralec glukuronidacije z UGT1A1 in vitro. Pri kombinaciji ciprofloksacina ali močnega *zaviralca CYP1A2* (npr. fluvoksaminal z erlotinibom je potrebna previdnost. V primeru pojava neželenih dogodkov, povezanih z erlotinibom, lahko odmerek erlotiniba zmanjšamo. Predhodno ali sočasno zdravljenje z zdravilom Tarceva ni spremenilo očistka prototipov *substratov CYP3A4*, midazolama in eritromicina. Inhibicija glukoronidacije lahko povzroči interakcije z zdravili, ki so *substrati UGT1A1* in se izločajo samo po tej poti. Močni *zaviralci aktivnosti CYP3A4* zmanjšajo presnovo erlotiniba in zvečajo koncentracije erlotiniba v plazmi. Pri sočasnem jemanju erlotiniba in močnih zaviralcev CYP3A4 je zato potrebna previdnost. Če je treba, odmerek erlotiniba zmanjšamo, še posebno pri pojavu toksičnosti. Močni *spodbujevalci aktivnosti CYP3A4* zvečajo presnovo erlotiniba in pomembno zmanjšajo plazemske koncentracije erlotiniba. Sočasnemu dajanju zdravila Tarceva in induktorjev CYP3A4 se je treba izogibati. Pri bolnikih, ki potrebujejo sočasno zdravljenje z zdravilom Tarceva in močnim induktorjem CYP3A4 je treba premisliti o povečanju odmerka do 300 mg ob skrbnem spremljanju njihove varnosti. Zmanjšana izpostavljenost se lahko pojavi tudi z drugimi induktorji, kot so fenitoin, karbamazepin, barbiturati ali šentjanževka. Če te zdravilne učinkovine kombiniramo z erlotinibom, je potrebna previdnost. Kadar je mogoče, je treba razmisliti o drugih načinih zdravljenja, ki ne vključujejo močnega spodbujanja aktivnosti CYP3A4.

Bolnikom, ki jemljejo varfarin ali druge *kumarinske antikoagulante*, je treba redno kontrolirati protrombinski čas ali INR. Sočasna uporaba *zaviralcev P-glikoproteina*, kot sta ciklosporin in verapamil, lahko vodi v spremenjeno porazdelitev in/ali spremenjeno izločanje erlotiniba. Za erlotinib je značilno zmanjšanje topnosti pri pH nad 5. Zdravila, ki spremenijo pH v zgornjem delu prebavil, kot so *zaviralci protonske črpalke*, *H2 antagonisti* in antacidi, lahko spremenijo topnost erlotiniba in posledično njegovo biološko uporabnost. Kombinaciji erlotiniba in zaviralcev protonske črpalke se je treba izogibati. Učinki sočasnega dajanja erlotiniba in H2 antagonistov ali antacidov niso znani, vendar je zmanjšana biološka uporabnost verjetna. Zato se je treba sočasnemu dajanju teh kombinacij izogibati. V študiji faze Ib ni bilo pomembnih učinkov *gemcitabina* na farmakokinetiko erlotiniba, prav tako ni bilo pomembnih učinkov erlotiniba na farmakokinetiko gemcitabina. Erlotinib poveča koncentracijo platine. Pomembnih učinkov *karboplatina* ali paklitaksela na farmakokinetiko erlotiniba ni bilo. *Kapecitabin* lahko poveča koncentracijo erlotiniba. Pomembnih učinkov erlotiniba na farmakokinetiko kapecitabina ni bilo.

Neželeni učinki: *Zelo pogosti neželeni učinki* so kožni izpuščaj in driska, kot tudi utrujenost, anoreksija, dispneja, kašelj, okužba, navzeja, bruhanje, stomatitis, bolečina v trebuhu, pruritus, suha koža, suhi keratokonjunktivitis, konjunktivitis, zmanjšanje telesne mase, depresija, glavobol, nevropatija, dispepsija, flatulenca, alopecija, okorelost, preraja. *Pogosti neželeni učinki* so gastrointestinalna krvavitve, krvavitev iz nosu, nenormalnosti testov jetrne funkcije, keratitis, zanohtnica. *Redko* so poročali o jetrni odpovedi. *Občasno* pa o poraščenosti moškega tipa pri ženskah, spremembah trepalnic/obrvi, krhkih nohtih, odstopanju nohtov od kože, resni intersticijski pljučni bolezni, vključno s smrtnimi primeri.

Režim izdaje zdravila: H/Rp

Imetnik dovoljenja za promet: Roche Registration Limited, 6 Falcon Way, Shire Park, Welwyn Garden City, AL7 1TW, Velika Britanija.

Informacija pripravljena: 1. april 2008.

DODATNE INFORMACIJE SO NA VOLJO PRI
Roche farmacevtska družba d.o.o.
Vodovodna cesta 109, 1000 Ljubljana
Povzetek glavnih značilnosti zdravila
je dosegljiv na www.roche.si

Roche

95-08-TAR

Tarceva®
erlotinib

ČAS ZA ŽIVLJENJE.

DOKAZANO PODALJŠA PREŽIVETJE PRI BOLNIKIH:

- z lokalno napredovalim ali metastatskim nedrobnoceličnim rakom pljuč[1]
- z metastatskim rakom trebušne slinavke[1]

Povzetek glavnih značilnosti zdravila TARCEVA, www.emea.europa.eu

Že desetletje prinašamo rešitve v Vaš laboratorij!

Za področja:

- bioznanosti **SYNGENE, INVITROGEN: DYNAL, ZYMED, MOLECULAR PROBES, CALTAG**
- diagnostike **MINERVA, MEDAC, BIOTEK**
- gojenja celičnih kultur **INVITROGEN-GIBCO, TPP, GREINER** in **SANYO**
- merjenja absorbance, fluorescence in luminiscence **BIOTEK**
- pipetiranja **BIOHIT** in **BIOTEK**
- laboratorijske opreme **SANYO**
- čiste vode za laboratorije **ELGA LABWATER**
- HPLC in GC kolon, vial in filtrov **PHENOMENEX** in **CHROMACOL/NATIONAL SCIENTIFIC**

KEMOMED
Prinašamo rešitve

SVETOVANJE, TRGOVINA, TRŽENJE d.o.o. • Kališka 9 • PE: Stritarjeva 5 • 4000 KRANJ • Slovenija
t: +386 4 20 15 050 • f: +386 4 20 15 055 • e-mail: info@kemomed.si • www.kemomed.si

TANTUM® VERDE
(benzidamin)

Lajša lokalizirano bolečino in oteklino pri vnetju v ustih in žrelu!

BLAŽI ZNAKE VNETJA
- Zmanjšuje oteklino

HITRO UMIRI BOLEČINO
- Zmanjšuje težave pri požiranju

TANTUM VERDE

- učinkovit in enostaven za uporabo ter varen;
- brez sladkorja, primeren tudi za diabetike;
- primeren za otroke, starejše od 6 let.

IMETNIK DOVOLJENJA ZA PROMET

TANTUM® VERDE se lahko kupi brez recepta v lekarni. Dodatne informacije dobite pri imetniku dovoljenja za promet.

Pred uporabo natančno preberite navodilo! O tveganju in neželenih učinkih se posvetujte z zdravnikom ali s farmacevtom.

gelclair®

UČINKOVITO, DOLGOTRAJNO OLAJŠANJE BOLEČIN ZA BOLNIKE Z ORALNIM MUKOZITISOM

GELCLAIR® je bioadherenten gel za oralno uporabo. Prekrije sluznico v ustni votlini in žrelu ter tako ustvari zaščitno plast, ki za več ur pomiri oralni mukozitis. GELCLAIR® odlikuje enostavna uporaba in zelo dobra prenosljivost, brez zabeleženih neželenih stranskih učinkov in interakcij z zdravili.

HELSINN

PharmaSwiss
Choose more Life

PharmaSwiss d.o.o.
Dolenjska cesta 242c, 1000 Ljubljana
telefon: + 386 1 256 47 00, faks: +386 1 256 47 05

NOVO

NAVELBINE®

vinorelbin

Koncentrat za raztopino za infundiranje 10 mg/ml, 50 mg/5ml

Novost za zdravljenje: nedrobnoceličnega raka pljuč in napredovalega raka dojke

Izkušnje z več kot 1 mio bolnikov po svetu

- Odlična učinkovitost v kombinaciji s cisplatinom ali kot monoterapija za bolnike, ki niso primerni za polikemoterapijo
- Dobra prenosljivost:
  - blaga alopecija
  - zelo nizka stopnja emetogenosti (< 10 %)
  - ni kardiotoksičnosti
  - ni nevrotoksičnosti
- Premedikacija ni potrebna
- Sinergistično delovanje s tarčnim zdravilom trastuzumab

Pred predpisovanjem zdravila Navelbine® preberite povzetek temeljnih značilnosti, ki ga dobite pri naših strokovnih sodelavcih.

Pierre Fabre Médicament

MEDIS | www.medis.si | onkologija@medis.si

Editorial policy

Editorial policy of the journal *Radiology and Oncology* is to publish original scientific papers, professional papers, review articles, case reports and varia (editorials, reviews, short communications, professional information, book reviews, letters, etc.) pertinent to diagnostic and interventional radiology, computerized tomography, magnetic resonance, ultrasound, nuclear medicine, radiotherapy, clinical and experimental oncology, radiobiology, radiophysics and radiation protection. The Editorial Board requires that the paper has not been published or submitted for publication elsewhere: the authors are responsible for all statements in their papers. Accepted articles become the property of the journal and therefore cannot be published elsewhere without written permission from the editorial board. Papers concerning the work on humans, must comply with the principles of the declaration of Helsinki (1964). The approval of the ethical committee must then be stated on the manuscript. Papers with questionable justification will be rejected.

Manuscript written in English should be submitted to the Editorial Office in triplicate (the original and two copies), including the illustrations*: Radiology and Oncology*, Institute of Oncology, Zaloska 2, SI-1000 Ljubljana, Slovenia; (Phone: +386 (0)1 5879 369, Tel./Fax: +386 (0)1 5879 434, E-mail: gsersa@onko-i.si). Authors are also asked to submit their manuscripts electronically, either by E-mail or on CD rom. The type of computer and word-processing package should be specified (Word for Windows is preferred).

All articles are subjected to editorial review and review by independent referee selected by the editorial board. Manuscripts which do not comply with the technical requirements stated herein will be returned to the authors for correction before peer-review. Rejected manuscripts are generally returned to authors, however, the journal cannot be held responsible for their loss. The editorial board reserves the right to ask authors to make appropriate changes in the contents as well as grammatical and stylistic corrections when necessary. The expenses of additional editorial work and requests for reprints will be charged to the authors.

General instructions•• Radiology and Oncology will consider manuscripts prepared according to the Vancouver Agreement (*N Engl J Med* 1991; **324:** 424-8, *BMJ* 1991; **302:** 6772; *JAMA* 1997; **277:** 927-34.). Type the manuscript double spaced on one side with a 4 cm margin at the top and left hand side of the sheet. Write the paper in grammatically and stylistically correct language. Avoid abbreviations unless previously explained. The technical data should conform to the SI system. The manuscript, including the references may not exceed 20 typewritten pages, and the number of figures and tables is limited to 8. If appropriate, organize the text so that it includes: Introduction, Material and methods, Results and Discussion. Exceptionally, the results and discussion can be combined in a single section. Start each section on a new page, and number each page consecutively with Arabic numerals.

Title page should include a concise and informative title, followed by the full name(s) of the author(s); the institutional affiliation of each author; the name and address of the corresponding author (includ-

ing telephone, fax and e-mail), and an abbreviated title. This should be followed by the *abstract page*, summarising in less than 200 words the reasons for the study, experimental approach, the major findings (with specific data if possible), and the principal conclusions, and providing 3-6 key words for indexing purposes. The text of the report should then proceed as follows:

Introduction should state the purpose of the article and summarize the rationale for the study or observation, citing only the essential references and stating the aim of the study.

Material and methods should provide enough information to enable experiments to be repeated. New methods should be described in detail. Reports on human and animal subjects should include a statement that ethical approval of the study was obtained.

Results should be presented clearly and concisely without repeating the data in the tables and figures. Emphasis should be on clear and precise presentation of results and their significance in relation to the aim of the investigation.

Discussion should explain the results rather than simply repeating them and interpret their significance and draw conclusions. It should review the results of the study in the light of previously published work.

Illustrations and tables must be numbered and referred to in the text, with appropriate location indicated in the text margin. Illustrations must be labelled on the back with the author's name, figure number and orientation, and should be accompanied by a descriptive legend on a separate page. Line drawings should be supplied in a form suitable for high-quality reproduction. Photographs should be glossy prints of high quality with as much contrast as the subject allows. They should be cropped as close as possible to the area of interest. In photographs mask the identities of the patients. Tables should be typed double spaced, with descriptive title and, if appropriate, units of numerical measurements included in column heading.

References· must be numbered in the order in which they appear in the text and their corresponding numbers quoted in the text. Authors are responsible for the accuracy of their references. References to the Abstracts and Letters to the Editor must be identified as such. Citation of papers in preparation, or submitted for publication, unpublished observations, and personal communications should not be included in the reference list. If essential, such material may be incorporated in the appropriate place in the text. References follow the style of Index Medicus. All authors should be listed when their number does not exceed six; when there are seven or more authors, the first six listed are followed by "et al". The following are some examples of references from articles, books and book chapters:

Dent RAG, Cole P. *In vitro* maturation of monocytes in squamous carcinoma of the lung. *Br J Cancer* 1981; **43:** 486-95.

Chapman S, Nakielny R. *A guide to radiological procedures.* London: Bailliere Tindall; 1986.

Evans R, Alexander P. Mechanisms of extracellular killing of nucleated mammalian cells by macrophages. In: Nelson DS, editor. *Immunobiology of macrophage.* New York: Academic Press; 1976. p. 45-74.

Page proofs will be faxed or sent by E-mail to the corresponding author. It is their responsibility to check the proofs carefully and fax a list of essential corrections to the editorial office within 48 hours of receipt. If corrections are not received by the stated deadline, proof-reading will be carried out by the editors.

Eli Lilly farmacevtska družba, d.o.o.
Dunajska 156, 1000 Ljubljana, Slovenija
Tel.: (01) 5800 010,
Faks: (01) 569 1705